University of Sao Paulo
"Luiz de Queiroz" College of Agriculture

Functional, structural and agrohydrological sugarcane crop modelling: towards a simulation platform for Brazilian farming systems

Murilo dos Santos Vianna

Thesis presented to obtain the degree of Doctor in Science. Area: Agricultural Systems Engineering

Piracicaba
2018

Murilo dos Santos Vianna
Environmental Engineer

Functional, structural and agrohydrological sugarcane crop modelling: towards a simulation platform for Brazilian farming systems

versão revisada de acordo com a resolução CoPGr 6018 de 2011

Advisor:
Prof. Dr. **FÁBIO RICARDO MARIN**

Thesis presented to obtain the degree of Doctor in Science. Area: Agricultural Systems Engineering

Piracicaba
2018

Dados Internacionais de Catalogação na Publicação
DIVISÃO DE BIBLIOTECA – DIBD/ESALQ/USP

Vianna, Murilo dos Santos

Functional, structural and agrohydrological sugarcane crop modelling: towards a simulation platform for Brazilian farming systems / Murilo dos Santos Vianna. - - versão revisada de acordo com a resolução CoPGr 6018 de 2011. - - Piracicaba, 2018.

113 p.

Tese (Doutorado) - - USP / Escola Superior de Agricultura “Luiz de Queiroz”.

1. *Saccharum officinarum* L. 2. Modelagem de culturas 3. Modelo funcional estrutura de plantas 4. Modelo de cultura baseado em processos I. Título

ACKNOWLEDGEMENTS

To my family, especially my wife, Raissa Carneiro for their love, support, teaching and much of patience during all the way through here;

To my professor advisor, Dr. Fábio Ricardo Marin, for his mentoring and assistance during the development of this research and since under graduation (2008), as well as, the friendship, teaching and motivational support to keep on crop modelling research;

To FAPESP, by the financial support (36 months) through the Ph.D. scholarship (Process n° 2014/05887-6) and the scholarship for the abroad internship (9 months) at Wageningen University and Research Centre (Process n° 2015/16214-5);

To my supervisors, Dr. Klaas Metselaar and Jochem Evers, for their mentoring, assistance and teachings during development of my abroad internship at Wageningen University and Research Centre which contributed a lot to this thesis development and to my professional carrier;

To graduate colleagues and friends, Daniel Nassif and Leandro Costa for the support on field experiment and provide the datasets of 1st and 2nd years of long-term experiment, and especial thanks to Kássio Carvalho for supporting in many experimental measurements in the 3rd year of long-term experiment;

To professors and employees of "Luiz de Queiroz" College of Agriculture for teaching and support, especially to Davilmar, Angela and Fernando to support me on paper work, Lino and Afonso (in memorian) for supporting on field experiment;

To "Luiz de Queiroz" College of Agriculture, University of Sao Paulo, for the infrastructure for experimental field and many possibilities to improve my skills in research and teaching in Biosystem Engineering through the Graduate Program of Agricultural Systems Engineering;

To GEPEMA/AGRIMET group for tremendous support on field experiment, and especially by collecting and providing the 4th year dataset of the long-term experiment and also for workshops and practicing teaching and mentoring skills with undergraduate students;

To everyone that in some way contributed for my personal and professional evolution, helping to obtain the degree of Doctor in Science in Agricultural Systems Engineering.

EPIGRAPH

"Not only does god play dice, but he sometimes throws them where they cannot be seen"
Stephen Hawking

CONTENTS

RESUMO

Modelagem funcional, estrutural e agro-hidrológica da cultura da cana-de-açúcar: rumo a uma plataforma de simulação de sistemas agrícolas brasileiros

A cultura da cana-de-açúcar é a principal fonte de açúcar e a segunda maior fonte de biocombustíveis do mundo. O Brasil é o maior produtor mundial desde a década de 80 e atualmente representa metade da produção mundial, enquanto que ao mesmo tempo o etanol e a biomassa correspondem a mais de 15% da fonte de energia do país. Contudo, a produtividade comercial da cana-de-açúcar brasileira atingiu um limiar de cerca de 75 t ha^{-1} e para atender à crescente demanda de açúcar e etanol, a cultura expandiu-se fortemente para a região centro-oeste, onde a irrigação é obrigatória para manter os níveis de produção e diminuir riscos de quebra de safra. Para dar suporte a tomada de decisão e avanço científico sobre onde e como a cultura deve se expandir e/ou aumentar a produtividade, é necessária uma visão heurística do sistema agrícola brasileiro que pode ser traduzida matematicamente para um modelo de cultura. Desta forma, os efeitos do manejo e tipo de solo, variabilidade climática e fatores econômicos na produtividade de culturas agrícolas podem ser avaliados quantitativamente por meio de modelos de culturas baseados em processos (MBP). No entanto, em contraste a outras culturas, a cana-de-açúcar possui apenas dois MBPs disponíveis para usuários finais (DSSAT-CANEGRO e APSIM-Sugar) que requerem calibração e parametrização para melhor representar o sistema agrícola de cana-de-açúcar do Brasil. Portanto, este estudo teve como objetivo desenvolver, calibrar e avaliar diferentes abordagens de modelagem de culturas voltadas a produção de cana-de-açúcar no Brasil, para servir como ferramenta de tomada de decisão para o setor público e privado, auxilio no manejo da água e avaliação dos impactos nas mudanças climáticas. Portanto, uma nova versão do modelo baseado em processo de cana-de-açúcar (SAMUCA) foi desenvolvida para operar a nível de fitômeros, incluindo os efeitos no crescimento e desenvolvimento da cana com base na cobertura da palha no solo, competição por luz no processo de perfilhamento e acúmulo de sacarose com base nas relações fonte-dreno. O modelo foi incorporado em uma plataforma modular dedicada a simular o sistema solo-planta-atmosfera e manejo do sistema agrícola. Além disso, a versão anterior do SAMUCA também foi reestruturada e acoplada à plataforma agro-hidrológica SWAP ("Soil, Water, Atmosphere and Plant") com objetivo de aprimorar as simulações de balanço hídrico no solo e efeito no crescimento da cana-de-açúcar. Por fim, um Modelo Funcional-Estrutural de Plantas (MFEP) para a cana-de-açúcar foi desenvolvido integrando os principais componentes da cultura a nível de órgãos (fitômeros) com base em uma abordagem de fonte-dreno e um modelo robusto de radiação que foram introduzidos em uma plataforma de modelagem tridimensional (GroIMP). As três abordagens foram avaliadas e seu desempenho foi determinado com base em condições experimentais para diferentes regiões brasileiras. O desempenho da nova versão do modelo SAMUCA em experimento de longo prazo e em diferentes condições brasileiras foi satisfatório e os índices de concordância foram próximos de outros modelos de cana-de-açúcar amplamente utilizados (CANEGRO e APSIM-Sugar). Além disso, a plataforma de simulação de culturas modulada pode ser usada para hospedar mais modelos de culturas e integrar novas características do sistema de cultivo brasileiro. O acoplamento do modelo SWAP-SAMUCA foi realizado e apesar não apresentar melhorias expressivas no desempenho do modelo em simular os componentes da cultura (com erro médio quadrático [RMSE] 6% menor), a habilidade do modelo SWAP-SAMUCA em simular o teor de água no solo mostrou-se consideravelmente superior em comparação ao modelo original (RMSE 32% menor). O MFEP para cana-de-açúcar foi capaz de simular o desenvolvimento do dossel, o processo de perfilhamento e o acúmulo de sacarose ao nível de órgãos e planta de forma satisfatória. Além de sua capacidade em simular com precisão a interceptação da radiação por cada estrutura do dossel, podendo auxiliar na compreensão do processo de competição intraespecífica entre perfilhos, a estrutura do MFEP da cana-de-açúcar também pode ser usada no apoio à pesquisa focando os mecanismos de acúmulo de sacarose e translocação de açúcares bem como em estudos de consórcio em cana-de-açúcar, como têm sido realizado com sucesso para outras culturas nos últimos anos.

Palavras-chave: *Saccharum officinarum* L.; Modelagem de culturas; Modelo funcional estrutural de plantas; Modelo de cultura baseado em processos

ABSTRACT

Functional, structural and agrohydrological sugarcane crop modelling: towards a simulation platform for Brazilian farming systems

Sugarcane crop is the main source of sugar and the second largest source of biofuel in the world. Since the 1980s, Brazil has been the largest sugarcane producing nation, producing half of the global amount. Ethanol and biomass from sugarcane account for more than 15% of the country´s energy source. Nevertheless, commercial Brazilian sugarcane yield has plateaued at 75 t ha^{-1}, and to meet the increasing demand for sugar and ethanol, the crop has strongly expanded towards central-western regions, where irrigation is mandatory to offset water stress risks. To support decision making and scientific guidance towards where and how the crop should expand and/or to increase yields, a heuristic view of the crop system is needed, which can mathematically be translated into a crop model. In turn, the effects of crop management, land use change, climate variability and agro-economic change factors on crop production and associated quantities can and have been assessed by using crop process-based models (PBM). In contrast to other crops, however, sugarcane has only two PBMs available for end users (DSSAT-CANEGRO and APSIM-Sugar), and further modifications of these models are required to better assess and support sustainable sugarcane production in Brazil. Therefore, this study aimed to develop, calibrate and evaluate different crop modelling approaches for Brazilian sugarcane farming systems, water management strategies, climate change impacts and canopy structures to support improved decisions for private and public stakeholders in the sugarcane sector, provide scientific guidance and establish a Brazilian platform of crop simulations. A new version of the sugarcane process-based model (SAMUCA) was developed to operate at phytomer level, focusing on soil mulch effects on crop growth and development, tillering process under competition for light and sucrose accumulation based on source-sink relations. The model was embedded into a modular platform dedicated to simulating the soil-plant-atmosphere and the management of the sugarcane farm system. The previous version of SAMUCA was also re-structured and coupled to the SWAP (Soil, Water, Atmosphere and Plant) agrohydrological model platform, focusing on soil water relations to crop growth. Moreover, a Functional-Structural Plant Model (FSPM) for sugarcane was developed by integrating the main crop components at the organ level (phytomer), based on a relative source-sink approach and a robust light model embedded into a three-dimensional modelling platform (GroIMP). All approaches were evaluated, and the performance under experimental conditions for different Brazilian conditions was determined. The performance of the new version of SAMUCA in a long-term experiment and under different Brazilian conditions was satisfactory, with agreement indices close to those of other widely used sugarcane crop models (CANEGRO and APSIM-Sugar). In addition, the modulated crop simulation platform can be used to host more crop models and integrate new features of Brazilian farming systems. The coupling of the SWAP-SAMUCA model was accomplished, and although non-expressive improvements in model performance regarding crop yield were noticed (with an overall 6% lower RMSE), the ability of SWAP-SAMUCA to simulate soil water content was higher than that of the original "tipping bucket" approach (32% lower RMSE). The Functional-Structural Plant Model for sugarcane was able to satisfactorily simulate canopy development, tillering and sucrose accumulation at the organ level and its integration at the whole-plant level. Besides its ability to simulate competition for light, helping to understand intra-specific competition among tillers, the sugarcane FSPM framework can be used to support sucrose accumulation and translocation mechanism studies as well as intercropping studies for sugarcane, which has already successfully been done for other crops.

Keywords: *Saccharum officinarum* L.; Crop modelling; Functional-structural plant model; Crop process based model

1. INTRODUCTION

Sugarcane (*Saccharum officinarum L.*) is one of the world's most productive crops, with biomass accumulation rates as high as 550 kg ha^{-1} day^{-1}. Apart from being the main source of sugar in the world, the ability to produce large amounts of biomass over a relatively short time makes this species extremely attractive in a biomass-dependent economy (Moore and Botha, 2013b). Over the last three decades, sugarcane has emerged as the second largest source of biofuel, with major social, economic and environmental importance in many tropical and sub-tropical countries (Scheiterle *et al.*, 2017; Tapia Carpio and Simone de Souza, 2017). Globally, it is the 6th most economically significant crop and the 2nd most important C4 species, after maize (Sage, Peixoto and Sage, 2013; FAO, 2016).

More than 70% of the global sugarcane crop are produced in Brazil, India, China, Thailand and Pakistan (FAO, 2016), and Brazil has become the major sugarcane producer in the world since the late 1970s, after Brazilian government incentives to sugarcane production and the shifting of the fuel program (PROALCOOL); currently accounting for half of the global production (FAO, 2016; Marin, 2016). Sugar is not the only major Brazilian end product; ethanol and biomass correspond to more than 15% of the country's energy source (including gasoline mandatory mixture), mainly used for electricity and heating in sugarcane mills (Walter *et al.*, 2014; EPE, 2015; Marin, 2016; Fortunato *et al.*, 2017).

As a result of the mechanisation of sugarcane harvesting in Brazil, together with the increased demand for ethanol by the major "*flexfuel*" vehicle fleet, areas under sugarcane cultivation have been expanding at the rate of one hectare per minute over the last 10 years (Rudorff *et al.*, 2010; Vianna and Sentelhas, 2015; F. V. Scarpare *et al.*, 2016), extending into marginal regions with adverse soil and climate conditions. These conditions result in a wide yield variability and require improved management strategies. On the hand, irrigation has become an important management tool, while on the other hand, the crop's response to different soil conditions, weather and management is still rather uncertain. In addition to this, climate change is already occurring and is expected to intensify in the coming decades, imposing a further production risk to all crops, including sugarcane (Stocker *et al.*, 2013).

Under these scenarios, crop modelling has been widely applied to understand the key biophysical processes involved in crop growth and production (Jones *et al.*, 2003; Keating *et al.*, 2003; van Ittersum K *et al.*, 2003). Pioneering crop system studies, focusing on quantifying these processes, have been initiated in the early 1960s through Dutch and US research program initiatives (Passioura and Passioura, 1996; Sinclair and Seligman, 1996; van Ittersum K *et al.*, 2003). Thereafter, many process-based crop models (PBM) have been developed, and by including the underlying processes and crop function, such models could be applied in general situations (outside of experimental conditions). Apart from being a crop system heuristic tool, PBM has become an important support tool in research and decision making (van Diepen *et al.*, 1989; Brisson *et al.*, 1998; Jones *et al.*, 2003; Keating *et al.*, 2003; van Ittersum K *et al.*, 2003; Vos, Marcelis and Evers, 2007; Raes *et al.*, 2009). Further advantages of crop modelling have been reported by Vos et al. (2007) as, such as (i) integration of knowledge (exceeding the capacity of the human brain), (ii) quantitative testing of hypotheses, (iii) extrapolation of effects of factors beyond the range of conditions covered experimentally, (iv) revelation of knowledge gaps and 'guiding' research and (v) to support practical management decisions (input of resources, climate control in greenhouses, planning of processes).

Nowadays, at least five generic PBMs (J. R. Williams *et al.*, 1989; van Diepen *et al.*, 1989; Brisson *et al.*, 1998; Jones *et al.*, 2003; Keating *et al.*, 2003) and around 32 specific crop PBMs are available for end users. Besides, some crops have several specific PBMs (e.g. wheat has 27 available models) representing different modelling approaches or options to include crop and management specificities for growth and development simulation. In addition, it has

recently been found that PBM ensembles to reduce the uncertainty of predictions for a number of crops (Tebaldi *et al.*, 2007; Asseng, 2013; Rosenzweig *et al.*, 2013; Marin *et al.*, 2015; Martre *et al.*, 2015; Maiorano *et al.*, 2016; Battisti, Sentelhas and Boote, 2017; Dias and Sentelhas, 2017). Although the reasons for this are still unclear, there is now clear evidence that the development of new crop models can improve long-term time-space simulations, esp. in the context of climate change issues. Several PBMs have been developed for sugarcane (Keating *et al.*, 1999; Singels and Donaldson, 2000; Liu and Bull, 2001; J.F. and Todoroff, 2002; Villegas *et al.*, 2005; Singels, Jones and Berg, 2008). However, in contrast to other crops, only two of these models are fully available for end users: DSSAT-CANEGRO and the APSIM-Sugar. Both have been extensively used and tested for sugarcane crops worldwide (Inman-Bamber, Muchow and Robertson, 2002; Inman-Bamber and McGlinchey, 2003; Knox *et al.*, 2010; Singels *et al.*, 2014; Everingham *et al.*, 2015), including in Brazil (Marin *et al.*, 2011, 2013, 2015; Costa *et al.*, 2014; Vianna and Sentelhas, 2014, 2015). Because of the heuristic character of modelling and due to the specific features of sugarcane farming systems in Brazil, Marin & Jones (2014) presented a standalone sugarcane PBM (SAMUCA - *Agronomic Modular Simulator for Sugarcane*). Marin et al. (2017) applied the SAMUCA model for stochastic simulation of sugarcane production and uncertainty analysis. In these publications, the authors verified the need for improving soil-water balance routines to better represent crop growth and water use under rainfed and irrigated conditions. In addition, widely used and tested PBMs for sugarcane, such as CANEGRO and APSIM-Sugar, are embedded in robust crop modelling platforms and including some of these features (i.e. soil mulch cover and soil water balance) to the SAMUCA model structure could reduce its simulation uncertainties, improving its ability to support decision making (Marin, 2017) and to assess climate change impacts on sugarcane (Stokes *et al.*, 2016).

The components commonly simulated in PBM are leaves, stems, roots and reproductive or storage organs (state variables), of which attributes are expressed as quantities (i.e. weight, surface area, N content) per unit area of soil surface (van Ittersum K *et al.*, 2003; Vos *et al.*, 2010). Despite of the remarkable advances in crop production and the enormous contribution that PBMs have made to crop system analysis, there is still room for further refinement of models to include processes involving plant structures and organ level (Vos, Marcelis and Evers, 2007). Besides this, in contrast to other crops, all aerial parts of the sugarcane crop are harvested, and a considerably high amount of biomass (around 75 t ha^{-1} in Brazil, FAO (2016)) is processed for sugar and ethanol production, increasing the importance of its structural composition (sugars and fibre). Moreover, different row spacings have been adopted to decrease damage to plants and soil structure from harvest equipment, although potentially effecting the tillering process and productivity due to increased shading (Singels and Smit, 2009; Wang *et al.*, 2017). Yet, recently, efforts have been made to better understand the process of sucrose accumulation and feedback responses of sucrose in whole plant net photosynthesis (Mccormick, Cramer and Watt, 2006; Inman-Bamber *et al.*, 2009; R. V Ribeiro *et al.*, 2017; Verma *et al.*, 2017). Hence an FSPM for sugarcane might be a promising tool to support scientific studies and to quantitatively test hypotheses on the sucrose accumulation process (Uys *et al.*, 2007; Wang *et al.*, 2013) and source-sink relations on the whole plant level (Mccormick, Cramer and Watt, 2006), with the aim to improve tillering process simulation (Singels and Smit, 2009), optimize row spacing arrangements (Wang *et al.*, 2017) and evaluate intercropping options for sugarcane farming systems (Li, Mu and Cheng, 2013).

In the last two decades, computational advances on graphical processing units (GPUs), ray-tracking algorithms and extensible languages have enabled plant processes and structures to be simultaneously simulated under a three-dimensional approach, the so-called "Functional-Structural Plant Models" (FSPM) (Vos *et al.*, 2010). In such an approach, modelers explicitly describe plant growth and development over time by physiological rules of creation (Prusinkiewicz and Lindenmayer, 2012) and by modifying three-dimensional (3D) plant structures depending on

environmental factors (Vos *et al.*, 2010). The ray-tracking algorithms are able to precisely simulate light intensity and quality distribution of each structure (leaves, petioles, stems, axillary buds) within plant canopies, considering optical properties (Hemmerling *et al.*, 2008; De Visser *et al.*, 2012; Henke and Buck-sorlin, 2015). During the last decade, FSPM has been largely used in studies of light-dependent processes such as intercropping, planting row arrangements, tillering process, organ source-sink relations and sugar translocation, as well as greenhouse light optimisation (Evers *et al.*, 2007; Xu *et al.*, 2010; Dejong *et al.*, 2011; De Visser, Buck-Sorlin and Van Der Heijden, 2014; Mao *et al.*, 2016).

Based on the exposed rational, this dissertation tested the following hypotheses: (i) It is possible to develop a sugarcane process-based model adapted to Brazilian farming systems to support improved decisions for the private and public stakeholders in the sugarcane sector; (ii) simulation uncertainties could be reduced by including robust soil-water balance subroutines in a sugarcane model; (iii) a Functional Structural Plant Modelling framework for sugarcane can benefit future studies on sucrose accumulation, tillering and breeding programs.

1.1. OBJECTIVES

Based on the hypotheses presented above, the overall objective of this study was to develop, calibrate and evaluate different crop modelling approaches for Brazilian sugarcane farming systems, considering water management, climate change impacts, and canopy structure for improving the support on decisions for the sugarcane sector and contributing to the development of a Brazilian platform for crop simulations.

1.1.1. Specific objectives

This objective, in turn, can be subdivided into specific objectives, as follows:

i) To improve the structure of a sugarcane process-based model for the Brazilian farming systems, with focus on new and improved algorithms for water consumption, mulch cover effect and crop growth and development;

ii) to couple a robust agrohydrological model to a sugarcane process-based crop model in order to reduce crop and water simulation uncertainties;

iii) to develop new algorithms to describe the tillering process, light-interception, sucrose accumulation and carbohydrate partitioning based on the Functional-Structural Plant Model (FSPM) approach;

iv) to calibrate and evaluate the performance of each modelling methodology based on collected field experiment datasets and under different soil and climatic conditions in Brazil.

REFERENCES

ASSENG, S. Uncertainty in simulating wheat yields under climate change. **Nature Climate Change**, v. 3, n. 9, p. 627–632, 2013.

BATTISTI, R.; SENTELHAS, P. C.; BOOTE, K. J. Inter-comparison of performance of soybean crop simulation models and their ensemble in southern Brazil. **Field Crops Research**, v. 200, p. 28–37, 2017.

BRISSON, N. *et al.* STICS: a generic model for the simulation of crops and their water and nitrogen balances. I. Theory and parameterization applied to wheat and corn. **Agronomie**, v. 18, n. 5–6, p. 311–346, 1998.

COSTA, L. G.; MARIN, F. R.; NASSIF, D. S. P.; PINTO, H. M. S.; LOPES-ASSAD, M. L. R. C. Simulação do efeito do manejo da palha e do nitrogênio na produtividade da cana-de-açúcar. **Revista Brasileira de Engenharia Agrícola e Ambiental**, v. 18, n. 5, p. 469–474, 2014.

DEJONG, T. M.; SILVA, D. DA; VOS, J.; ESCOBAR-GUTIRREZ, A. J. Using functionalstructural plant models to study, understand and integrate plant development and ecophysiology. **Annals of Botany**, v. 108, n. 6, p. 987–989, 2011.

DIAS, H. B.; SENTELHAS, P. C. Evaluation of three sugarcane simulation models and their ensemble for yield estimation in commercially managed fields. **Field Crops Research**, v. 213, p. 174–185, 2017.

DIEPEN, C. A. VAN; WOLF, J.; KEULEN, H. VAN; RAPPOLDT, C. WOFOST: a Simulation Model of Crop Production. **Soil Use and Management**, v. 5, n. 1, p. 16–24, 1989.

EPE. **Balanço Energético NacionalNational Report**. [s.l: s.n.]. Available at: <https://ben.epe.gov.br/>. Last time accessed: 10 out. 2016.

EVERINGHAM, Y.; INMAN-BAMBER, G.; SEXTON, J.; STOKES, C. A Dual Ensemble Agroclimate Modelling Procedure to Assess Climate Change Impacts on Sugarcane Production in Australia. **Agricultural Sciences**, n. August, p. 870–888, 2015.

EVERS, J. B.; VOS, J.; CHELLE, M.; ANDRIEU, B.; FOURNIER, C.; STRUIK, P. C. Simulating the effects of localized red: far-red ratio on tillering in spring wheat (Triticum aestivum) using a three-dimensional virtual plant model. **New Phytologist**, v. 176, n. 2, p. 325–336, 2007.

FAO. **FAOSTAT DataBase**. Available at: <http://faostat.fao.org/>. Last time accessed: 10 out. 2016.

FORTUNATO, F. M.; VIEIRA, A. L.; GOMES NETO, J. A.; DONATI, G. L.; JONES, B. T. Expanding the potentialities of standard dilution analysis: Determination of ethanol in gasoline by Raman spectroscopy. **Microchemical Journal**, v. 133, p. 76–80, 2017.

HEMMERLING, R.; KNIEMEYER, O.; LANWERT, D.; KURTH, W.; BUCK-SORLIN, G. The rule-based language XL and the modelling environment GroIMP illustrated with simulated tree competition. **Functional Plant Biology**, v. 35, n. 10, p. 739–750, 2008.

HENKE, M.; BUCK-SORLIN, G. Advanced light modelling with GroIMP Table of Contents Introduction. 2015.

INMAN-BAMBER, N. G.; BONNETT, G. D.; SPILLMAN, M. F.; HEWITT, M. L.; XU, J. Source--sink differences in genotypes and water regimes influencing sucrose accumulation in sugarcane stalks. **Crop and Pasture Science**, v. 60, n. 4, p. 316–327, 2009.

INMAN-BAMBER, N. G.; MCGLINCHEY, M. G. Crop coefficients and water-use estimates for sugarcane based on long-term bowen ratio energy balance measurements. **Field Crops Research**, v. 83, n. 2, p. 125–138, 2003.

INMAN-BAMBER, N. G.; MUCHOW, R. C.; ROBERTSON, M. J. Dry matter partitioning of sugarcane in Australia and South Africa. **Field Crops Research**, v. 76, n. 1, p. 71–84, 2002.

ITTERSUM K, M. VAN; LEFFELAAR, P. A.; KEULEN, H. VAN; KROPFF, M. J.; BASTIAANS, L.; GOUDRIAAN, J. On approaches and applications of the Wageningen crop models. **European Journal of Agronomy**, v. 18, p. 201–234, 2003.

J. R. WILLIAMS, J. R.; C. A. JONES, C. A.; J. R. KINIRY, J. R.; D. A. SPANEL, D. A. The EPIC Crop Growth Model. **Transactions of the ASAE**, v. 32, n. 2, p. 0497–0511, 1989.

J.F., M.; TODOROFF, P. **Le modèle de croissance mosicas et sa plateforme de simulation simulex: état des lieux et perspectives**Congrès de la Sociéte de technologie agricole et sucrière de Maurice. **Anais**...2002Available at: <http://publications.cirad.fr/en/une_notice.php?dk=519377>

JONES, J. W.; HOOGENBOOM, G.; PORTER, C. H.; BOOTE, K. J.; BATCHELOR, W. D.; HUNT, L. A.; WILKENS, P. W.; SINGH, U.; GIJSMAN, A. J.; RITCHIE, J. T. **The DSSAT cropping system model**. [s.l: s.n.]. v. 18

KEATING, B. A. *et al.* An overview of APSIM, a model designed for farming systems simulation. **European Journal of Agronomy**, v. 18, n. 3–4, p. 267–288, 2003.

KEATING, B. A.; ROBERTSON, M. J.; MUCHOW, R. C.; HUTH, N. I. Modelling sugarcane production systems I. Development and performance of the sugarcane module. **Field Crops Research**, v. 61, n. 3, p. 253–271, 1999.

KNOX, J. W.; RODR??GUEZ D??AZ, J. A.; NIXON, D. J.; MKHWANAZI, M. A preliminary assessment of climate change impacts on sugarcane in Swaziland. **Agricultural Systems**, v. 103, n. 2, p. 63–72, 2010.

LI, X.; MU, Y.; CHENG, Y. Effects of intercropping sugarcane and soybean on growth , rhizosphere soil microbes , nitrogen and phosphorus availability. **Acta Physiologiae Plantarum**, v. 35, p. 1113–1119, 2013.

LIU, D. L.; BULL, T. A. Simulation of biomass and sugar accumulation in sugarcane using a process-based model. v. 144, p. 181–211, 2001.

MAIORANO, A. *et al.* Crop model improvement reduces the uncertainty of the response to temperature of multi-model ensembles. **Field Crops Research**, p. 1–16, 2016.

MAO, L.; ZHANG, L.; EVERS, J. B.; HENKE, M.; WERF, W. VAN DER; LIU, S.; ZHANG, S.; ZHAO, X.; WANG, B.; LI, Z. Identification of plant configurations maximizing radiation capture in relay strip cotton using a functional-structural plant model. **Field Crops Research**, v. 187, p. 1–11, 2016.

MARIN, F. R. **Tempocampo: A System for Operational Forecasting of Brazilian Sugarcane and Soybean Yield**MANAGING GLOBAL RESOURCES FOR A SECURE FUTURE (Annual Meeting). **Anais**...Tampa: ASA, CSSA, SSSA, 2017

MARIN, F. R.; JONES, J. W.; ROYCE, F.; SUGUITANI, C.; DONZELI, J. L.; FILHO, W. J. P.; NASSIF, D. S. P. Parameterization and evaluation of predictions of DSSAT/CANEGRO for Brazilian sugarcane. **Agronomy Journal**, v. 103, n. 2, p. 304–315, 2011.

MARIN, F. R.; JONES, J. W.; SINGELS, A.; ROYCE, F.; ASSAD, E. D.; PELLEGRINO, G. Q.; JUSTINO, F. Climate change impacts on sugarcane attainable yield in southern Brazil. **Climatic Change**, v. 117, n. 1–2, p. 227–239, 2013.

MARIN, F. R.; THORBURN, P. J.; NASSIF, D. S. P.; COSTA, L. G. Sugarcane model intercomparison: Structural differences and uncertainties under current and potential future climates. **Environmental Modelling & Software**, v. 72, p. 372–386, 2015.

MARIN, R. Understanding sugarcane production , biofuels , and market volatility in Brazil — A research perspective. v. 45, n. 2, p. 75–77, 2016.

MARTRE, P. *et al.* Multimodel ensembles of wheat growth: Many models are better than one. **Global Change Biology**, v. 21, n. 2, p. 911–925, 2015.

MCCORMICK, A. J.; CRAMER, M. D.; WATT, D. A. Sink strength regulates photosynthesis in sugarcane. 2006.

MOORE, P. H.; BOTHA, F. C. **Sugarcane: physiology, biochemistry and functional biology**. [s.l.] John Wiley & Sons, 2013.

PASSIOURA, J. B.; PASSIOURA, J. B. Simulation models: science, snake oil, education, or engineering? **Agronomy Journal**, v. 88, n. 5, p. 690–694, 1996.

PRUSINKIEWICZ, P.; LINDENMAYER, A. **The algorithmic beauty of plants**. [s.l.] Springer Science & Business Media, 2012.

RAES, D.; STEDUTO, P.; HSIAO, T. C.; FERERES, E. Aquacrop-The FAO crop model to simulate yield response to water: II. main algorithms and software description. **Agronomy Journal**, v. 101, n. 3, p. 438–447, 2009.

RIBEIRO, R. V; MACHADO, E. C.; MAGALHÃES FILHO, J. R.; LOBO, A. K. M.; MARTINS, M. O.; SILVEIRA, J. A. G.; YIN, X.; STRUIK, P. C. Increased sink strength offsets the inhibitory effect of sucrose on sugarcane photosynthesis. **Journal of plant physiology**, v. 208, p. 61–69, 2017.

ROSENZWEIG, C. *et al.* The Agricultural Model Intercomparison and Improvement Project (AgMIP): Protocols and pilot studies. **Agricultural and Forest Meteorology**, v. 170, p. 166–182, 2013.

RUDORFF, B. F. T.; AGUIAR, D. A. DE; SILVA, W. F. DA; SUGAWARA, L. M.; ADAMI, M.; MOREIRA, M. A. Studies on the rapid expansion of sugarcane for ethanol production in S??o Paulo state (Brazil) using Landsat data. **Remote Sensing**, v. 2, n. 4, p. 1057–1076, 2010.

SAGE, R. F.; PEIXOTO, M. M.; SAGE, T. L. Photosynthesis in Sugarcane. **Sugarcane: Physiology, Biochemistry, and Functional Biology**, n. DECEMBER, p. 121–154, 2013.

SCARPARE, F. V.; HERNANDES, T. A. D.; RUIZ-CORRÊA, S. T.; PICOLI, M. C. A.; SCANLON, B. R. .; CHAGAS, M. F.; DUFT, D. G.; CARDOSO, T. DE F. Sugarcane land use and water resources assessment in the expansion area in Brazil. **Journal of Cleaner Production**, v. 133, p. 1318–1327, 2016.

SCHEITERLE, L.; ULMER, A.; BIRNER, R.; PYKA, A. From Commodity-Based Value Chains to Biomass-Based Value Webs: The Case of Sugarcane in Brazil's Bioeconomy. **Journal of Cleaner Production**, 2017.

SINCLAIR, T. R.; SELIGMAN, N. G. Crop modeling: from infancy to maturity. **Agronomy Journal**, v. 88, n. 5, p. 698–704, 1996.

SINGELS, A.; DONALDSON, R. A. A simple model of unstressed sugarcane canopy development. **Proceedings of the South African Sugar Technologists' Association**, v. 74, p. 151–154, 2000.

SINGELS, A.; JONES, M.; BERG, M. VAN DEN. DSSAT v4. 5 Canegro sugarcane plant module: scientific documentation. **South African Sugarcane Research Inst. Mount …**, p. 1–34, 2008.

SINGELS, A.; JONES, M.; MARIN, F. R.; RUANE, A.; THORBURN, P. Predicting Climate Change Impacts on Sugarcane Production at Sites in Australia, Brazil and South Africa Using the Canegro Model. **Sugar Tech**, v. 16, n. 4, p. 347–355, 2014.

SINGELS, A.; SMIT, M. A. Sugarcane response to row spacing-induced competition for light. **Field Crops Research**, v. 113, n. 2, p. 149–155, 2009.

STOCKER, T. F.; QIN, D.; PLATTNER, G.-K.; TIGNOR, M.; ALLEN, S. K.; BOSCHUNG, J.; NAUELS, A.; XIA, Y.; BEX, V.; MIDGLEY, P. M.; OTHERS. Climate change 2013: The physical science basis. **Intergovernmental Panel on Climate Change, Working Group I Contribution to the IPCC Fifth Assessment Report (AR5)(Cambridge Univ Press, New York)**, 2013.

STOKES, C. J.; INMAN-BAMBER, N. G.; EVERINGHAM, Y. L.; SEXTON, J. Measuring and modelling CO2 effects on sugarcane. **Environmental Modelling and Software**, v. 78, p. 68–78, 2016.

TAPIA CARPIO, L. G.; SIMONE DE SOUZA, F. Optimal allocation of sugarcane bagasse for producing bioelectricity and second generation ethanol in Brazil: Scenarios of cost reductions. **Renewable Energy**, v. 111, 2017.

TEBALDI, C. *et al.* The use of the multi-model ensemble in probabilistic climate projections. **Philosophical transactions. Series A, Mathematical, physical, and engineering sciences**, v. 365, n. 1857, p. 2053–75, 2007.

UYS, L.; BOTHA, F. C.; HOFMEYR, J. S.; ROHWER, J. M. Kinetic model of sucrose accumulation in maturing sugarcane culm tissue. v. 68, p. 2375–2392, 2007.

VERMA, I.; ROOPENDRA, K.; SHARMA, A.; JAIN, R.; SINGH, R. K.; CHANDRA, A. Expression analysis of genes associated with sucrose accumulation in sugarcane under normal and GA3-induced source--sink perturbed conditions. **Acta Physiologiae Plantarum**, v. 39, n. 6, p. 133, 2017.

VIANNA, M.; SENTELHAS, P. C. Performance of DSSAT CSM-CANEGRO Under Operational Conditions and its Use in Determining the "Saving Irrigation" Impact on Sugarcane Crop. **Sugar Tech**, v. 18, n. 1, p. 75–86, 2015.

VIANNA, S.; SENTELHAS, C. Risco de deficit hídrico para a cultura da cana - de - açúcar em diferentes regiões brasileiras. **Pesquisa Agropecuária Brasileira** n. 1, p. 1–10, 2014.

VILLEGAS, F. D.; HALL, F. R.; BOX, P. O.; JONES, J. W.; HALL, F. R.; BOX, P. O.; ROYCE, F. S.; HALL, F. R.; BOX, P. O. CASUPRO : An industry-driven sugarcane model. **South African Sugarcane Research Inst. Mount** v. 300, n. 5, 2005.

VISSER, P. H. B. DE; BUCK-SORLIN, G. H.; HEIJDEN, G. VAN DER; MARCELIS, L. F. M. **A 3D model of illumination, light distribution and crop photosynthesis to simulate lighting strategies in greenhouses** VII International Symposium on Light in Horticultural Systems 956. **Anais**...2012

VISSER, P. H. B. DE; BUCK-SORLIN, G. H.; HEIJDEN, G. W. A. M. VAN DER. Optimizing illumination in the greenhouse using a 3D model of tomato and a ray tracer. **Frontiers in plant science**, v. 5, 2014.

VOS, J.; EVERS, J. B.; BUCK-SORLIN, G. H.; ANDRIEU, B.; CHELLE, M.; VISSER, P. H. B. DE. Functional-structural plant modelling: A new versatile tool in crop science. **Journal of Experimental Botany**, v. 61, n. 8, p. 2101–2115, 2010.

VOS, J.; MARCELIS, L. F. M.; EVERS, J. B. CHAPTER 1 FUNCTIONAL-STRUCTURAL PLANT MODELLING IN. *In*: **FunctionalStructural Plant Modelling in Crop Production**. [s.l.] Springer, 2007. p. 1–12.

WALTER, A.; GALDOS, M. V.; SCARPARE, F. V.; LEAL, M. R. L. V.; SEABRA, J. E. A.; CUNHA, M. P. DA; PICOLI, M. C. A.; OLIVEIRA, C. O. F. DE. Brazilian sugarcane ethanol: Developments so far and challenges for the future. **Wiley Interdisciplinary Reviews: Energy and Environment**, v. 3, n. 1, p. 70–92, 2014.

WANG, J.; NAYAK, S.; KOCH, K.; MING, R. Carbon partitioning in sugarcane (Saccharum species). **Frontiers in Plant Science**, v. 4, n. June, p. 2005–2010, 2013.

WANG, Y.; SONG, Q.; JAISWAL, D.; P. DE SOUZA, A.; LONG, S. P.; ZHU, X. G. Development of a Three-Dimensional Ray-Tracing Model of Sugarcane Canopy Photosynthesis and Its Application in Assessing Impacts of Varied Row Spacing. **Bioenergy Research**, p. 1–9, 2017.

XU, L.; HENKE, M.; ZHU, J.; KURTH, W.; BUCK-SORLIN, G. A rule-based functional-structural model of rice considering source and sink functions. **Plant Growth Modeling, Simulation, Visualization and Applications, Proceedings - PMA09**, p. 245–252, 2010.

2. AGRONOMIC MODULAR SIMULATOR FOR SUGARCANE (SAMUCA): SCIENTIFIC MODEL OVERVIEW, IMPROVEMENTS AND EVALUATION FOR BRAZILIAN CONDITIONS

ABSTRACT

Sugarcane is the main source of sugar and the second largest source of biofuel in the world. Since the 1980s, Brazil has been the largest sugarcane-producing nation, accounting for half of the global production. Ethanol and biomass correspond to more than 15% of the national energy source and have been used as feedstock for the paper and plastic industry. Nevertheless, the commercial Brazilian sugarcane yield has reached a plateau of around 75 t ha^{-1}, and to meet the increasing demand for sugar and ethanol, the crop has strongly expanded towards the central-western region, where irrigation is mandatory to offset water stress. The effects of crop management, land use change, climate variability and the economy on crop production and associated quantities can and have been assessed by using crop process-based models (PBM). In contrast to other crops, however, sugarcane has only two PBMs available for end users (DSSAT-CANEGRO and APSIM-Sugar), and further modifications of these models are required to better assess and support sustainable sugarcane production in Brazil. Therefore, this study aimed to develop, calibrate and evaluate a sugarcane PBM (SAMUCA), with focus on soil-water balance, including the mulch cover and its effects on crop growth and development. Therefore, a new version of the SAMUCA model was developed to operate at phytomer level, focusing on soil mulch effects on crop growth and development, tillering process under competition for light and sucrose accumulation based on source-sink relations. The model was embedded into a modular platform dedicated to simulating the soil-plant-atmosphere and the management of the sugarcane farm system. A calibration routine in R environment was implemented to optimise the model parameters, and its performance was determined for long-term experiments and for different Brazilian conditions. The overall performance of the new version of SAMUCA under long-term experiments and in different Brazilian conditions was satisfactory, and the agreement indices were close to those of other widely used sugarcane crop models (CANEGRO and APSIM-Sugar). In addition, the modulated crop simulation platform could be used to host more crop models and integrate new features of Brazilian farming systems, thereby supporting decision making and crop system analysis.

Keywords: *Saccharum officinarum* L.; Crop modelling; Process based crop model; Modelling platform

2.1. INTRODUCTION

Sugarcane crop is the main source of sugar in the world, with significant social, economic and environmental importance in many tropical countries. Compared to other crops, it is the 6st most economically significant and the 2nd most important C4 species after maize (FAO, 2016). Globally, more than 70% of sugarcane are produced in Brazil, India, China, Thailand and Pakistan, with Brazil being the largest producer (50% of the global production); sugarcane is also used for the production of ethanol ("*flexfuel*" vehicles) and biomass energy (electricity and heating) (Walter *et al.*, 2014). Sugarcane covers an area of about 8.8 million hectares in Brazil, with a total average production of 645 million tons per year. The state of São Paulo in Southern Brazil accounts for 50% of the national production, where the crop is mainly managed under rainfed conditions (CONAB, 2017).

Nevertheless, commercial sugarcane yield has reached a plateau of around 75 t ha^{-1}, and in order to meet the increasing demand for sugar and ethanol, sugarcane areas have been expanding at the rate of 1 hectare per minute

over the last 10 years (Vianna and Sentelhas, 2015; F. V. Scarpare *et al.*, 2016) towards marginal areas in the central-western region of the country (area of the original Cerrado biome). In these areas, sugarcane production is confronted with new challenges, mainly related to climate restrictions in the states of Goiás, Mato Grosso, Mato Grosso do Sul, Minas Gerais and Tocantins, whereas intense water deficits throughout the year substantially reduce yields and increase plant mortality (Loarie *et al.*, 2011; Vianna and Sentelhas, 2014). In addition, the last decade, mechanisation and non-burning (green cane) harvesting systems, employed in practically all Brazilian sugarcane fields, have resulted in the maintenance of a layer of residue on the soil, the so-called "mulch cover".

Mulch cover management contributes to the cycling of soil nutrients (Oliveira *et al.*, 2000; Van Antwerpen *et al.*, 2002), the preservation of soil structure and physical and chemical properties (Graham, Haynes and Meyer, 2002) and can be related to a significant reduction of pests, diseases and weeds (Azania *et al.*, 2002; Araújo *et al.*, 2005) as well as to indirect yield increase (Gava *et al.*, 2001; Kingston, 2013). Nonetheless, one of the most important effects is the maintenance of soil moisture by the reduction of evaporation, reaching a reduction of up to 200 mm per year (Denmead, Mayocchi and Dunin, 1997; Thorburn *et al.*, 1999; Olivier and Singels, 2012). Despite the benefits of the mulch cover in terms of soil health and water savings, new technologies of electricity and second-generation ethanol production (Dias *et al.*, 2011) from crop residue have raised the questions of the optimal point between mulch cover and energy production from crop residues.

To support decision making on where and how the crop should expand and be managed in a sustainable way, understanding crop responses to water deficit is mandatory. In this context, process-based models (PBM) integrate soil, plant, atmosphere and management responses, considering physical and biological processes at field level. More than five generic PBMs (J. R. Williams *et al.*, 1989; van Diepen *et al.*, 1989; Brisson *et al.*, 1998; Jones *et al.*, 2003; Keating *et al.*, 2003) and around 32 specific crop PBMs are available for end users. Besides, some crops have several specific PBMs, i.e. wheat with 27 available models, representing different modelling approaches or options to include crop and management specificities. In addition, the use of PBM ensembles reduces the uncertainty of predictions for many crops (Tebaldi *et al.*, 2007; Asseng, 2013; Marin *et al.*, 2015; Martre *et al.*, 2015; Battisti, Sentelhas and Boote, 2017; Dias and Sentelhas, 2017). However, the reason for that is still unclear, mainly because the specificity of each model and the complexity of simulated interactions and strategies on how to overcome possible impacts remain uncertain.

Several PBMs for sugarcane have been developed and are described in the literature (Keating *et al.*, 1999; Singels and Donaldson, 2000; Liu and Bull, 2001; J.F. and Todoroff, 2002; Villegas *et al.*, 2005; Singels, Jones and Berg, 2008). However, in contrast to other crops, only two of these are available for end users, namely the DSSAT-CANEGRO model and the APSIM-Sugar model. Both have been extensively used and tested in sugarcane studies worldwide (Inman-Bamber, Muchow and Robertson, 2002; Inman-Bamber and McGlinchey, 2003; Knox *et al.*, 2010; Singels *et al.*, 2014; Everingham *et al.*, 2015), including Brazil (Marin *et al.*, 2011, 2013, 2015; Costa *et al.*, 2014; Vianna and Sentelhas, 2014, 2015). Because of the heuristic character of modelling and the specific features of sugarcane farming systems in Brazil, such as mulch cover management, tropical soil characteristics and compaction due to heavy machinery and green-cane harvesting, Marin & Jones (2014) presented a standalone sugarcane PBM (SAMUCA - *Agronomic Modular Simulator for Sugarcane*). Marin et al. (2017) applied the SAMUCA model for stochastic simulation of sugarcane production and uncertainty analysis. In these publications, the authors verified the need for improved soil-water balance routines to better represent crop growth and water use under rainfed and irrigated conditions. In addition, widely used and tested PBMs for sugarcane, such as CANEGRO and APSIM-Sugar, are embedded in robust crop modelling platforms, and including some of these features (i.e. soil mulch cover and soil-water balance) into the

SAMUCA model structure could reduce its simulation uncertainties, improving its ability to support decision making (Marin, 2017) and to assess climate change impacts in sugarcane (Stokes *et al.*, 2016).

Generally, a crop PBM operates in a modular form, and algorithms are organized as subroutines responsible for the computation of processes inherent to the simulated system (Jones *et al.*, 2003; Keating *et al.*, 2003; van Ittersum K *et al.*, 2003). As an example, a growth subroutine (biomass gain) would include the equations representing the photosynthetic processes; in another sub-routine, partitioning would the use the results of the growth routine to simulate the partitioning of assimilated carbohydrates between tissue culture, and so on. systemin agricultural systems, it is often necessary to subdivide subroutines for soil, plant and the atmosphere, where each module will have its sub-modules, responsible for the calculation of each process. This is the concept of the modelling platform, which allows to maintain the organisational level of the equations and approaches within the model, besides facilitating the interface between the modules and the implementation of new algorithms or even couplings among models (van Ittersum K *et al.*, 2003; Jones, 2013). In addition to the structural scope, all modules must be compatible with the time-step of the processes to be simulated, thus determining the functions of rate of change and integration of state variables. Although several models are available for the simulation of sugarcane growth, only APSIM-Sugar (Keating et al., 1999) and DSSAT-CANEGRO (Inman-bamber, 1991; Singels et al., 2008) are actually available to end users (Marin et al., 2015). To obtain the heuristic benefits of developing a new model as well as to reduce the uncertainty in simulations (Asseng et al., 2013), Marin and Jones (2014) proposed a new, simple sugarcane model evaluated for several Brazilians regions. This structure, however, requires the development of new algorithms and improvements, with a focus on two aspects: soil-water balance and trash cover effects in crop development.

Therefore, the aims of this study were: (i) to improve a structure of dynamic sugarcane growth for Brazilian conditions; (ii) to develop the model with new algorithms related to the water consumption of a sugarcane field experiment, considering the mulch cover effect; (iii) to develop, based on the literature, processes involved in the response of sugarcane to different concentrations of atmospheric CO_2; (iv) to develop, based on literature and experimental data, processes involved in the differentiation of growth between planted cane and ratooned cane; and (v) to calibrate the new model and evaluate its performance in simulating the components of sugarcane under different soil and climatic conditions, based on experimental data previously collected with the same variety in five Brazilian locations.

2.2. MATERIAL AND METHODS

2.2.1. Modelling structure and information flow

The new version of the SAMUCA model proposed here operates at daily and hourly time-steps and is organised in modular subroutines. The model was embedded in a platform shell implemented to be compatible with further crop models to be included in the future. The SAMUCA model operates following a typical logical sequence for the simulation, with the following steps: (1) reading and initialisation of the state variables, (2) potential and actual crop daily rate calculation and (3) integration, which is replicated for almost all subroutines within the platform and changes as the simulation triggers are actioned (i.e. planting or harvesting dates) (Figure 1). Hierarchically, the modulation shell is subdivided in a control subroutine, responsible to read and organise all control files and simulations, thereby controlling the sub-modules Soil, Plant and Atmosphere. The Soil subroutine is responsible for the soil-water balance, soil temperature and operations (i.e. mulch cover); the Plant subroutine contains the crop model for

simulations, i.e. SAMUCA; the Atmosphere subroutine is responsible for astronomic calculation, evapotranspiration demand and air temperature simulations.

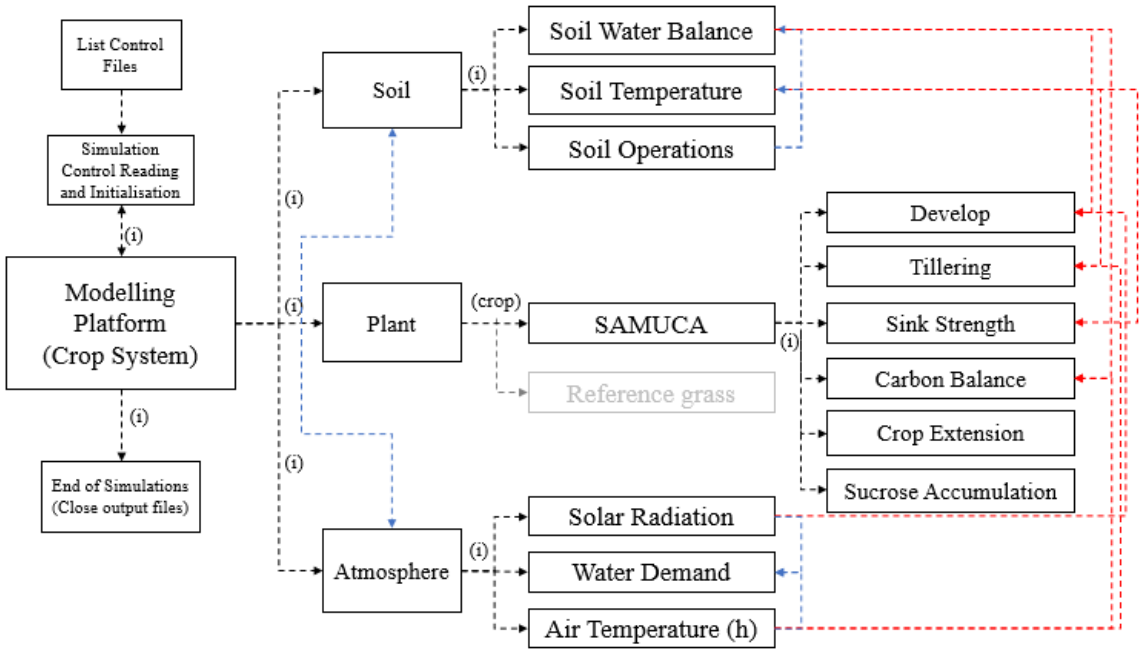

Figure 1. Information logical flowchart of SAMUCA and crop model shell showing the model subroutines and information flow through the simulation process

The complete simulation of SAMUCA, disregarding daily and hourly loops, contains 23 summarised steps by its main subroutines in Figure 1. The directory structure for simulation should contain a root folder containing the executable file (".exe") and the directories for crop parameters, weather input data, soil profile, simulation control files and output file folder ("C:\ ... \Crop ", "C:\ ... \Weather ","C:\ ... \Soil", "C:\ ... \Control" and "C:\ ... \ Output "). Simulation control files containing planting and harvest dates, simulation site, crop, soil type, field operation (mulch cover) and simulation options must be in the "Control" directory; files containing the soil, climate and crop characteristics must be within the "Soil", "Weather" and "Crop" directories, respectively; the "Output" directory is dedicated for storing the output files resulting from the simulations. The entire platform shell and subroutines were implemented through the Microsoft Visual Studio 2013 compiler in FORTRAN language, still one of the most efficient languages for mathematical calculations (Chapman, 2008).

Table 1. Main subroutines description and logical sequential order of a simulation in the new version of SAMUCA model and shell. Where i is the step task (i=1 initialization, 2 = state rate and 3 = integration)

Subroutine	(i)	Description
Runtime	1	Compute simulation initial time
Output	1	Open warning files
Readfile	1	Read list and control files (.sam)
TimeControl	1	Time control initialization
Readfile	2	Read simulation control operations and settings (.ctl)
Output	2	Open output files (.out)
Weather	1	Open weather files (.met)
SoilWat	1	Read soil parameters (.spd) file and initialization of soil water balance
soiltemp	1	Soil temperature initialization
soplat	1	Atmosphere state variables initialization
TimeControl	2	Time flag control and initialization of crop simulation
Plant	1	Read and initialize crop parameters (.crp) and state variables
Weather	2	Daily weather data reading
SoilWat	2	Soil water balance state/rate
SoilTemp	2	Soil temperature state/rate
Soplat	2	Atmospheric water demand state/rate
Plant	2	Potential and Actual crop state/rate
Plant	3	Potential and Actual Crop state integration
Soplat	3	Water use update and integration
SoilWat	3	Root water uptake update and soil water content rate integration
TimeControl	3	Time and flag control (field operations,for next day)
Output	3	Close output files
Runtime	2	Simulation final Time and duration

2.2.1.1. Soil

The new soil-water balance implemented operates the one-dimensional "tipping bucket" soil-water balance routine (Figure 2), which has been widely tested to calculate the amount of water available to the crop over longer periods of time, such as a season (Jones *et al.*, 2003; Keating *et al.*, 2003; van Ittersum K *et al.*, 2003). The soil profile is described by consecutive layers containing depth information (cm), saturation point, field capacity, wilting and saturation point ($cm^3\ cm^{-3}$) and hydraulic conductivity ($cm\ h^{-1}$), as stated previously (Ritchie, 1998; Jones *et al.*, 2003; Porter *et al.*, 2010). The daily changes in soil water content ($cm_{H2O}^3\ cm_{soil}^{-3}$) are computed in each soil layer due to rainfall and irrigation infiltration, drainage, soil evaporation and root water uptake (crop transpiration). Daily rainfall and gross irrigation values are used to compute surface runoff and infiltration by the Curve Number method (Boughton, 1989). Upward unsaturated flow is also computed using a conservative estimate of the soil water diffusivity and differences in the volumetric soil water content of adjacent layers (Ritchie, 1998). The water amount passing through soil layer is limited to underlying saturated hydraulic conductivity (*ksat*, parameter) and could be discharged to runoff (when top layer) or accumulated into the above soil layer up to its saturation capacity (Jones *et al.*, 2003).

In a broad view, this new version brings the following improvements compared with the original version of SAMUCA (Marin and Jones, 2014): (i) the possibility of including up to 30 soil layers; (ii) its approach has been widely tested on a daily scale, unlike the original Teh (2006) approach, implemented for a 5-day scale; and (iii) it already includes the effect of mulch cover on soil evaporation.

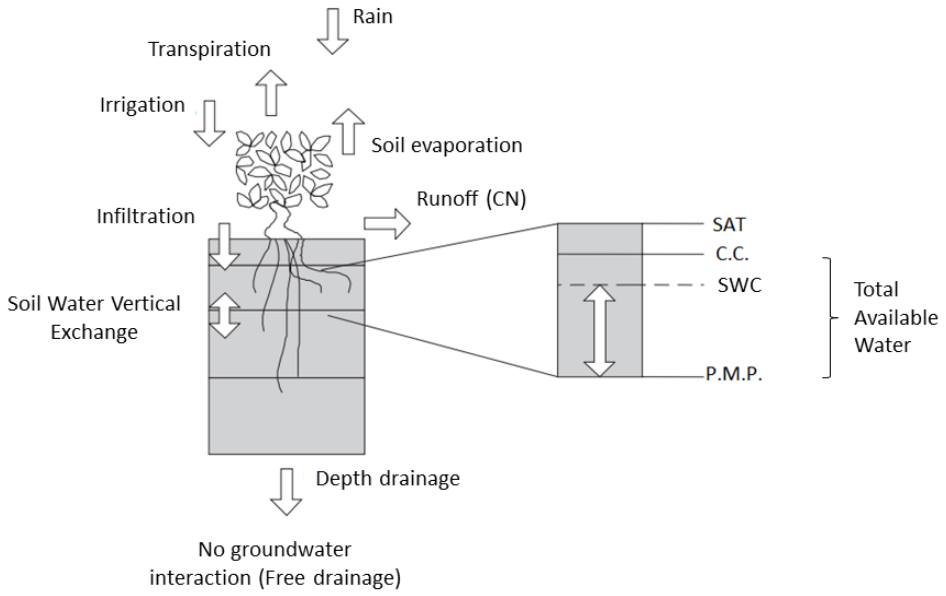

Figure 2. Schematic representation of the "tipping bucket" soil water balance routine implemented (Porter et al. 2010)

The soil temperature algorithm was developed based on the literature (Brown *et al.*, 2000; Kroes *et al.*, 2009; Monteith and Unsworth, 2012) and empirical evidences (Figure 19) collected during the field experiment (described in section 2.2.2.1 of this chapter) that soil mulch cover has an indirect effect on sugarcane tillering by reducing temperature. The differential equation for soil heat flow (Equation 1) is solved numerically by the Thomas algorithm (Muller, Normale and Lyon, 2006), following the SWAP model approach (Kroes *et al.*, 2009).

$$C_{heat}\ \frac{dT}{dt} = \frac{d\left(\lambda_{heat}\ \frac{dT}{dz}\right)}{dz} \quad (1)$$

where C_{heat} is soil heat capacity (J cm^{-3} °C^{-1}); dT is soil temperature variation (°C); dt is the time step (fraction of day); λ_{heat} is the soil thermal conductivity (J cm^{-1} °C^{-1} d^{-1}); dz is the nodal distance between soil layers (cm). Solid components of soil must by specified, and volumetric heat capacity is calculated as the weighted mean of the heat capacities of induvial components (Table 2). Water and air content are simulated during the crop season and have a strong influence on C_{heat} and λ_{heat}; an initial value of the soil temperature layer must also be provided to start the numerical procedure. When the mulch cover is added to the field, a top layer is added to the soil profile, with no sand, clay or organic matter content, and only a value of mulch volumetric saturation point is assumed (Equation 5). The lower mulch layer C_{heat} and λ_{heat} was expected to decrease the vertical heat flux to the soil surface, reducing overall soil temperature.

Table 2. Volumetric heat capacity and thermal conductivity for each soil mineral component (Kroes et al. 2009)

Component	Volumetric heat capacity (J cm^{-3} °C^{-1})	Thermal conductivity (J cm^{-1} °C^{-1} d^{-1})
Sand	2.128	7603
Clay	2.385	2523
Organic	2.496	216
Water	4.18	492
Air (20°C)	1.212	22

To solve the numerical system, the temperature below the last layer (bottom boundary) was analytically computed by a synodal equation, relating annual mean and amplitude temperature, soil depth and soil thermal diffusivity ($cm^2\ d^{-1}$) (Kroes *et al.*, 2009). Surface temperature was determined by Equation 2, as described by Monteith and Unsworth (2012). For the use of Equation 2, it was necessary to determine the energy balance (Rn) below the vegetative canopy, which was calculated by net short and longwave radiation, as proposed in FAO-56 (Allen, Luis, *et al.*, 1998). The shortwave balance computed at the soil surface level took into account the radiation transmitted through the canopy and the surface albedo (assuming mulch = 0.4, bare soil = 0.13). The heat diffusion resistance (rH) at ground level was obtained via Equation 2, using surface temperature data throughout the season. A curve representing the heat diffusion resistance (rH) at ground level was adjusted in relation to leaf area index data and used to estimate rH values during the simulations (Figure 3).

$$T_0 = T + \frac{(\gamma^* rH/\rho c_p)Rn}{\Delta + \gamma^*} - \frac{\{e_s(T) - e\}}{\Delta + \gamma^*} \qquad (2)$$

where To is the surface temperature (°C); T is the air temperature (°C); γ^* is the psychrometric constant (kPa $°C^{-1}$); rH is the heat diffusion resistance (s m^{-1}); ρ is the air density (kg m^{-3}); Cp is the air specific heat (kj kg^{-1} $°C^{-1}$); e_s and e are saturation and actual vapor pressure (kPa); Δ is the slope of air vapor pressure to temperature (kPa $°C^{-1}$).

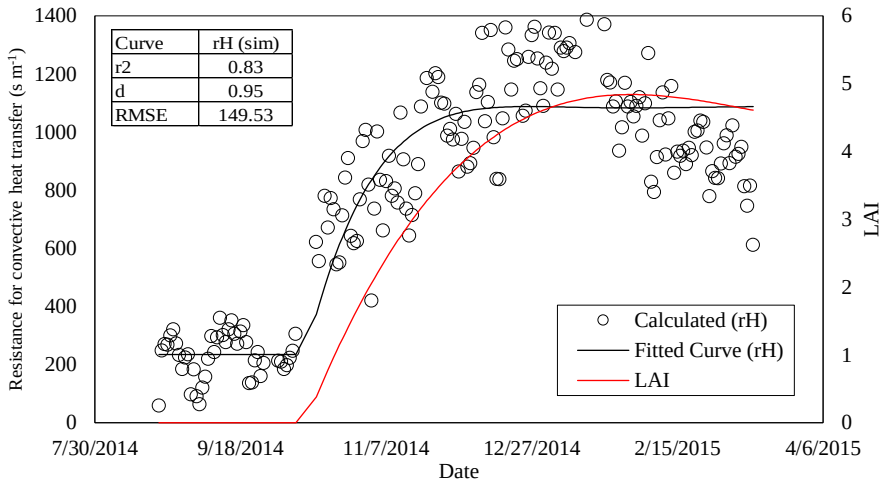

Figure 3. Heat resistance to vapor diffusion (rH) at the soil surface level obtained by equation 1 (circles), fitted curve (asymmetric asymptote, equation 13 modified to compute rH(LAI)) relating leaf area index (LAI) and rH (continuous line) and LAI over the cycle

2.2.1.2. Atmosphere

Potential evapotranspiration is simulated by a Penman-Monteith subroutine (Allen, Pereira, Raes and Martin Smith, 1998). The Priestley-Taylor (1972) method was also implanted in case of limited weather data, and additionally, reference evapotranspiration can be added as a weather input data. Crop potential evapotranspiration (EO, mm d^{-1}) is derived from the LAI, and reference evapotranspiration relation (EORATIO) is described by (Singels, Jones and Berg, 2008). Potential soil evaporation (EOS, mm d^{-1}) is then simulated as a fraction of EO, according to an exponential relation of LAI, similar to the previous version (Marin and Jones, 2014). Soil actual evaporation (ES, mm d^{-1}) is derived by the implementation of the SALUS evaporation method (Ritchie *et al.*, 2009), which represents

an empirical adaptation of a physically-based model using the diffusion theory to simulate second-stage soil evaporation and water redistribution (when swc <= fcp) (Suleiman and Ritchie, 2003b). Empirical coefficients are used regarding the soil profile status, which can be (i) wet, (ii) equilibrium and (iii) dry, to estimate a transfer coefficient (ES_{coef}, dimensionless) (Equation 3). The soil profile is considered wet when volumetric soil water content (SWC) of at least one soil layer in top 50 cm is greater than the field capacity point (FCP) and greater than a threshold for transference equilibrium. When the soil is in wet condition, but the SWC of the top layer is lower than the equilibrium threshold, the soil status is considered at equilibrium; a dry condition is assumed when all layers SWC are lower than FCP (Ritchie *et al.*, 2009). Daily soil evaporation is then integrated from all soil layers´ evaporation fractions (Equation 4).

$$ES_{coef(L)} = a_{z(i)}.meandep_{(L)}{}^{b_{z(i)}} \quad (3)$$

$$ES = \sum_{L=1}^{nsl}\left[max\left(0.,SWC_{(L)} - 0.3WPP_{(L)}\right)ES_{coef(L)}.Thick_{(L)}\right] \quad (4)$$

where $ES_{coef(L)}$ is the transfer coefficient (dimensionless) of layer (L); $a_{z(i)}$ and $b_{z(i)}$ are the empirical transfer coefficients (dimensionless) of layer (L) at wet, equilibrium or dry states (i) (Table 3); $meandep_{(L)}$ is the central depth point of the soil layer (cm); ES is the actual daily evaporation (cm d^{-1}); $SWC_{(L)}$ is the soil layer (L) water content (cm^3 cm^{-3}); $WPP_{(L)}$ is the wilting point of soil layer (L); $Thick_{(L)}$ is the thickness of the soil layer (cm).

Table 3. Empirical coefficients for transmission of Ritchie (2009) soil evaporation algorithm for dry, equilibrium and wet condition

Empirical Coefficients	Dry	Equilibrium	Wet
a_z	0.524	0.011	0.260
b_z	-2.020	0.000	-0.700

The soil mulch cover effect on evaporative demand is accounted by the methods proposed by Porter et al. (2009), whereas the mulch cover has the effect of buffering the water content in the upper soil layers by preventing rapid depletion due to evaporation. A saturation water content of mulch is computed based on a residue-type parameter (Sm) and the mass of the mulch cover (M_{mulch}) (Equation 5). The amount of rainfall or irrigation intercepted by the mulch layer is equal to the difference between the current and saturation water contents of the mulch (θ_{SATm} - θ_m). A mulch area index (MAI) is computed to reduce the fractional of water intercepted by mulch and for mulch layer evaporation (Equation 6).

$$\theta_{SATm} = S_m.M_{mulch}.10^{-4} \quad (5)$$

$$MAI = A_m.M_{mulch}.10^5 \quad (6)$$

where θ_{SATm} is the water content of the mulch at saturation (mm), M_{mulch} is the mass of surface mulch (Kg $_{DM}$ ha^{-1}) and S_m is the saturation water content of surface mulch (Kg_{H2O} Kg_{DM}^{-1}); *MAI* is the mulch area index ($m_{mulch}{}^2$ m_{soil}^{-2}); A_m the area covered per unit dry weight of residue (cm^2 g^{-1}). Water absorbed by mulch is reduced by the fractional surface coverage (Fc) (Equation 7) and the rainfall, minus the amount absorbed by the mulch which runs off or infiltrates. Mulch potential evaporation is related to the energy available at the surface and is reduced in the presence of a crop canopy. Thus, calculation corresponds to a Beer's law equivalent (Equation 8). To account for the entire mulch layer,

the potential evaporation from the mulch layer is proportional to the energy received by the mulch after accounting for plant canopy interception (Equation 9).

$$F_c = 1 - e^{-MAI} \quad (7)$$

$$EO_{surf} = EO \,.\, e^{(-k_{can}\, LAI)} \quad (8)$$

$$EO_{mulch} = EO_{surf} \,.\, \left[1 - e^{(-k_m . MAI)}\right] \quad (9)$$

where *Fc* is the fraction surface coverage by mulch; *MAI* is the mulch area index ($m_{mulch}^2\ m_{soil}^{-2}$); EO_{surf} is the surface evaporation, including both soil and mulch evaporation (mm d^{-1}); *EO* is the potential reference evapotranspiration (mm d^{-1}); k_{can} is the canopy light extinction coefficient (dimensionless); EO_{mulch} is the mulch layer evaporation (mm d^{-1}); k_m is the mulch cover light extinction coefficient (dimensionless). Actual mulch evaporation is computed by multiplying by the fractional mulch coverage and is limited to 85% of the total mulch water stored (Equation 10). Potential soil surface (EOS) is then computed as the difference between potential surface evaporation (EO_{surf}) and actual mulch evaporation (E_m). Actual soil evaporation (ES) is not supposed to exceed potential soil evaporation and is reduced indirectly:

$$E_m = min[EO_m, (0.85 \,.\, \theta_m)]Fc \quad (10)$$

Potential transpiration (EOP) is simulated in the form of the previous version, but including the CO_2 concentration effect on stomatal resistance to reduce the potential rate, described in section 2.2.1.3.6. Actual transpiration is computed as the ratio of atmospheric demand (EOP) and the potential root water uptake (PRWU). Potential root water uptake is computed by the methodology described by Ritchie (1998), similar to that used in the CERES-Maize model. Root length density (RLD, $cm_{root}\ cm_{soil}^{-3}$) simulated by the crop module is used to compute the PRWU for each soil layer, assuming water movement to a single root and that the roots are uniformly distributed (Ritchie, 1998; Singels *et al.*, 2010). The PRWU is then integrated over the soil layers, and if greater than the atmospheric demand, the actual root water uptake (ARWU) is reduced to EOP and actual transpiration is at potential rate. If PRWU is lower than EOP, actual plant transpiration (EP) is reduced and water stress factors are updated.

2.2.1.3. Crop Model Overview

The new version of the SAMUCA model follows the same structure as previously described by Marin and Jones (2014). Three main steps are performed to simulate crop growth, following the classical structure of (i) initialisation of model state variables and axioms, (ii) time-step rate calculations and (iii) time-step integration of state variables and rates (Thornley and Johnson, 1990; Teh, 2006). Because sugarcane structures and organ composition are of major economic interest (sucrose and fibre), this new version simulates crop growth and development at the phytomer level. This concept is based on functional structural plant models (FSPM) and enables to downscale the relations of environmental conditions to sugarcane internode composition (Prusinkiewicz and Lindenmayer, 1990; Vos *et al.*, 2010; Singels and Inman-Bamber, 2011). Crop growth and development are explicitly distinguished. Development is simulated by successive phytomers, and tiller creation and growth represent the photosynthetic capacity to supply the demanded carbohydrates to sink organs (phytomers and the root system).

A sugarcane phytomer can be depicted as a plant repetition unit of one leaf, attached to its node, an axillary bud to the opposite side, and a subtending internode (encased by the leaf sheath) (Moore and Botha, 2013b). Because this model approach (process-based) cannot simulate this richness of organ structure without a high level of uncertainty, a phytomer is represented as a leaf and its subtending internode. The rate of phytomer initiation is simulated by a plastochron interval (C° days), which is closely related to the phyllochron interval, well known for different varieties of sugarcane (Keating *et al.*, 1999; Singels and Inman-Bamber, 2011). For simplicity, the model assumes they are equal, and no distinction is made between leaf initiation and appearance on the top parts of the sugarcane shoots. Based on these creation rules, successive phytomer initiation for the primary shoots is simulated and integrated for plant and field levels.

2.2.1.3.1. Initial Conditions

The spatial boundary is set to 1 square meter, wherein the initial plant population is computed based on row-spacing and linearly planted buds (bud m^{-1}). At the very first model time-step (planting date), these buds sprout, and the primary shoot is initiated at the planting depth with its 1st phytomer. The first distinction between ratoon and plant cane is made, whereas the initial planting depth (cm) parameter is used to set the belowground starting point for shoot (upward direction) and root (up and downward direction) growth. For ratoon sugarcane, the belowground starting point is a crop parameter (closer to soil surface), while for plant cane, the initial starting point is the planting depth; thereafter, a belowground shoot rate of the expansion (cm °C day^{-1}) parameter is used to simulate the time when primary shoots emerge at the soil surface. The difference between plant cane ("cana-planta") and ratoon ("soqueira") cane initial soil depth is the main mechanism to simulate the difference in sugarcane emergence time (Keating *et al.*, 1999; Singels, Jones and Berg, 2008).

Before emergence, the number of phytomers initiated is considered as belowground internodes which are shorter, but also have a sink strength for growth. Their substrate reserves are used for ratoon re-growth (Keating *et al.*, 1999; Matsuoka and Garcia, 2011), and this feature plays a role in the second distinction between plant and ratoon cane. The initial amount of substrate reserves (CH_2O) for plant cane is equal to the sugar fraction of chopped stalks at planting (Fsuc/DWcane), whilst in ratoon cane, the initial substrate reserves are equal to the sugar amounts of below-ground internodes of the previous season. If the substrate reserves (CH_2O) are not sufficient to sustain respiration and to meet the sink strength of the phytomers and the root system; as a result, the crop dies before emergence. Leaves are also considered organ sinks before emergence and responsible for the physical protection of younger short internodes and the apical meristem, as well as for shoot expanding towards the soil surface (Moore and Botha, 2013b).

2.2.1.3.2. Crop development

In contrast to grain crops, the major economic developmental stage of sugarcane is the vegetative stage, during which the stalk grows and sugar is accumulated in the internodes. In commercial fields, flowering is an undesired trait, since inflorescence organs impose a high sink strength to crop carbohydrates, withdrawing the sucrose content. Thus, the domesticated sugarcane crop is mostly grown in the vegetative stage, and when exposed to cooler temperatures or water stress, structural growth is limited, although assimilates are still produced and stored as sucrose

(Bonnett, 2013). Therefore, two forms of development are simulated in this new model version: (i) tillering, as regulated by a thermal time for tiller emergence rate and competition for light (Bezuidenhout *et al.*, 2003; Singels and Smit, 2009) and (ii) successive phytomer creations by its plastochron (Prusinkiewicz and Lindenmayer, 1990). Flowering is not considered in the model, but this framework is suitable to include the crop inflorescence as a competitive sink organ.

Initial tillering rate is computed analogous to the phytomer creation; after the emergence of primary tillers, successive new tillers emerges after a thermal time parameter (i.e. "tillochron", Evers (2006)) for tiller emergence (Bezuidenhout *et al.*, 2003). Tillering ceases when a threshold of light transmitted through the canopy is attained. Light transmission is simulated by using the Beer's Law, considering the green fraction of the shed leaf area (LAI_{MOD}). To avoid steeper tillering senescence rate (see Figure 59b), an empirical factor was added, depicted as the maximum rate of tiller senescence (tiller d^{-1}) under competition of light. Tiller senescence rate stops after equilibrium to a light threshold or a thermal time for stalk maturity (CHUMAT) is attained (Equations 11 and 12). Due to experimental evidences of the soil temperature effect on tillering rate (Figure 19), soil temperature is simulated and used as thermal time accumulation in the tillering process. Soil temperature is highly influenced by the soil mulch cover, and the sugarcane tillering process is indirectly affected:

$$dTill = \frac{dage_{soil}}{Tillochron} \qquad (Tage_{acc} < CHUMAT \text{ and } FTL > FTL_{threshold}) \qquad (11)$$

$$dTill = \left(1 - \frac{FTL_{threshold}}{FTL}\right) TSenRate \qquad (Tage_{acc} < CHUMAT \text{ and } FTL < FTL_{threshold}) \qquad (12)$$

where *dTill* is the daily tillering rate (tiller m^{-2}); $dage_{soil}$ is the thermal using soil temperature (degree day d^{-1}); *Tillochron* is the thermal time parameter for new tiller emergence (degree day $tiller^{-1}$); $FTL_{threshold}$ is the fraction of the transmitted light threshold to start tiller senescence (0-1); *FTL* is the fraction of the light threshold calculated by Beers Law (0-1), considering green and dead leaf areas; *TSenRate* is the maximum rate of tiller senescence under light threshold (tiller d^{-1}); $Tage_{acc}$ is the accumulated thermal time according to soil temperature; *CHUMAT* is the thermal time parameter for stalk maturity (Keating *et al.*, 1999; Singels, Jones and Berg, 2008; Marin and Jones, 2014). Because soil temperature is implemented, phytomer development will be based on soil temperature when the apical meristem (assumed here as the younger phytomer) is below the ground or on air temperature when it is above the ground.

2.2.1.3.3. Crop Growth

Biomass gain is simulated based on the carbon balance of source-to-sink organs and sugar reserves. Daily sink strengths are calculated separately for each organ pool and phytomer. Carbon balance take places for daily produced substrates to compute the allocation among organs, whereas the surplus substrates are stored in reserves (hexoses and sucrose). Total internode sugar reserves are constrained by lignin biosynthesis, and the sucrose fraction of total sugars is then simulated as a passive storage, increasing with internode maturity (Bottcher et al., 2013; Lingle and Thomson, 2012; Moore, 2005).

2.2.1.3.4. Carbon Balance

Most biological growing processes over time can be described by asymptote curves (Thornley and Johnson, 1990; Yin *et al.*, 2003). Under conditions with sufficient water and nutrients, sugarcane leaves and internode growth over thermal time can be described by an asymptotic curve (Fournier, 2001; Singels and Inman-Bamber, 2011; Lingle and Thomson, 2012). Based on this approach, the model simulates the daily amount of carbohydrates needed for each phytomer by the first derivative of Equation 13 (Equation 14), with respect to phytomer thermal age (Figure 5a):

$$y = y_{max} + \frac{y_{min} - y_{max}}{\left[1 + \left(\frac{age}{mid}\right)^{s}\right]^{m}} \tag{13}$$

$$\frac{dy}{dage} = -m(y_{min} - y_{max})\left\{\left[1 + \left(\frac{age}{mid}\right)^{s}\right]^{(-m-1)}\right\} s \left(\frac{age}{mid}\right)^{(s-1)} \frac{1}{mid} \frac{1}{(1 - gresp)} \tag{14}$$

where y is the theoretical dry weight of the internode or leaf (g) at the thermal age (*age*); y_{min} and y_{max} are initial and final dry weight from the beginning to the final growth stage; *mid* is the inflexion point of the growing curve; *s* is the shape parameter of the curve (the higher the value the steeper the growth rate); *m* is the asymmetric parameter for the inflexion point; 1/(1-*gresp)* is the substrates requirement for growing tissue (g_{CH2O} g_{Dw}^{-1}), where *gresp* for sugarcane is usually 0.242 (Inman-Bamber, 1991; Singels and Inman-Bamber, 2011). Note that Equation 14 can be simplified, as y_{min} is generally equal to zero and asymmetric growth is not often observed in a biological system with a limited life span and limited carbohydrates (m = 1) (Thornley and Johnson, 1990). Nevertheless, the model uses its full form to keep equation versatility. The sink strength computed for each organ is depicted in Figure 5a.

Sugarcane stalks usually have a constant number of green leaves during vegetative growth (around 10 green leaves per stalk), and for each senesced leaf, a new leaf is initiated, together with a phytomer on the stalk apical meristem (De Silva and De Costa, 2012; Bonnett, 2013; Rae, Martinelli and Dornellas, 2013). Thus, the life span (°C days) of each green leaf is calculated by multiplying the crop parameter maximum number of green leaves per stalk (MAXGL) and its phyllochron (PHY). Maximum green leaf dry weight ($y_{max.lf}$) is computed as the ratio of the maximum green leaf area (MLA, cm^2) and the specific leaf area parameter (SLA, cm^2 g^{-1}); the inflexion curve of leaf growth (mid_{lf}) is the half of its life span (°C days) (Equations 15 and 16). The shape (s) and asymmetry (m) of sink strength are also input parameters to adjust the growth function.

$$mid_{lf} = \frac{MAXGL\,.PHY}{2} \tag{15}$$

$$ymax_{lf} = \frac{MLA}{SLA} \tag{16}$$

The internode sink strength is computed only for its fibre fraction and ceases when the subtending leaf exceeds its life span. When internodes are above the young leaves´ natural breaking point, a minimum amount of 10% of its total dry weight is taken as total sugars, as 5% sucrose and 5% hexoses (Singels and Inman-Bamber, 2011; Lingle and Thomson, 2012). After this development stage, the internode starts to elongate and to increase its fibre sink strength, while the phytomer corresponding leaf is now considered fully developed. At the same time, a lignin deposition rate is calculated and ceases at the same time as the internode stops to function as a fibre sink. The approach depends on the mechanism via which the internodes act as reservoirs for sugars, in which case the amount of lignin is

strongly linked to the total amount of sugars and storage tissues. Much of this approach is based on the analysis of Lingle and Thomson (2012), who studied internode composition during sugarcane growth, and on the sugarcane phytomer model proposed by Singels and Inman-Bamber (2011). Reference values of internode fibre content ($y_{max.it}$), total sugars and length were obtained from their study (Figure 4a), and a strong relation of internode lignin amount to total sugar content was also found (Figure 4b). In this new version, the model simulates the lignin dry mass of each internode by heat unit accumulation and by computing the potential sugar amount of the corresponding internode by using the sugar/lignin ratio (SL_ratio, $g^1_{sugar}\ g^{-1}_{lignin}$) (Figure 4b).

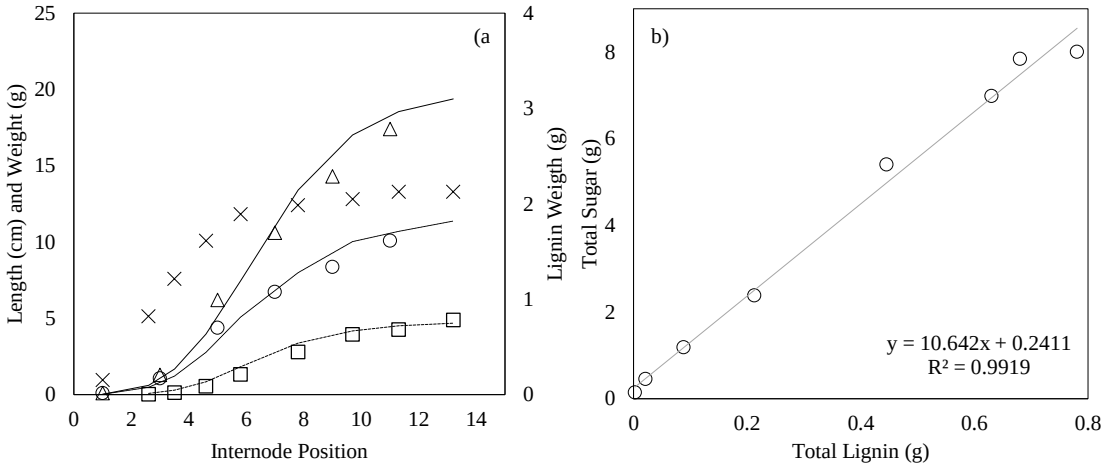

Figure 4. Internodes total dry weight (Δ), length (X), structural weight (O), lignin amount (□) and fitted curves for total dry weight (solid line), structural weight (dotted line) and lignin weight (dashed line) in relation to internode position (a); relation between total lignin dry mass and total sugar of single internode from position 1 to 14 (b). Results obtained from Lingle and Thomson (2012)

An assumption made here is that the base temperature for the fibre sink is equal to the stalk expansion rate (Tb = 16°C). The lignin deposition rate is computed using the crop development base temperature (Tb) of 12°C. This assumption is based on the fact that the fibre content is more related to plant expansion and the size of young internodes, whereas lignin deposition is related to the maturity level of the internode parenchyma (Ebrahim *et al.*, 1998; Bottcher *et al.*, 2013). Therefore, at higher temperatures and in young internodes, fibre contents are higher than sugar contents. On the other hand, at cooler temperatures or water stress condition, internode fibre contents and available assimilates (CH_2O) are smaller, while the sugar content is higher. Total leaf and internode per shoot are computed by integration of all organs´ daily rates. For simplicity, total leaf area and internode sink strength per area unit are scaled up by the number of shoots (tillers) per area unit and corrected by an age factor among shoot thermal age. For each new shoot emerged, its thermal age is stored and updated; rather than simulated individually for all shoot phytomers, the relative age of all shoots to the primary shoot is used (Equations 17, 18 and 19) to avoid overestimation of the total sink strength:

$$dleaf_{ss} = \sum_{n=1}^{ndlf} \left(\mathrm{dleaf}_{ss,n}\right) . nstk . tagefac \tag{17}$$

$$dint_{ss} = \sum_{n=1}^{ndlf} \left(\mathrm{dint}_{ss,n}\right) . nstk . tagefac \tag{18}$$

$$tagefac = \sum_{n=1}^{nstk} \left({till_{age,n}}/{till_{age,1}} \right) \frac{1}{nstk} \quad (19)$$

where $dleaf_{ss}$ and $dint_{ss}$ are the daily total sink strengths of leaf and fibre internodes (g m^{-2}); *nstk*, is the number of live tillers (tillers m^{-2}); *tagefac* is the tiller age correction factor (0-1). Note that *tagefac* approaches to its minimum value at the peak of the tiller population and gets closer to the unit at early growth and maturity. The whole root system is considered to be a sink organ; thus, root sink strength is computed based on a maximum root dry biomass per area ($y_{max,root}$) and the thermal time to maturity (Laclau and Laclau, 2009).

The available substrate is then distributed among all growing organs (leaves, internodes, panicles, roots), using the relative sink strength principle (Heuvelink, 1996) (Equation 20).

$$Rss_i = \frac{SS_i}{\left(SS_{rt} + SS_{lf} + SS_{it}\right)} \quad (20)$$

where Rss_i is the relative sink strength of the organ pool (0-1); SS_i is the absolute sink strength of the organ pool (i) in g m^{-2}; SS_{rt}, SS_{lf}, and SS_{it} are the absolute sink strength values of all organ pools, roots, leaves and internodes, respectively. This approach is based on a supply-demand carbon balance, whereas the daily amounts of assimilates are partitioned among the organ pools (Figure 5b), based on each organ sink strength. When the daily amounts of substrates are greater than the total organ demand, the surplus is stored in the stalk up to its potential sugar capacity. If the amount of substrates after carbon allocation exceeds the stalk potential sugar capacity, the daily substrate surplus is stored in roots, and the CO_2 assimilation rate is reduced (*fb_res*, parameter) as a feedback response of organs (Mccormick, Cramer and Watt, 2006; Mccormick, Watt and Cramer, 2009). When the daily amounts of substrates are lower than the organ demand, crop growth is reduced.

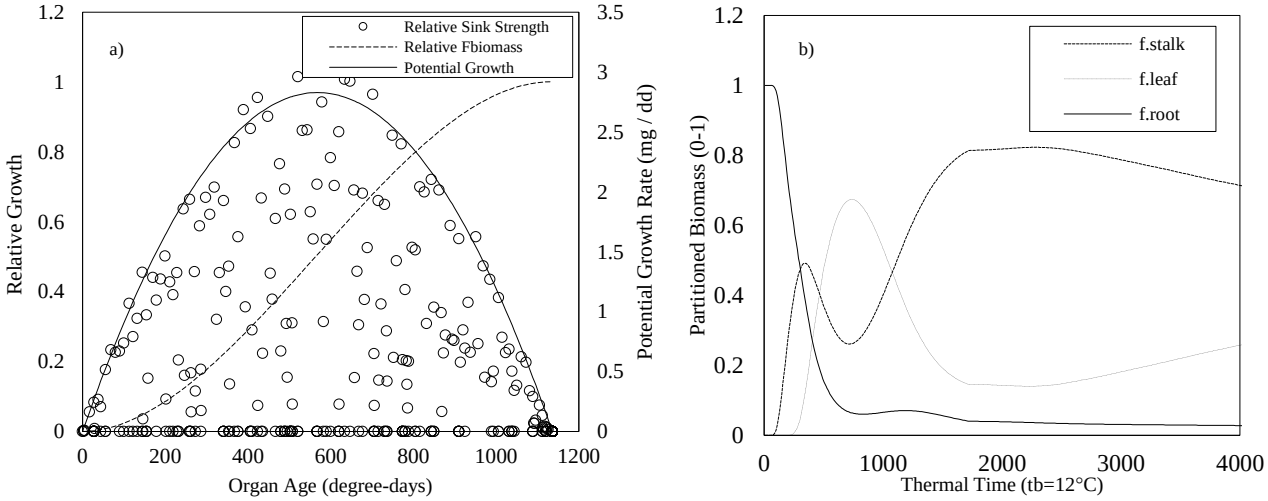

Figure 5. Potential growth, relative sink strength and fraction of potential biomass (*Fbiomass*) allocated to an organ under potential substrates supply (a) and fraction of total assimilates partitoned to each organ pool throughout crop season (b) (ymax root = 132 g m^{-2}, root tt develop = 3000°CDay, ymax leaf = 4g $leaf^{-1}$, ymax int. = 20 g $internode^{-1}$, plastochron = 120 °Cday, maxpop = 26 tiller m^{-2})

Daily total assimilate production is calculated by the three-point Gaussian integration method (Goudriaan, 1986, 2016). Input solar radiation is fractioned between the direct and diffuse proportion, based on the degree of

atmosphere light scattering, simplified by Spitters (1986) by ratios between incoming global radiation (Qg, MJ m^{-2} d^{-1}) and extraterrestrial solar radiation (Qo, MJ m^{-2} d^{-1}). Instantaneous flux densities of diffuse and direct radiation are calculated for three Gaussian steps, according to the sine of the solar elevation (Spitters, Van Keulen and Van Kraalingen, 1989). Half of the incoming radiation flux is considered as photosynthetically active radiation (PAR), and the reflected fraction is discounted and redistributed in the canopy, assuming a spherical leaf angle distribution (Monteith and Unsworth, 2012; Goudriaan, 2016). The 3-depth canopy radiation absorbed flux is then computed for the three-time step separately for shaded and sunlit leaf areas by the first derivative of Beers Law (Equations 21, 22 and 23):

$$I_{dif(L,n)} = k_{dif}\left(1 - \alpha_{dif}\right) PAR_{dif(n)} e^{\left(-k_{dif}\, L\right)} \tag{21}$$

$$I_{sca(L,n)} = k_{sca(n)}\left(1 - \alpha_{sca(n)}\right) PAR_{dir(n)} e^{\left(-k_{sca(n)}\, L\right)} \tag{22}$$

$$I_{dir(L,n)} = k_{dir(n)}(1 - \alpha_c) PAR_{dir(n)} e^{\left(-k_{dir(n)}\, L\right)} \tag{23}$$

where I_{dif}, I_{sca}, I_{dir} are the diffuse, scattered and direct intercepted PAR (W m^{-2}) by leaf area at the Gaussian time-step (n) and canopy layer (L); k_{dif} is the fixed canopy light extinction for diffuse radiation (dimensionless); k_{sca} is the canopy light extinction for scattered radiation (dimensionless), as a function of canopy reflectance, transmission and solar elevation angle (β) to the horizon (Goudriaan, 2016); k_{dir} is the canopy light extinction of direct beam solar radiation (dimensionless), equalling $0.5/\sin(\beta)$ for spherical leaf angle; α_{dif} and α_{sca} are the diffuse and scattered PAR reflectance coefficients (0-1), adjusted based on the fixed canopy reflectance coefficient (αc) and sin(β) (Cowan, 1968; Monteith, 1969); PAR_{dir} and PAR_{dif} are, respectively, instantaneous PAR direct and diffuse flux (W m^{-2}) at the time-step(n).

The sunlit leaf area receives both diffuse and direct flux radiation (I_{lit}) (Equation 25), while the shaded leaf area receives the diffuse flux and the scattered component of the direct flux (I_{shd}), which is the difference between the total scattered light and the direct light beam at canopy depth(L) (Equation 24). Instantaneous assimilation is then computed by an exponential light curve response (Equation 26) for both shaded and sunlit leaf areas. To obtain the instantaneous assimilation rate at the canopy layer (L), the fraction of the sunlit leaf area (fslla) at the canopy layer (L) is imposed (Equations 27 and 28):

$$I_{shd(L,n)} = I_{dif(L,n)} + I_{sca(L,n)} - I_{dir(L,n)} \tag{24}$$

$$I_{lit(L,n)} = I_{dif(L,n)} + I_{dir(L,n)} \tag{25}$$

$$Ass_{i(L,n)} = Amax\left[1 - e^{\left(-I_{ilf(L,n)}\, eff/Amax\right)}\right] \tag{26}$$

$$fslla_{(L,n)} = e^{\left(-kdir_{(n)}\, L\right)} \tag{27}$$

$$Ass_{L(L,n)} = fslla_{(L,n)}\, Ass_{lit(L,n)} + (1 - fslla_{(L,n)}) Ass_{shd(L,n)} \tag{28}$$

where Ass_i is the CO_2 assimilation rate (kg ha^{-1} h^{-1}) for diffuse or direct leaf area (i = *shd* or I = *lit*) at the Gaussian time-step(n) and the canopy layer (L); Ass_L is the CO_2 assimilation rate (kg ha^{-1} h^{-1}) of the layer canopy (L) at the Gaussian time-step(n); *Amax* is the maximum leaf assimilation rate at light saturation (kg ha^{-1} h^{-1}); *eff* is the initial light use efficiency of a leaf (kg J^{-1}). The assimilation rate is then integrated for each canopy layer, according to the Gaussian

step and weight procedure (three-point), and stored for carbon balance in kg CO_2 layer^{-1} d^{-1}, such that the sum of assimilates from the layers represents the daily crop total assimilation (kg_{CO2} m^{-2} d^{-1}). Carbohydrate production is obtained by converting the CO_2 atomic mass to CH_2O (kg_{CH2O} m^{-2} d^{-1}) by the 30/44 ratio.

Daily crop maintenance respiration (g_{CH2O} g_{DW}^{-1} d^{-1}) is accounted for leaf, internode and root pools separately by adjusted Q_{10} relation curves to temperature (Liu and Bull, 2001). Total crop maintenance respiration (kg_{CH2O} m^{-2} d^{-1}) is subtracted from daily carbohydrate production, and the remaining daily CH_2O is available for allocation in organs sinks (phytomers and root system) or stored. Phytomers are fed by substrates produced in their corresponding canopy layer (Figure 6), a fraction of all substrates produced by the canopy is allocated to root system according to the relative sink strength. Leaf area of each phytomer is integrated downwards the crop canopy, and the number of phytomers of the underlying canopy layer is counted by matching the cumulative leaf area. Within each canopy layer, the available substrates are then partitioned among the phytomers as function of the leaf area (Figure 6).

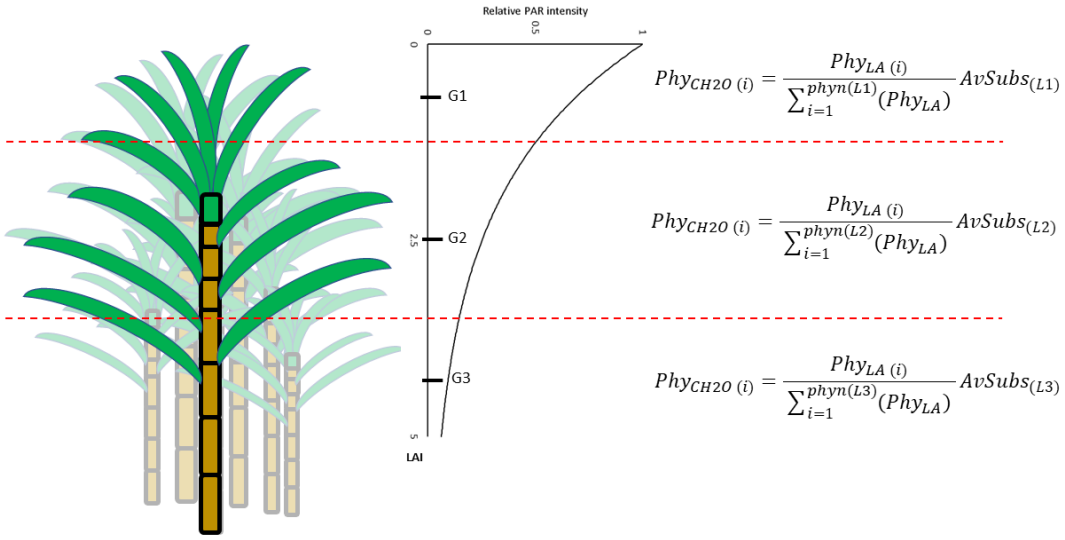

Figure 6. Schematic representation of the primary tiller substrates partitioning in relation to canopy layer substrates production (LAI = 5). $Phy_{CH2O(i)}$ is the phytomer total available substrates partitioned from underlying canopy layer (Li); Phy_{LA} is phytomer leaf area (cm^2); Phyn(Li) is the phytomer number of canopy layer (Li); AvSubs(Li) is the total available substrates produced at canopy layer (Li); G_i discrete points of Gaussian step integration over LAI, recall that a further 3-points are also integrated with time-step

If daily substrates are not sufficient to sustain respiration, the phytomers will use their own reserves to maintain crop metabolism. The crop is considered dead after all reserves have been used for the maintenance of respiration. When daily photosynthesis fully supplies maintenance respiration, the surplus income is then used to supply the sink demand of each phytomer ($leaf_{ss}$ + $internode_{ss}$) by a source-sink ration (ssfac) (Equations 29 and 30). When ssfac is lower than 1, growth is limited by source supply, and no exchange among phytomer reserves is allowed to avoid growth compensation by sink reserves of other phytomers. This assumption was made due to the lack of data regarding to which extent sugarcane phytomers share their reserves for structural growth and after model testing against data on yield overestimation when reserves were exchanged among phytomers.

$$ssfac_{(phy)} = \min\left(1, \frac{Phy_{CH2O}}{Phy_{ss}}\right) \tag{29}$$

$$dAlloc_{(phy)} = ssfac_{(phy)}\left(dleaf_{ss(phy)} + dint_{ss(phy)}\right) \tag{30}$$

When ssfac is greater than 1, allocation is fully supplied for growth, and surplus sugars are stored in the potential sugar reserves of the internodes, updated by its lignin content, as previously explained. If the phytomer CH_2O surplus exceeds its potential sugar storage, the remaining amounts are reallocated (bottom-up) among the phytomer potential sugar reserves, and if the remaining amount still exceeds the all phytomers potential storage, the substrates are stored in belowground internodes. Once the sugars exceed the potential reserves, a feedback response factor (*fbrespfac*) is imposed to reduce the maximum assimilation rate at an arbitrary value of 5% for the following day, and the maximum assimilation rate is restored (fbrespfac = 1) when no sugars are translocated to belowground parts (Mccormick, Cramer and Watt, 2006, 2008; Watt, McCormick and Cramer, 2013; R. V. Ribeiro *et al.*, 2017).

Sucrose accumulation at the phytomer level is simulated as the difference between total sugar reserves and hexoses (Equation 32). Total hexose is constrained so that it does not exceed the internode total sugar amount and is computed as the phytomer total growth and maintenance respiration. An empirical factor of the hexose usage rate (Hexuse, g_{hexose} d^{-1}) is imposed to mimic the hexose/sucrose fraction variations among internodes (Singels and Inman-Bamber, 2011) (Equation 31):

$$Hexose_{phy(i)} = \left\{dDW_{phy}\left[\frac{1}{(1-gresp)} - 1\right] + DW_{phy}.mresp\right\} + Hexose_{phy(i-1)}.Hexuse \quad (31)$$

$$Sucrose_{phy} = TotalSug_{phy} - Hexose_{phy} \quad (32)$$

where $Hexose_{phy(i)}$ is the current hexose amount (i) and the hexose amount of yesterday (i-1) (g), constrained by internode total sugar ($TotalSug_{phy}$); dDW_{phy} is the daily internode dry weight gain (g); gresp is the growth respiration (g_{CH2O} g_{DW}^{-1}); mresp is the maintenance respiration (g_{CH2O} g_{DW} d^{-1}); Hexuse is the empirical daily hexose use rate (frac $_{CH2O}$ d^{-1}); $Sucrose_{phy}$ is the internode sucrose amount (g).

Toot system depth growth was related to soil temperature (0.048 cm degree day^{-1}), similar to the results from Laclau and Laclau (2009). Growth in the upward direction, starting from planting depth, is also simulated at the same rate. In contrast, in the standalone version of SAMUCA, root length density (RLD) distribution is simulated considering the planting depth as starting point rather than the first soil layer, avoiding overestimating roots in the superficial soil layer. Instead of the geotropism function, two specific root length (SRL, cm g^{-1}) parameters are used, one for the root-deepening front and another for roots above the root front. Laclau and Laclau found that under rainfed and irrigated conditions, specific root length (m g^{-1}) can be three-fold higher at the root-deepening front than the rest of the root system. Root length density (RLD) is then computed by using a higher SRL parameter for the deepest soil layer with roots and a lower value for layers above the deepening front (Equations 33 and 34).

$$RGF_L = \frac{RVR_L}{\sum_{L=1}^{nsl}(RVR_L)} \quad (33)$$

$$dRLD_L = \frac{dDWroot\,.\,RGF_L.SRL_L}{Thick_L} \quad (34)$$

where RGF_L is the root growth partitioning factor (0-1) of the soil layer L; *nsl* is the number of soil layers with roots; RVS_L is the root vertical range of layer L (cm); $dRLD_L$ is the daily root length density increment at layer L (m_{root} m_{soil}^{-3}); dDW_{root} is the daily biomass allocated to roots (g m^{-2}); SRL_L is the specific root length at layer L (m_{root} g_{root}^{-1}); $Thick_L$

is the soil layer thickness (m). $dRLD_L$ is converted to $cm_{root}\ cm_{soil}^{-3}$ later on for integration and for the root water uptake module.

The length expansion of internodes was simulated based on Inman-Bamber et al. (2008). Similar to the previous version (Marin and Jones, 2014), stalk extension is related to air temperature and simulated hourly. The Parton and Logan (1981) model is employed to simulate hourly air temperature from daily maximum and minimum temperature (Vianna and Marin, 2017). Stalk extension starts at a higher base temperature than photosynthesis and reaches its maximum rate of expansion at optimum temperature (Tb = 16°C and To = 45°C, from Inman-Bamber et al. (2008)). The hourly effective temperature is used to simulate overall stalk extension (mm h^{-1}), whereas an age factor is also accounted for to reduce stalk expansion due to crop aging (Inman-bamber *et al.*, 2008) (Equation 35). Daily stalk extension is integrated and partitioned among growing internodes, according to the thermal age (Equations 36 and 37):

$$agefac = e^{-red.cropage} \tag{35}$$

$$dPER_h = min\left[1., \frac{\max(0., Tair_h - Tb)}{(To - Tb)}\right] PER_{max}.agefac \tag{36}$$

$$dPER_{int} = \frac{dAlloc_{int}}{\sum_{int=1}^{intn}(dAlloc_{int})} \sum_{h=1}^{24h}(dPER_h) \tag{37}$$

where *agefac* is the relative reduction factor due to crop age (0-1); *cropage* is the thermal age of primary shoots (degree.days); *red* is the empirical parameter for the age reduction factor (dimensionless); $dPER_h$ is the hourly stalk extension (mm h^{-1}); $Tair_h$ is the hourly air temperature (°C); *Tb* and *To* are the base and optimum temperature for stalk extension, respectively; PER_{max} is the stalk maximum extension rate (mm h^{-1}); $dPER_{phy}$ is the daily internode extension rate (mm d^{-1}); $dAlloc_{int}$ is the daily internode structural allocated carbon (g). Note that only growing internodes will extend; carbon allocation to structural internodes is described below.

2.2.1.3.5. Abiotic Stress

Cardinal temperatures are used to reduce the assimilation rate at light saturation point (Figure 7); relative reduction occurs when air temperature is below or above the optimum temperature range (To = and To_2) (Ebrahim *et al.*, 1998). Water stress is computed similarly as described in the previous version (Marin and Jones, 2014). Two water stress factors are used to reduce photosynthesis (SWFACP) and crop extension (SWFACE). The ratio of potential transpiration (Ptrans) and potential root water uptake (PRWU) is the demand-supply factor to reduce photosynthesis or extension (Ritchie, 1998) (Equation 38). In this approach, the PRWU is computed as a function of root length density (RLD) and soil water content, previously described by Ritchie (1998). This implies that the daily PRWU can be higher than the potential transpiration (Ptrans). Under this condition, actual root water uptake (ARWU) is reduced to Ptrans and actual transpiration (Atrans) is equal to Ptrans. If PRWU is lower than Ptrans, Atrans is reduced to PRWU and ARWU is equal to PRWU. Water stress sensitivity is different for photosynthesis and crop extension rate. When Ptrans/PRWU is lower than the photosynthesis or extension threshold (0-1), plant rate is reduced proportionally, adding a sensitive factor. Sugarcane water stress sensitivity for extension is higher than that for photosynthesis (Singels, Jones and Berg, 2008; Marin and Jones, 2014):

$$SWFAC_i = \frac{Ptrans}{PRWU}\frac{1}{Sens_i} \quad \text{(when Ptrans/PRWU} < S_{threshold(i)}) \quad (38)$$

where $SWFAC_i$ is the relative reduction factor (0-1) to process (i); Ptrans is the potential crop transpiration (mm d^{-1}); PRWU is the potential root water uptake (mm d^{-1}); $Sens_i$ is the sensibility of the process (i) to water stress; $S_{threshold(i)}$ is the demand/supply ratio at the beginning of water stress.

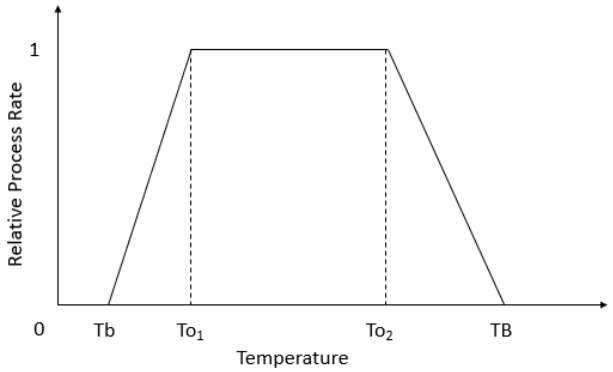

Figure 7. Relative process rate reduction factor as function of base and optimum temperatures

2.2.1.3.6. Atmospheric CO_2 effect

Elevated CO_2 concentrations are not expected to have a direct effect on sugarcane photosynthesis rates, since the C4 pathway allows Rubisco to operate at high efficiency (Sage, Peixoto and Sage, 2013). However, pronounced decreases in stomatal conductance (gs) under elevated CO_2 levels, leading to a reduction in transpiration rates, have been reported widely (Dugas et al., 1996; Long et al., 2004; Ainsworth and Long, 2005; Prior et al., 2010; Sage et al., 2013). In sugarcane, reductions in gs of up to 50% relative to current CO_2 levels have been reported (Ziska & Bunce, 1997), while the Florida varieties CP73-1547 and CP72-2086 showed a 30 to 40% reduction in leaf conductance during growth at elevated CO_2 concentrations (Vu et al. 2006; Vu & Allen 2009). As pointed out by Jones et al. (2015), some authors (Vu et al. (2006), de Souza et al. (2008) and Allen et al. (2011)) have reported increased photosynthesis rates at elevated CO_2 levels in pot experiments, but improved crop water status through stomatal response may have contributed significantly to these observed responses.

Stokes et al. (2016) decoupled direct and indirect effects of enriched CO_2 on sugarcane. Although the authors found a slight yield increase (3%) for sugarcane plants under high CO_2 concentrations, both whole-plant transpiration and stomatal conductance were 28% lower than under the control treatment (380 ppm of CO_2). Even with reduced transpiration, photosynthesis rates were not decreased, indicating that an indirect mechanism such as stomatal control dominates CO_2 responses in sugarcane. Therefore, it seems reasonable to accept that water use efficiency (WUE – defined as dry biomass produced per unit of transpiration) would be increased under elevated CO_2 conditions (Vu et al., 2006; Allen et al., 2011). The impact of atmospheric CO_2 concentrations on stomatal resistance was implemented following the relation proposed on the DSSAT (Decision Support System for Agrotechnology Transfer) platform (Equation 39), with a consistent response for sugarcane under elevated CO_2 concentrations (Marin *et al.*, 2015):

$$rs = \frac{(3.28.10^{-2} - 5.49.10^{-5}.[CO_2] + 2.96.10^{-8}.[CO_2]^2)^{-1}}{LAI} + rlb \quad (39)$$

where *rs* is the stomatal resistance to water vapor diffusion (s m^{-1}); *rlb* is leaf boundary layer resistance (assumed as fixed value of 10 s m^{-1}); *LAI* is the crop leaf area index; encased CO_2 is the CO_2 atmospheric concentration (μmol mol^{-1}) (Allen, Luis, *et al.*, 1998; Long *et al.*, 2004).

2.2.2. Model evaluation and calibration

2.2.2.1. Field Experiments Description

A field experiment was carried out in an irrigated second ratoon sugarcane field (2.5 ha), planted with the cultivar RB867515 at October 16, 2012; this cultivar is widely used and accounts for 27% of Brazilian sugarcane fields. This experiment was part of a long-term sugarcane experiment included in this thesis, carried out from October 2012 to July 2016. Planting was performed with a single line spacing of 1.4 m between rows, distributing 13-15 buds per linear meter to a depth of 0.25 m. The experiment started on July 17, 2014, with harvest on June 8, 2015 (after a total of 327 days). The experimental site was located at the Department of Biosystems Engineering of the College of Agriculture "Luiz de Queiroz", Piracicaba, São Paulo (Lat: 22°41'55"S Lon: 47°38'34"W Alt: 540m). The climate is characterised as hot and wet summer and dry winter (Cwa - Köppen classification), and the soil is a Hapludox (Soil Taxonomy, 2004). Fertilisation and agricultural pesticides were applied at the beginning of the second crop cycle, according to conventional practices in the state of São Paulo State; although an irrigation system was present, only two irrigations were performed in January due to severe droughts (Coutinho, Kraenkel and Prado, 2015; Marengo *et al.*, 2015) (low water level on reservoirs); the treatments were therefore mainly conducted under rainfed conditions. The experiment had two treatments, one with mulch cover (WM) and one without mulch cover (NW) (Figure 8). Attempting to represent a mechanised sugarcane field, 12 t ha^{-1} of mulch were applied at day 15 after ratooning to the WM treatment.

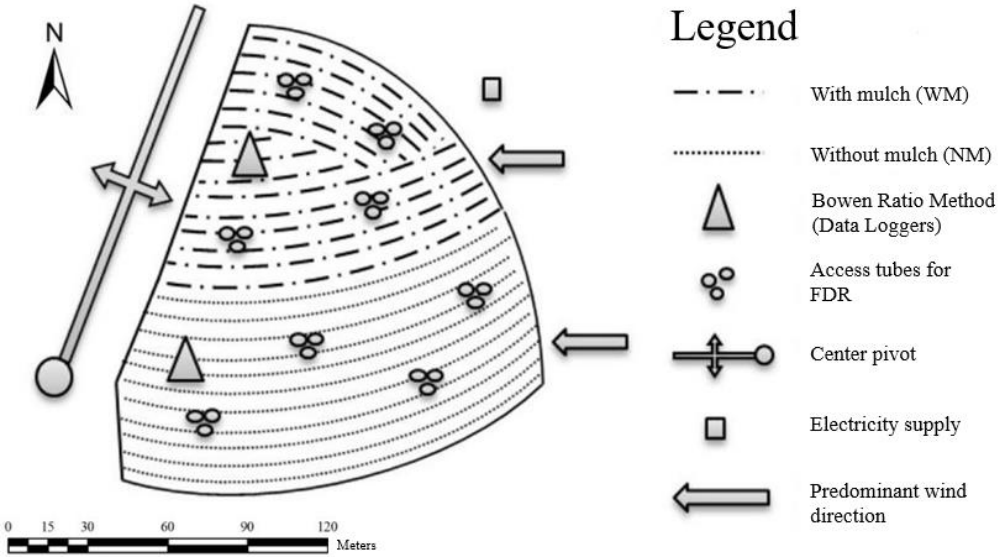

Figure 8. Experimental area sketch describing the central pivot, predominant wind direction, location of evapotranspiration measurements (Bowen Ratio Method) and access tubes for FDR soil moisture probe in treatment with mulch (WM) and without mulch (NM)

Crop evapotranspiration was measured by the Bowen Ratio Method (BRM), and soil water moisture was monitored via Frequency Domain Reflectometry (FDR). A BRM set of equipment was installed on each treatment, consisting of one net radiometer (Kipp Zonen, model NR-Lite) placed above the crop canopy, a soil heat flux sensor (Hukseflux, model HFP01) installed at a depth of 2 cm and two aspirated psychrometers (Marin *et al.*, 2001) placed above the crop canopy at a distance of 1 m. In addition, soil temperature measurements were conducted in both treatments via thermocouples placed at soil depths of 1, 5, 20 and 40 cm. A tipping bucket pluviometer (Campbell Scientific, model TE525MM) and one anemometer (Young, model 05103) were installed at treatments T1 and T2. Equipment sets were located northwest (NW) of each treatment, according to the predominant wind direction determined by Wiendll and Angelocci (1995), to ensure an adequate fetch; data derived from different wind directions were discarded. Data were measured every 30 seconds, averaged over 15 minutes and stored in a CR1000 Datalogger (Campbell Scientific) for each treatment. Net radiation (Nr, MJ m^{-2} $15_{min^{-1}}$), soil heat flux (G, MJ m^{-2} 15 $_{min^{-1}}$), temperature and vapor pressure difference between psychrometers (ΔT, °C and Δe, KPa) and psychrometric constant (γ, kPa $°C^{-1}$) were used for the BRM method (Equations 40 and 41):

$$\beta = \gamma \frac{\Delta T}{\Delta e} \tag{40}$$

$$\lambda E = \frac{Rn - G}{1 + \beta} \tag{41}$$

where β is the Bowen ratio, the ratio of sensible and latent heat flux; E is the latent heat flux (MJ m^{-2} $15_{min^{-1}}$); λ is the water latent heat of vaporisation (MJ $Kg_{H2O^{-1}}$). All data were tested using the filter described by Perez et al. (1999) to ensure physical consistency and quality of measurements.

A total of 24 FDR access tubes were widely placed within the treatments at a depth of 80 cm; they were installed in the middle of the 1st ratoon season, following the recommendations of the manufacturer (Silva, 2007; Sentek, 2011; Provenzano *et al.*, 2016). Four measurement points were located at each treatment, composed of three access tubes, two at crop row and one at inter-row (Figure 8). Measurements were undertaken at a 3-day time step and after each rain or irrigation event. Undisturbed samples of five depths at four locations inside the experimental area (two at each treatment) were taken to obtain soil water retention curves. Three replicates were collected at depths of 5, 15, 30, 60 and 100 cm and taken to the laboratory to obtain volumetric moisture values at potentials of 10, 20, 60, 100, 330, 1,000, 3,000 and 15,000 kPa (Figure 9). Wilting point, field capacity point and saturation point were then derived from the retention curves at 1.5, 0.33 and 0.1 MPa, respectively (Table 4).

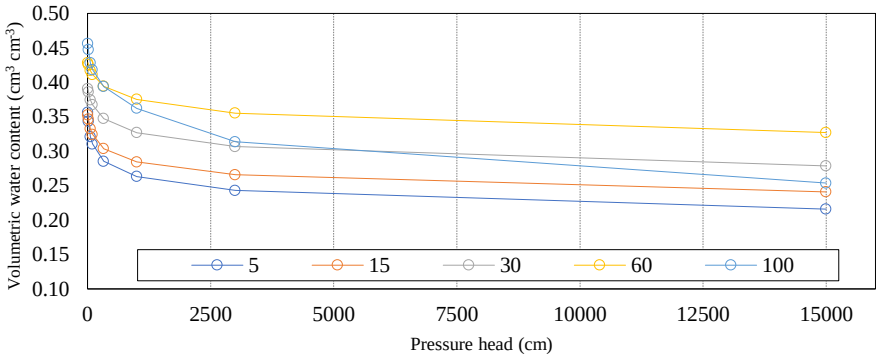

Figure 9. Soil water retention curves of the experimental area determined for 5, 15, 30, 60 and 100 cm depth (average values of 12 repetitions in four different locations within the experimental area, Figure 8)

Table 4. Soil depth (DP), wilting point (WPp), field capacity (FCp), saturation point (STp), saturated hydraulic conductivity (KSAT), sand (Psand), silt (Psilt), clay (Pclay) and organic (Porgm) matter fractions for each soil layer of the experiment

DP (cm)	WPp ($cm^3\ cm^{-3}$)	FCp ($cm^3\ cm^{-3}$)	STp ($cm^3\ cm^{-3}$)	KSAT ($cm\ h^{-1}$)	Psand* ($g\ g^{-1}$)	Psilt* ($g\ g^{-1}$)	Pclay* ($g\ g^{-1}$)	Porgm* ($g\ g^{-1}$)
5	0.216	0.285	0.380	1.70	0.185	0.150	0.650	0.015
15	0.240	0.303	0.352	1.01	0.185	0.150	0.650	0.015
30	0.278	0.347	0.390	0.49	0.199	0.170	0.620	0.011
60	0.307	0.394	0.428	0.21	0.199	0.170	0.620	0.011
100	0.253	0.393	0.456	0.21	0.211	0.160	0.620	0.009

*Obtained from predominant soil profile data base (RADAMBRASIL)

Biometric crop growth and development data were collected, including tillering, stalk diameter and stalk height, number of green and dried leaves, leaf area index (LAI), leaf insertion angle, length and width, stalk weight and leaf dry and fresh mass (NASSIF, MARIN and COSTA, 2013). Additional data from the plant cane, 1st and 3st ratoon seasons in the same experimental field, were measured as part of the long-term detailed field experiment. The other six sites were used to evaluate PBM performance for different soil and weather conditions in Brazil (Table 5).

Table 5. Different Brazilian regions datasets description used for modelling development and assessment

Site	Planting and harvesting dates	Weather	Water treatment	Soil Type	Soil depth
União/PI 4°51'S,42°52'W, 68 m	9/29/2007 and 06/16/2008	27 °C, 1500 mm, Aw	Irrigated and Rainfed	Oxisol*	125 cm
Coruripe/AL 10°07'S,36°10'W, 16 m	8/11/2007 and 11/15/2008	24.4 °C, 1400 mm, As´	2 irrigation levels	Typic Hapludox*	40 cm
Coruripe/AL 10°07'S,36°10'W, 16 m	8/16/2005 and 09/15/2006	21.6 °C 1400 mm, As´	Rainfed	Typic Hapludox*	40 cm
Aparecida do Tab./MS 20º05S,51º18'W,335 m	7/1/2006 and 09/08/2007	23.5 °C, 1560 mm, Aw	Rainfed	Typic Hapludox*	400 cm
Colina/SP 20°25'S,48°19'W, 590 m	2/10/2004 and 12/01/2005	22.8 °C, 1363 mm, Cwa	Rainfed	Typic Hapludox*	400 cm
Olímpia/SP 20°26'S,48°32'W, 500 m	2/10/2004 and 12/01/2005	23.3 °C, 1349 mm, Cwa	Rainfed	Typic Hapludox*	400 cm

* Classification nearest according to U.S. Soil Taxonomy.

2.2.2.2. Calibration routine and model evaluation

A simple calibration routine was implemented to optimise any crop parameter, based on specific field data. An R-script was created, designed to read field data and run the crop modelling platform as a function by using the parameter file as an input array (i.e. Sugarcane.crop). The function simply runs the model and compare its results with field data, calculating the root mean squared error (RMSE) or any other statistical index of agreement (Wallach *et al.*, 2014). A General-Purpose function ("optim(x,fun)") is then employed to run the function with the PBM and try the convergence of RMSE by changing its parameter array (Figure 10). By default, optim() runs an implementation of that of Nelder and Mead (1965), but it is also possible to run it using quasi-Newton and conjugate-gradient algorithms with box-constrained optimisation and simulated annealing (R. and Reeves, 1964; Nelder and Mead, 1965; Nash, 1990; Byrd *et al.*, 1995; Vanderplaats, 1995).

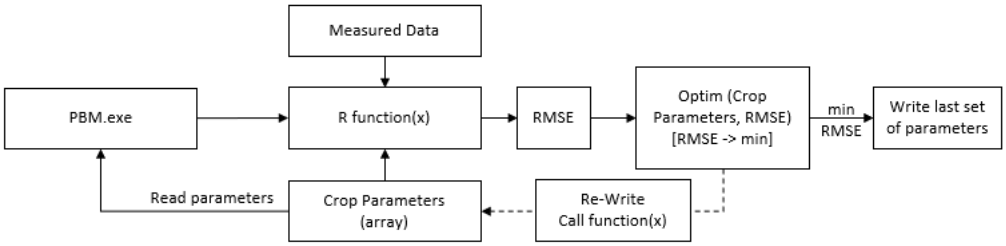

Figure 10. Schematic framework of a general-purpose calibration routine developed in R-Script. Where PBM is process based model in the compiled executable form; and RMSE is the root mean squared error set to be minimized by Optim() function

The constrained BFGS (Broyden–Fletcher–Goldfarb–Shanno) optimisation method (Byrd *et al.*, 1995) was selected to calibrate the SAMUCA model, focusing on tillering and canopy parameters. Initial parameter values and constrains were selected according to Marin and Jones (2014) and Singels and Inman-Bamber (2011). Because some state variables are dependent on others (i.e. soil surface temperature and crop canopy), the crop model shell includes a feature allowing to include the measured state variable value as input during simulation. This allowed to reduce the self-dependence between state variables, thereby improving calibration quality and time.

The soil evaporation and soil temperature algorithms were first calibrated with focus on empirical parameters of the evaporation method (a_z and b_z), soil mulch cover and bottom boundary conditions for soil temperature. Therefore, crop LAI were fixed by a fitted polynomial as a function of days after planting (only 2nd ratoon season), and the calibration procedure was applied to reduce the SWC measurement error for the first soil layer (10 cm). Soil temperature was then calibrated to obtain the mulch sand, silt, clay and organic matter content to meet the soil surface temperature measurements (below mulch). After soil water and temperature calibration, the crop parameters of the sugarcane model were then calibrated for the long-term (4 years) detailed experiment. Model performance was evaluated for the long-term experiment and for other sites (Table 5), based on mean averaged error (BIAS), root mean squared error (RMSE), correlation (r^2), agreement indices (d) and Nash-Sutcliffe model efficiency (E) (Wallach *et al.*, 2014). Because of the lack of information on soil composition, planting depth, mulch management and whether the crop cycle was of plant or ratoon, simulations for the other sites (Table 5) were performed considering only air temperature, and parameters related to soil temperature, such as tillering rate, emergence and root growth, were re-calibrated.

2.3. RESULTS AND DISCUSSION

2.3.1. Detailed Experimental Field (2nd ratoon)

Crop emergence occurred on 08/12/2014 (28 days after harvesting [DAH]), marked by slow growth and development until mid-September, mostly due to the cool temperatures and the lower rainfall amount in this period (Figure 12). With temperature and rainfall intensification in October, an overall increase in crop growth and development rate was observed, whereas the tillering peak occurred around 11/15/2014 (DAH = 123) in both treatments, characterising the beginning of the vegetative canopy closure phase (Figure 11). From 02/12/2015 (DAH = 140), the formation of the first mature aboveground culms was observed, indicating the beginning of the stalk extension stage and concomitant tillering senescence. At mid-March (DAH = 242), tiller senescence was stable, with

about 10 tillers m^{-2} in both treatments, while stalk height exceeded 2 m. During this period, the senescence rate of green leaves increased with the formation of new green leaves, making dry leaves appear at the base of the stalks.

Daily maximum temperature during the crop season was maintained at an average of 29°C, while daily minimum temperature presented an average of around 16°C (Figure 12). Daily global solar radiation averaged 22 MJ m^{-2} d^{-1} throughout the season, with values ranging between 25 and 30 MJ m^{-2} d^{-1} in summer and below 25 MJ m^{-2} d^{-1} in winter (beginning and end of season). Total rainfall during the crop cycle was 1,178 mm, with the dry season starting at the beginning to mid-October and more pronounced rains until mid-March. For operational reasons, irrigation was started in February with a single application of 30 mm on 02/24/2015 (DAH = 224) and another of 10 mm on 04/03/2015 (DAH = 232).

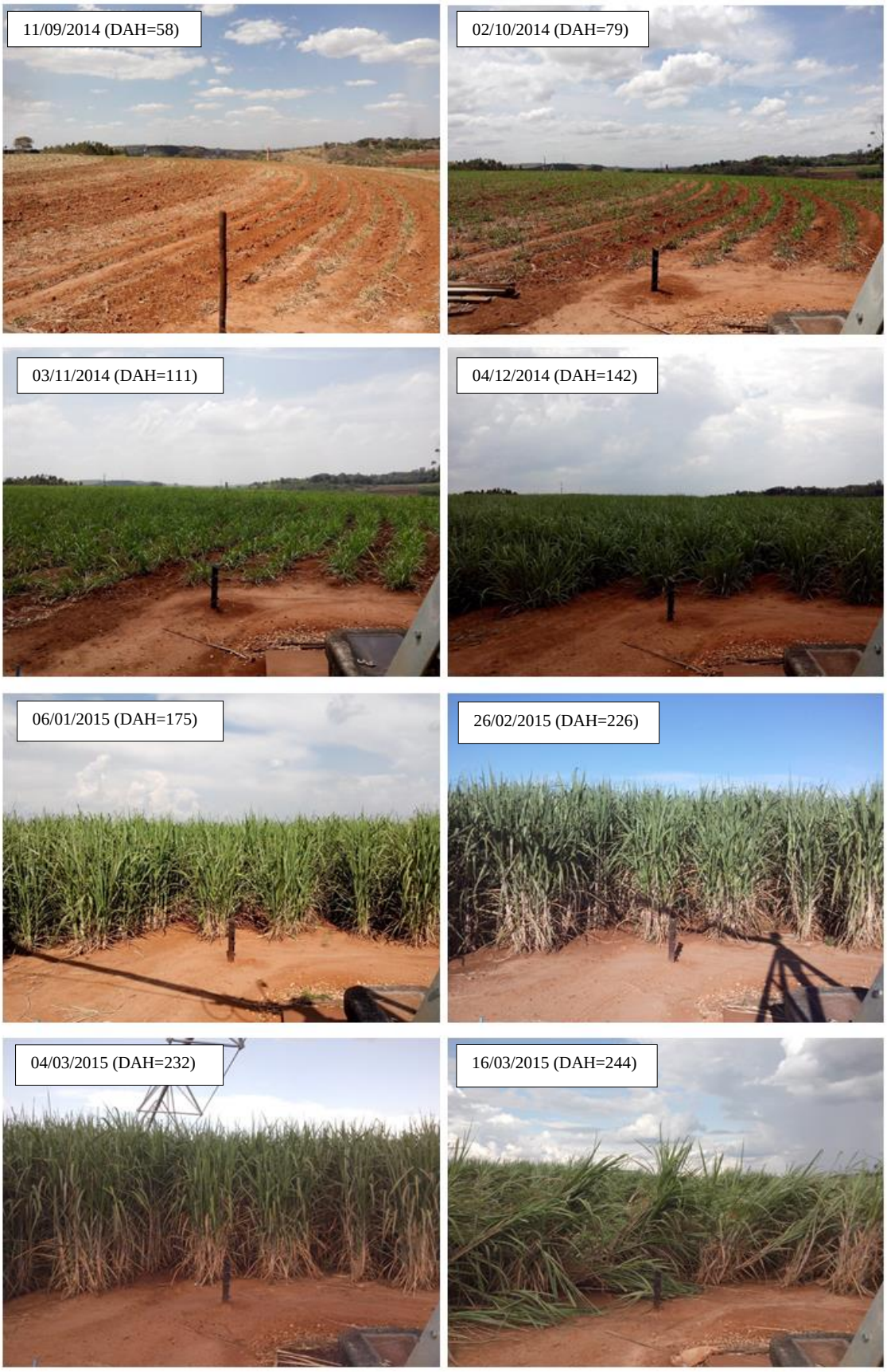

Figure 11. Crop growth and development throughout the 2nd ratoon season (wood stake height = 0.8m, as reference)

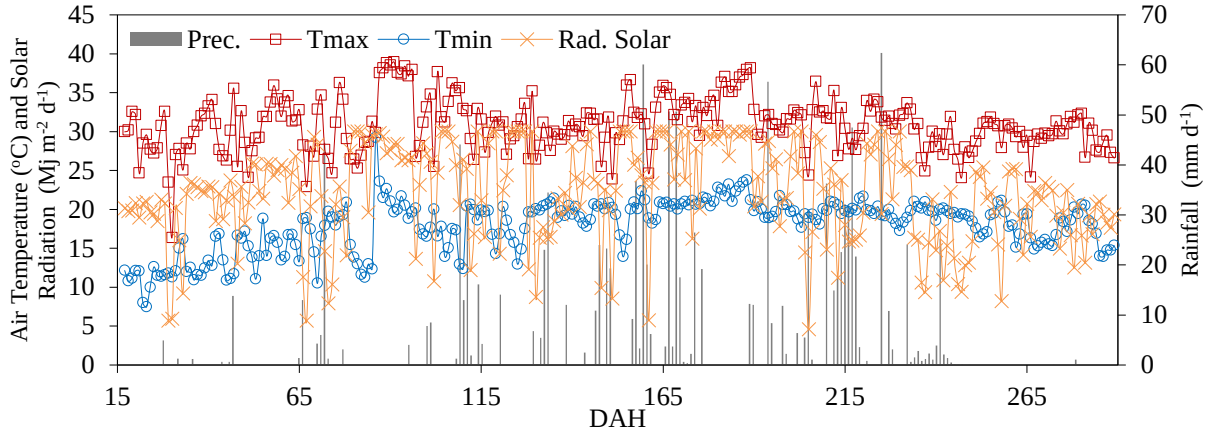

Figure 12. Maximum and minimum air temperatures, solar radiation and rainfall amount during the field experiment, in days after harvesting (DAH)

Crop lodging occurred at 03/15/2015 (DAH = 243) after a storm with 17 mm of rain over 2 hours and wind speeds of up to 60 km h^{-1} (Figure 11). Thereafter, growth of bended stalks and axial bud sprouting were noticed in lodged plants, while stand plants presented no morphological changes. Lodging in sugarcane fields is not a rare event, and besides of complicating harvest operations, it can reduce the crop sugar content used for laterally sprouted buds and/or for bending stalks (Bonnett et al., 2005; Bonnett, Salter e Albertson, 2001; Heerden, van et al., 2015; Singh et al., 2002). The lodging effect is not included in the model yet, but the collected data will support future implementation and testing of new algorithms to capture lodging effects (Baker, Sterling and Berry, 2014).

Most of the measured crop variables indicated no statistical difference throughout the season (Table 6). Leaf area index measurements were initiated on early October at 1.1 $m^2 m^{-2}$ and was 3.6 at mid-March, with an average variation of around 10%. The number of developed green leaves and the stalk diameter were constant throughout the season (Figure 14a and Figure 15b). The first dry leaf per plant was noticed at the time as the first mature internodes were emerged (Figure 14b) and ended at around 10 dry leaves per plant, revealing that most of the dry leaves of RB867515 in this experiment remained attached to stalks. This amount of dead biomass might decrease the radiation transmitted through the canopy and should be accounted for in light-dependent processes (i.e. tillering). Tillering was the only crop variable which was significantly impacted by the mulch cover (Figure 13b and Table 6). Tiller rate emergence was higher in the treatment without mulch until the peak of the population (DAH = 122); both treatments reached the tillering peak at the same time. After canopy closure and high competition for light, young tillers senesced until the establishment of around 10 tillers m^{-2}. Values of the leaf index area indicate that the contribution of young tillers to canopy formation is low, since no statistical difference was noticed, while a large difference (1.5-fold) was found for the plant population (Figure 13).

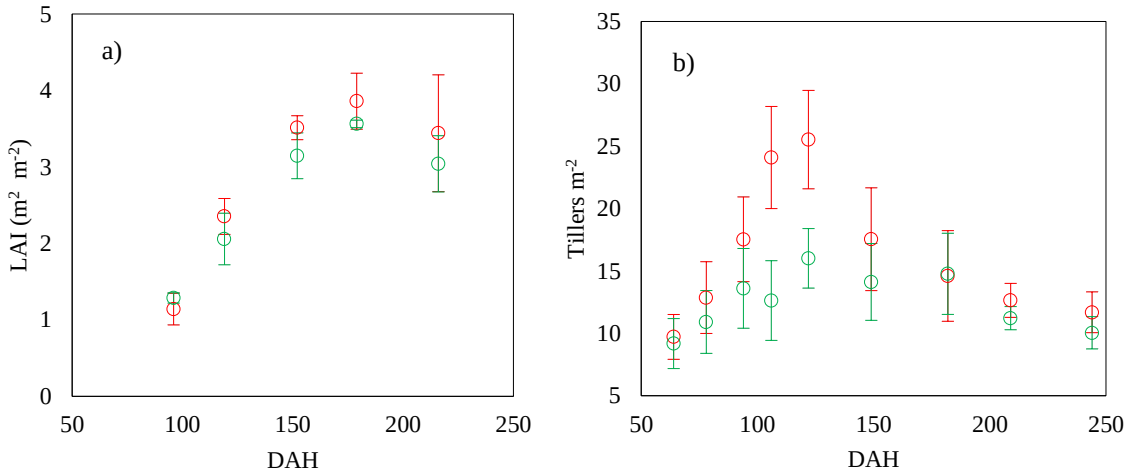

Figure 13. Measurements of leaf area index (a) and tillering (b), during the 2nd ratoon experiment for WM (green) and NM (red) treatments throughout days after harvesting (DAH)

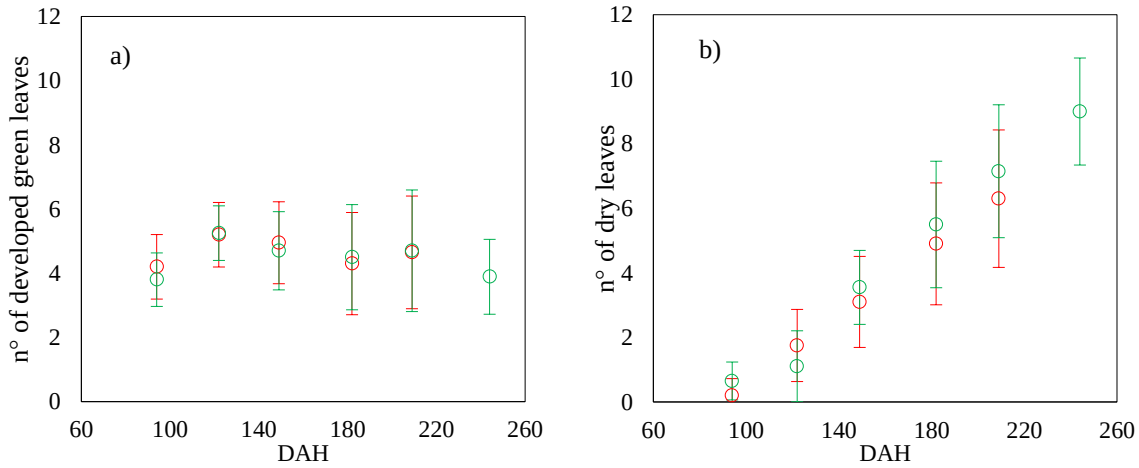

Figure 14. Measurements of number of developed green leaves per stalk (a) and number of dry leaves per stalk (b), during the 2nd ratoon experiment for WM (green) and NM (red) treatments throughout days after harvesting (DAH)

Stalk height was very similar in both experiments, starting to expand at a constant rate through 90 to 210 DAH and stabilising at a height of around 250 cm. It should be noted that only mature internodes (up to first leaf with dewlap formed) were measured for stalk height, while total plant height (stalks + canopy) was always higher. Fresh and dry stalk mass growth started after 100 DAH, when the first mature internodes appeared at the bottom of the plants (Figure 16). Stalk dry mass final yield was around 30 t ha^{-1}, whilst fresh mass yielded around 145 t ha^{-1}, with no statistical difference between treatments. Stalk water content usually ranged from 70 to 80% of total fresh mass, and the average water content in stalks throughout the season was 21 and 26% for the treatments WM and NM, respectively. Sucrose stalk accumulation and total extractable sugars were increased after 200 DAH, starting at 4% at 232 DAH and reaching up to 15% after 300 DAH (Figure 17).

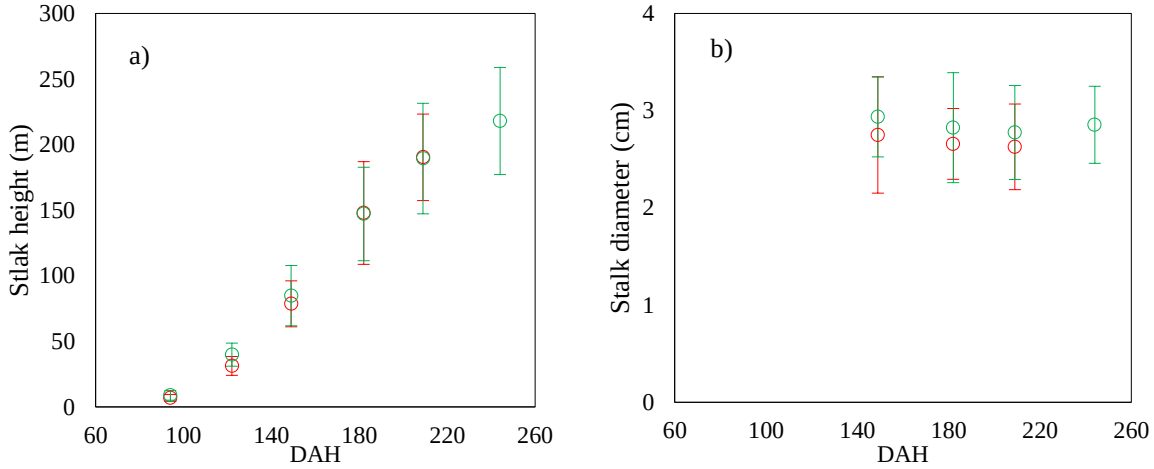

Figure 15. Measurements of stalk height (a) and stalk diameter (b), during the 2nd ratoon experiment for WM (green) and NM (red) treatments throughout days after harvesting (DAH)

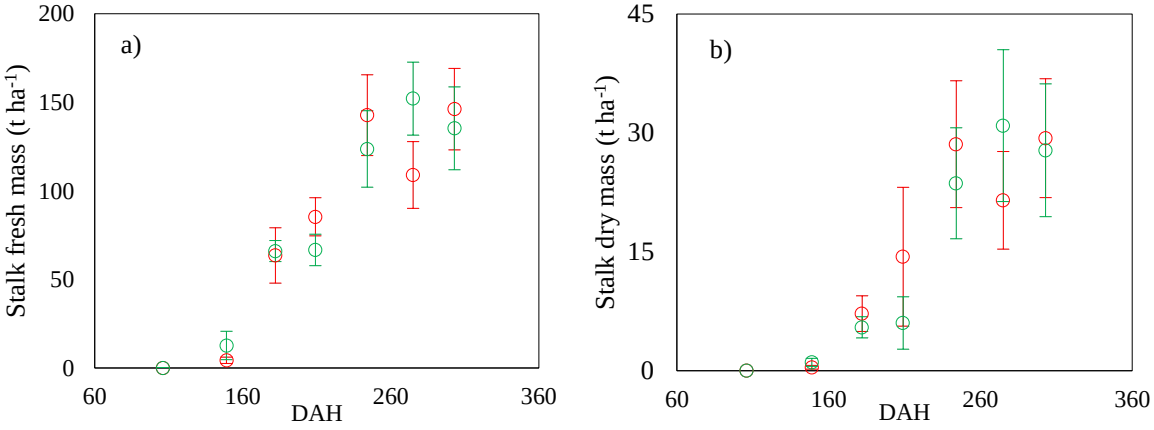

Figure 16. Measurements of stalk fresh mass (a) and stalk dry mass (b), during the 2nd ratoon experiment for WM (green) and NM (red) treatments throughout days after harvesting (DAH)

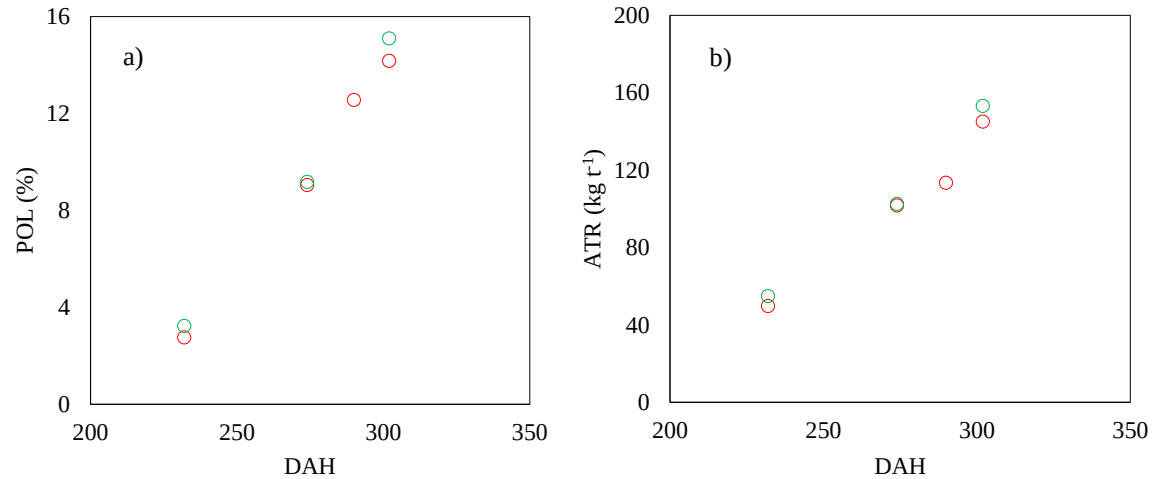

Figure 17. Measurements of sucrose content on fresh stalks (a) and total extractable sugars (b), during the 2nd ratoon experiment for WM (green) and NM (red) treatments throughout days after harvesting (DAH)

The most pronounced effects of mulch were observed for crop tillering, which was significantly lower in the mulch treatment at tillering peak (Figure 13b). In addition, a similar effect was found for soil temperature, which was considerably lower and with lower fluctuations in the treatment with mulch cover (Figure 18 and Figure 19). One of the hypotheses raised was that soil temperature, not only air temperature, should be considered in tillering simulation. Tillering could also be affected by a lack of nitrogen (Garside *et al.*, 2000), whereas the mulch cover could immobilise a considerable fraction of available nitrogen in the soil. However, measurements of chlorophyll content (leaf nitrogen level indicator) and leaf analysis indicated that nitrogen levels in the mulch treatment were even higher than in the treatment without mulch (Table 7), strongly suggesting that soil temperature was the main factor driving initial tillering. Therefore, a new model approach was implemented to simulate tillering based on soil temperature (Equations 11 and 12), indirectly including the effect of mulch on tillering and the fraction of light transmitted through the crop canopy in terms of intra-specific competition for light.

Table 6. Tillering (TILL), Leaf Area Index (LAI), Stalk Height (HGT), Stalk Fresh Mass (SFM) and Stalk Dry Mass (SDM) measured, variation coefficient (CV) throughout the season (months and DAH in brackets) and statistical differences (Tukey test p<5%) for With Mulch (WM) and Without Mulch (NM) treatments

Variable	Treatment	Sep (63)	Oct (105)	Nov (121)	Dec (148)	Jan (181)	Feb (208)	Mar (243)	Apr (274)
TILL (# plot^{-1})	WM	211.6 a	476.25 a	560.50 a	494.25 a	517.00 a	392.50 a	-	-
	NM	296.1 a	613.75 b	893.50 b	614.00 a	511.00 a	442.50 a	-	-
	C.V. (%)	12.2	10.46	7.87	22.44	22.07	7.07	-	-
LAI (m^2 m^{-2})	WM	-	1.14 a	2.35 a	3.51 a	3.86 a	-	-	-
	NM	-	1.29 a	2.06 a	3.15 a	3.56 a	-	-	-
	C.V. (%)	-	12.47	13.2	7.17	7.02	-	-	-
HGT (cm)	WM	-	8.80 a	39.85 a	84.83 a	147.10 a	189.35 a	-	-
	NM	-	6.85 a	31.25 a	78.60 a	147.85 a	190.30 a	-	-
	C.V. (%)	-	25.87	14.16	15.26	11.35	14	-	-
SFM (t ha^{-1})	WM	-	-	12.71 a	66.00 a	66.65 a	149.10 a	132.52 a	152.33 a
	NM	-	-	4.36 a	63.53 a	85.34 a	126.39 b	146.34 a	137.65 a
	C.V. (%)	-	-	68.16	18.22	13	14.35	16.68	11.69
SDM (t ha^{-1})	WM	-	-	1.06 a	5.47 a	6.02 a	29.82 a	23.20 a	30.34 a
	NM	-	-	0.44 a	7.20 a	14.38 a	24.30 a	29.27 a	27.67 a
	C.V. (%)	-	-	52.84	29.19	64.85	38.03	21.17	12.08

Table 7. Chlorophyll index (clorifiLOG, FALKER®) for Leaf +1 (CHLIDX) and nitrogen content (NCONT) sampled for Leaf+1 (n = 12) in December 2014 for With Mulch (WM) and Without Mulch (NM) treatments. Equal vertical letters do not differ from each other by the Tukey test at p <0.05 (n = 16)

Variable	Treatment	Nov	Dec	Jan	Feb	Mar
CHLIDX (dimensionless)	WM	56.17 a	55.23 a	46.93 a	53.54 a	51.03 a
	NM	53.41 b	50.22 b	42.22 b	48.88 b	48.22 b
NCONT (g kg^{-1})	WM	-	14.13 a	-	-	-
	NM	-	13.86 b	-	-	-

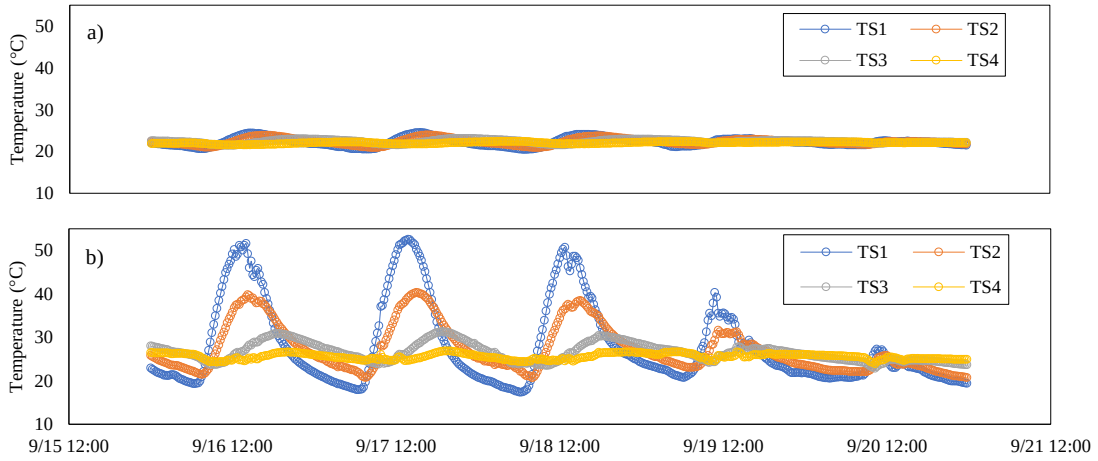

Figure 18. Soil temperature measurements from 9/16/2014 to 9/20/2014 at soil surface (TS1, 1cm), 5cm (TS2), 20cm (TS3) and 40cm (TS4) depth in 15 minutes time step for WM (a) and NM (b) treatments

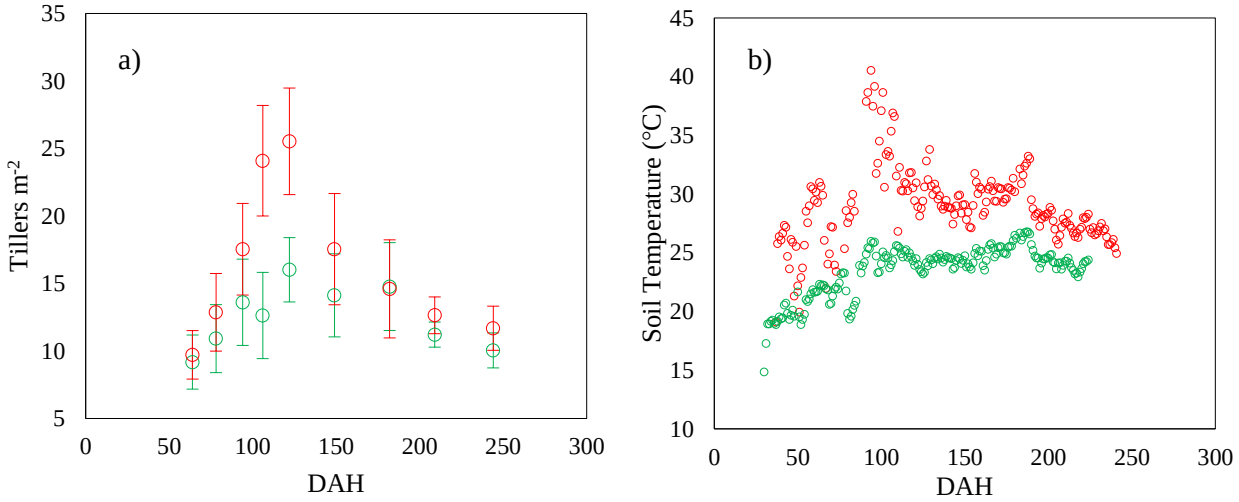

Figure 19. Average tillering and standard deviation (a) and soil temperatures (b) during the experiment for WM (green) and NM (red) treatment throughout days after harvesting (DAH)

No consistent nor statistical differences between treatments were found for the BRM measurements. Evapotranspiration was lower than reference evapotranspiration (ETo) from early crop development to canopy closure (DAH = 122). Thereafter, crop evapotranspiration was higher in the reference (Kc > 1) until lodging (Figure 20). This kind of field perturbation is not included in model predictions, leading to a prediction mismatch. Lodging is frequent in "Cwa" climates and has increased over the past years (Silva Dias *et al.*, 2013). The expected effect of lodging on soil-plant-atmosphere systems is at least a reduction of evapotranspiration rates, mainly due to a reduction in plant (i) transpiration caused by damaged stems and/or root systems; and (ii) in evaporation because of increased soil cover by biomass. Lodging affects not only sugarcane crops, but many crops cultivated under irrigated and windy conditions (Baker, Sterling and Berry, 2014). Physiologically, lodging is commonly accounted for in sugarcane crop models by reducing radiation use efficiency and sucrose levels due to stalk damage and geotropism expansion. This can be simulated by empirical relations to plant height and wind speed (van Heerden *et al.*, 2015) or physically through moment forces, soil conditions and crop canopy and root systems (Baker, Sterling and Berry, 2014).

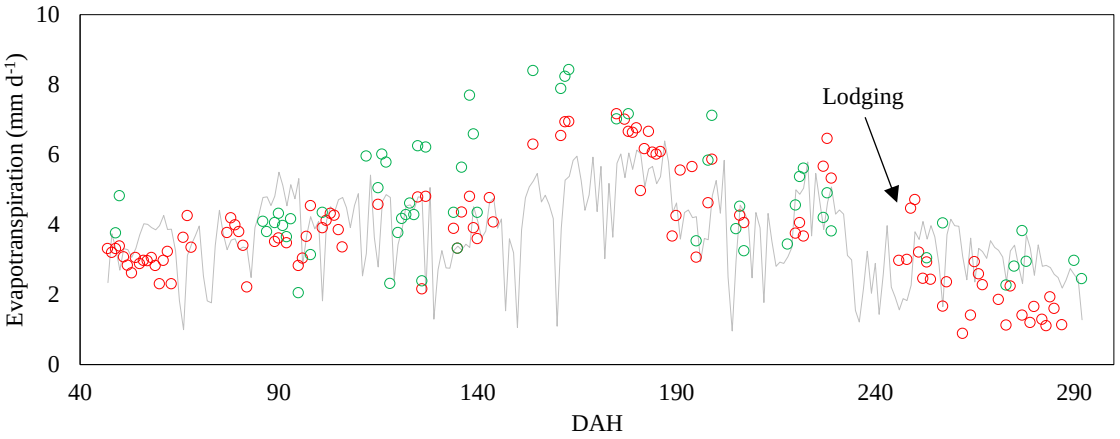

Figure 20. Sugarcane evapotranspiration for WM (green open circles) and NM (red open circles) treatments, and reference evapotranspiration (grey line) throughout days after harvesting (DAH)

Soil moisture was slightly higher in the treatment WM (> 10% average at a depth of 10 cm) from early crop development until canopy closure. After canopy closure, no differences in soil moisture were noticed (Figure 21). Mulch cover is expected to reduce soil evaporation and could potentially reduce evaporation losses up to 200 mm year^{-1} in sugarcane fields (Porter *et al.*, 2009; Olivier and Singels, 2012). Prior to canopy closure, soil evaporation is the dominant component of evapotranspiration; when the canopy is completely formed, transpiration accounts for more than 95% of evapotranspiration (Nassif, 2015). In addition, the most pronounced effect of the soil mulch cover was observed at a depth of 10 cm, albeit only for inter-row measurements, while measurements in the crop rows presented no consistent difference between treatments (Figure 22). Based on this result, crop fields with rapid canopy closure or/and shorter row spaces might offset the beneficial effect of mulch cover in terms of evaporation reduction. Besides, mulch cover has a range of other benefits, such as facilitating soil microbial growth and improving the soil structure (Costa *et al.*, 2014).

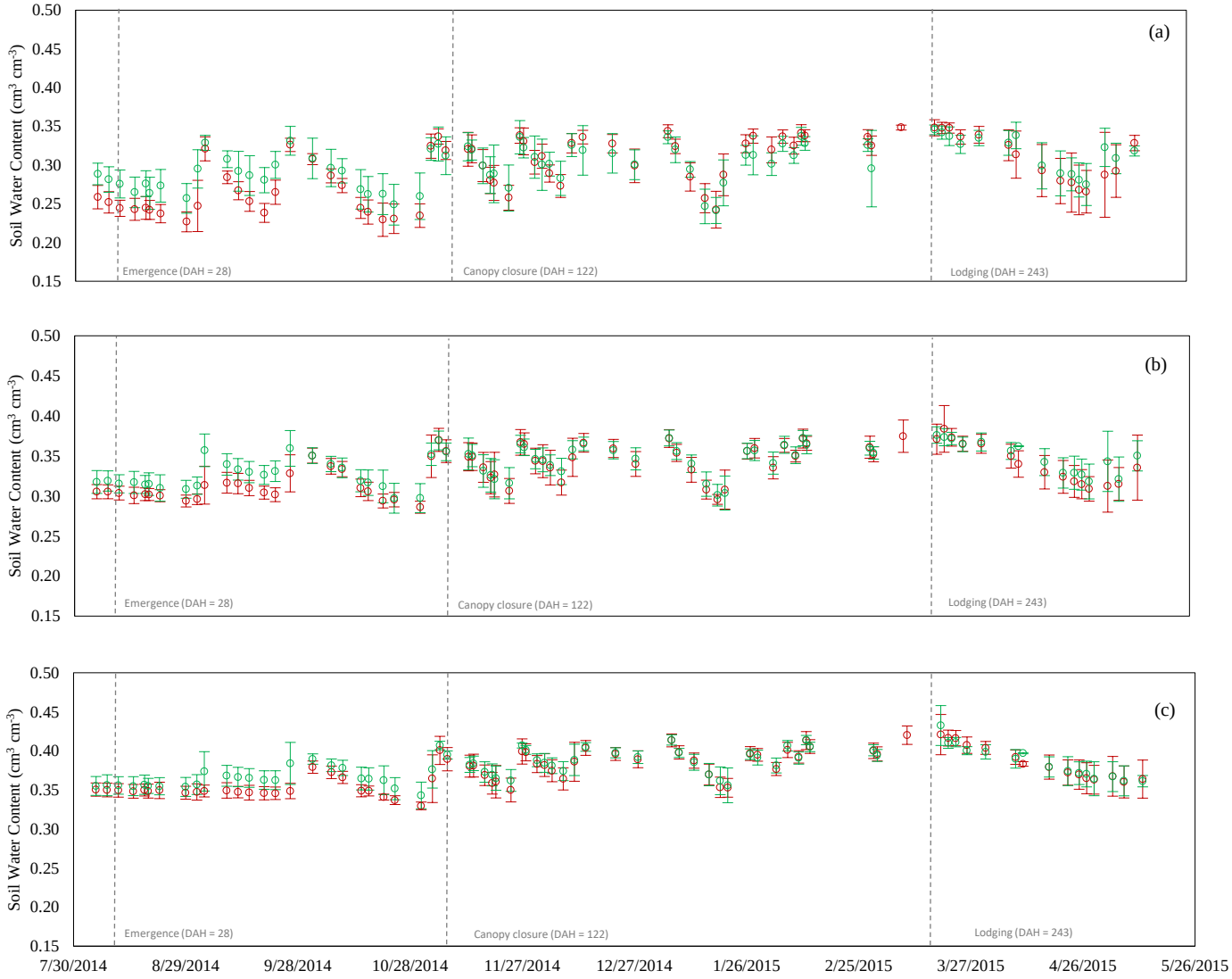

Figure 21. Measured soil water content ($cm^3\ cm^{-3}$) at 10cm (a), 30cm (b) and 60cm (c) depth for WM (green circles) and NM (red circles) treatments. Standard deviation is included as underlying bars (n=12) throughout dates and Days After Harvesting (DAH)

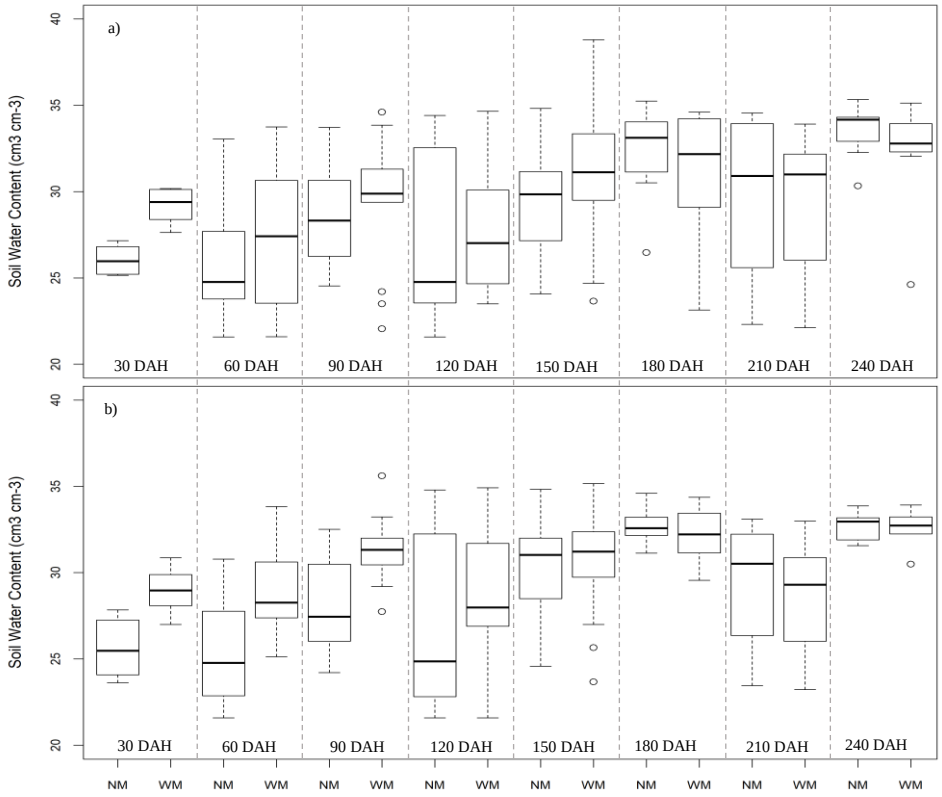

Figure 22. Soil water content measurements distribution (BoxPlot) at 10cm depth throughout the crop season (30 days ensembles) for the with mulch (WM) and without mulch (NM) treatment at planting row (b) and at inter-row (a). Vertical dashed lines separate values ensembles by 30 DAH

2.3.2. Model calibration and performance: Long term experiment

The calibrated soil evaporation algorithm (Ritchie *et al.*, 2009) was able to simulate differences between treatments (Figure 23). By providing the initial soil content (FDR, measurements) of the first soil layer, the calibration algorithm yielded the empirical parameters (Table 8), with minimum RMSE values of 0.034 and 0.041 $cm^3\ cm^{-3}$ for the treatments WM and NM, respectively. The method was able to capture soil moisture variations due to evaporation rates at early crop development, and as transpiration rates increase, evaporation becomes the smaller fraction (less than 5%) of the total evapotranspiration flux. The parameters used for calibration were residue cover (M_{mulch} = 12 t ha^{-1}), mulch water content capacity (Sm = 3.8 kg kg^{-1}), area covered (A_m = 32 g cm^{-2}), mulch extinction coefficient (0.8) and mulch albedo (0.4) (Porter *et al.*, 2009).

Table 8. Calibrated empirical coefficients for transmission of Ritchie (2009) soil evaporation algorithm for dry, equilibrium and wet condition

Empirical Coefficients	Dry	Equilibrium	Wet
a_z	0.568	0.011	0.260
b_z	2.11	0.000	-0.91

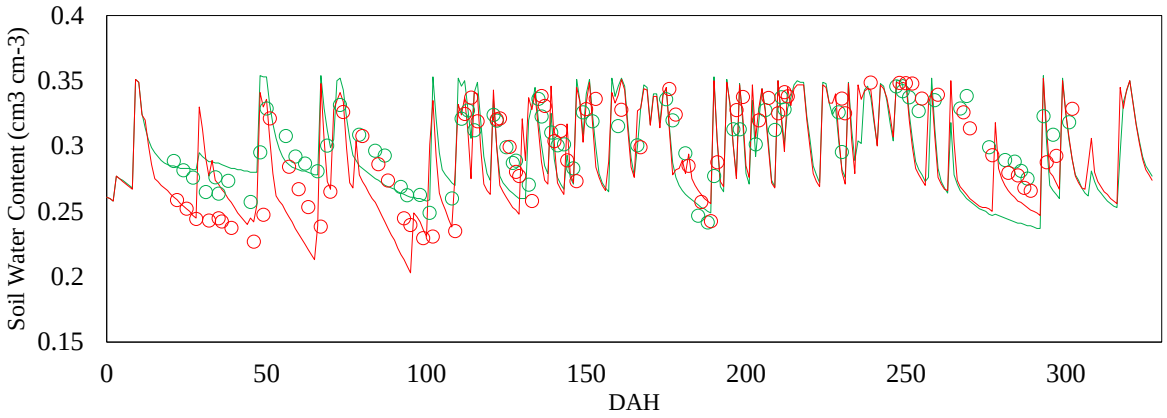

Figure 23. Measured (open circles) and simulated (lines) soil water content at 10cm depth for WM (green) and NM (red) treatments. Calibration procedure only for 2nd season

The calibrated soil temperature algorithm was able to reproduce temperature changes with soil depth (Figure 24). It should be noted that the soil water evaporation routine was first calibrated due to the dependence of soil water moisture on soil heat capacity and conductance (Kroes *et al.*, 2009). In addition, for calibration, the measured surface soil temperature was used as input, and only the bottom condition was computed by the synodal equation, relating annual mean and amplitude temperature, soil depth and soil thermal diffusivity (Tmean = 21°C; Ampli = 5°C; Ddamp = 350 $cm^2\ d^{-1}$). For calibration, initial mulch layer sand, silt and clay contents were set to zero, and an arbitrary organic matter content of 100% was assumed; mulch thickness was computed based on total area coverage and mass (h = 4.3 cm) (Porter *et al.*, 2009). Because mulch surface temperature was unknown, Equation 2 was used to simulate mulch surface temperature (mulch albedo = 0.4) (Figure 24b). Therefore, the soil surface temperature beneath the mulch layer was fitted, keeping mineral contents at zero, while the mulch organic matter content was optimised to 37.16%. The temperature dampening effect of mulch was obtained after calibration with a reduction of up to 10°C of soil temperature (Figure 24b). After canopy closure, soil surface temperature agreement beneath the mulch was weaker than in early development; however, the temperature range simulated agreed with the measured data, stabilising at 24°C (Figure 24b). Despite the uncertainty in terms of mulch surface temperature, the damping effect of temperature was accomplished by the mulch layer, and further mulch surface temperature measurements must be taken to reduce uncertainty.

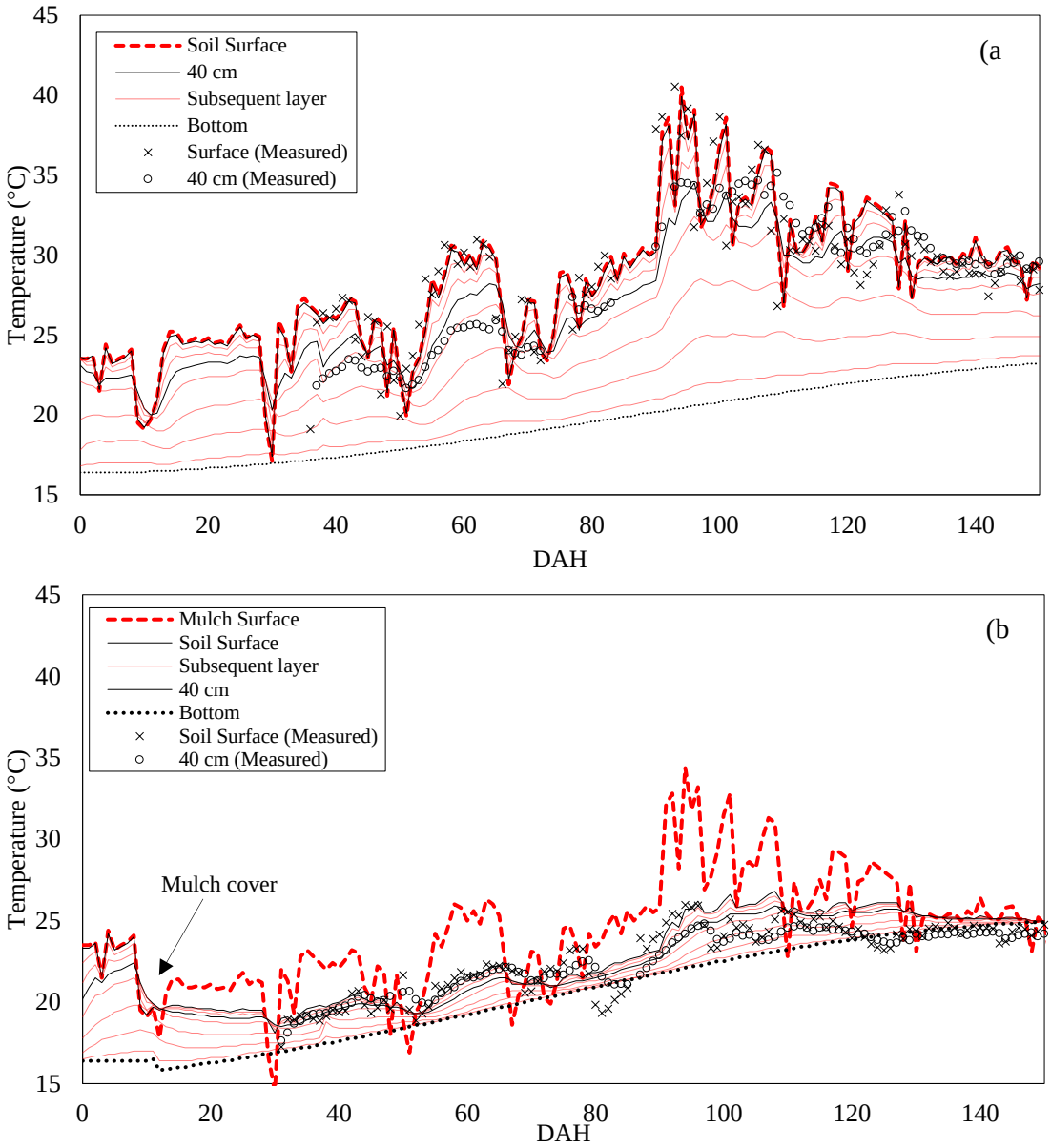

Figure 24. Simulated (lines) and measured (markers) temperature at soil surface, in subsequent layers and at bottom soil profile for without mulch treatment (a); Simulated (lines) and measured (markers) temperature at mulch surface, soil surface beneath mulch, subsequent layers and at bottom soil profile for with mulch treatment (b). Canopy closure was at around 120 DAH (DAH is Days after Harvesting)

Calibrated crop parameters for the long-term experiment are shown in Table 9. Parameters related to phytomer initiation, tillering, lignin content and hexoses use rate, shoot growth rate and ratooning depth were optimised, while the others were derived from experimental data or the literature. The photosynthesis curve was fitted to assimilation measurements of the first year (plant cane), and base temperatures were maintained at levels described for the previous version.

Table 9. Crop parameters for cultivar RB867515 based on long term experiment. Values with (*) were calibrated by the constrained BFGS method. Values separated by slashes are those assumed for simulations with (left) or without (right) soil temperature

Parameter	Value	Unit	Parameter	Value	Unit
Amax	67.8	Kg_{CO2} $ha^{-1}{}_{leaf}$ h^{-1}	Tbper	16	°C
Eff	0.33	Kg_{CO2} J^{-1} absorbed	tbMax_per	45	°C
TB	12	°C	tb0pho	10	°C
CHUMAT	4000	°C days	tb1pho	16	°C
PHYLOC	114*/102*	°C days $leaf^{-1}$	tb2pho	36	°C
MRDP	100	Cm	Tbfpho	42	°C
K	0.55	-	Hexuserate	0.05*	frac d^{-1}
DPERCORF	6.5	mm h^{-1}	Maxlignin	1.82*	g $internode^{-1}$
MAXGL	10	#	Mxitstrucw	8.5	g $internode^{-1}$
SLA	160	cm^2 g^{-1}	init_plantdepth_ratoon	12.1*	cm
MLA	780	cm^2	dswat_ddws	4.01*	t_{water} $t_{drymass}^{-1}$
lfshape	5	-	dswat_dsuc	1.49*	t_{water} $t_{sucmass}^{-1}$
maxndgl	5	#	SrlRF	22	m_{root} g_{root}^{-1}
kmr_leaf	0.00292	g_{CH2O} $g^{-1}{}_{DW}$ d^{-1}	srl	16	m_{root} g_{root}^{-1}
kmr_root	0.00292	g_{CH2O} $g^{-1}{}_{DW}$ d^{-1}	Mxrtw	152	g m^{-2}
kmr_stor	0.00121	g_{CH2O} $g^{-1}{}_{DW}$ d^{-1}	Rssshape	4	-
tref_mr	25	°C	rtdvp_time	2000	°C days
Q10MR	1.68	-	Rootleftfrac	0.03	0-1
init_it_diameter	2.5	cm	Rootdrate	0.036*/0.048*	cm °C $days^{-1}$
init_leaf_area	15	cm^2	shootgrowthrate	0.05*/0.09*	cm °C $days^{-1}$
init_stalkfw	1.5	kg $stalk^{-1}$	sens_pho	1	-
init_stalkht	2	m	sens_exp	1.5	-
nstalks_planting	2	#	KcMin	0.75	-
ltthreshold	0.18*	0-1	KcMax	1.15	-
tillochron	55*/49*	°C days $tiller^{-1}$	SWSP	0.3	0-1
tillerdeadrate	0.1*	frac d^{-1}	SWSE	0.9	0-1
nsenesleaf_effect	3*	#	fb_res	0.05	0-1

Simulations of soil water content agreed with measured data mostly when sugarcane was in the rapid growth phase, while transition periods, when the crop was not emerged, were more problematic. At the final season of the 1st ratooning (DAS = 610), a steeper water withdrawal was observed in both treatments, most likely due to root water uptake (Figure 25). Despite being widely used and tested (Ritchie, 1998), the implemented routine of root water uptake also overestimates soil water depletion due to its logarithmic relation to root length density (Singels *et al.*, 2010). Evapotranspiration was limited in the same period by the low soil water availability due to rapid depletion. After lodging (DAS = 958), simulated soil water content was underestimated because the model is not designed to simulate lodging events in sugarcane; in turn, simulations were not affected by lodging considering (erroneously) normal soil-plant-atmosphere conditions. Even though mismatching the initial soil conditions, especially at season transitions, soil water content simulation during canopy development and stalk growth showed satisfactory results. For both treatment simulations, the accuracy level was higher than 0.85, with an averaged error of 0.03 cm^3 cm^{-3} (Table 10). In addition, the soil water routine was able to simulate the mulch cover effect on soil evaporation, showing consistent differences in soil moisture at season transitions, when soil evaporation is the major fraction of evapotranspiration.

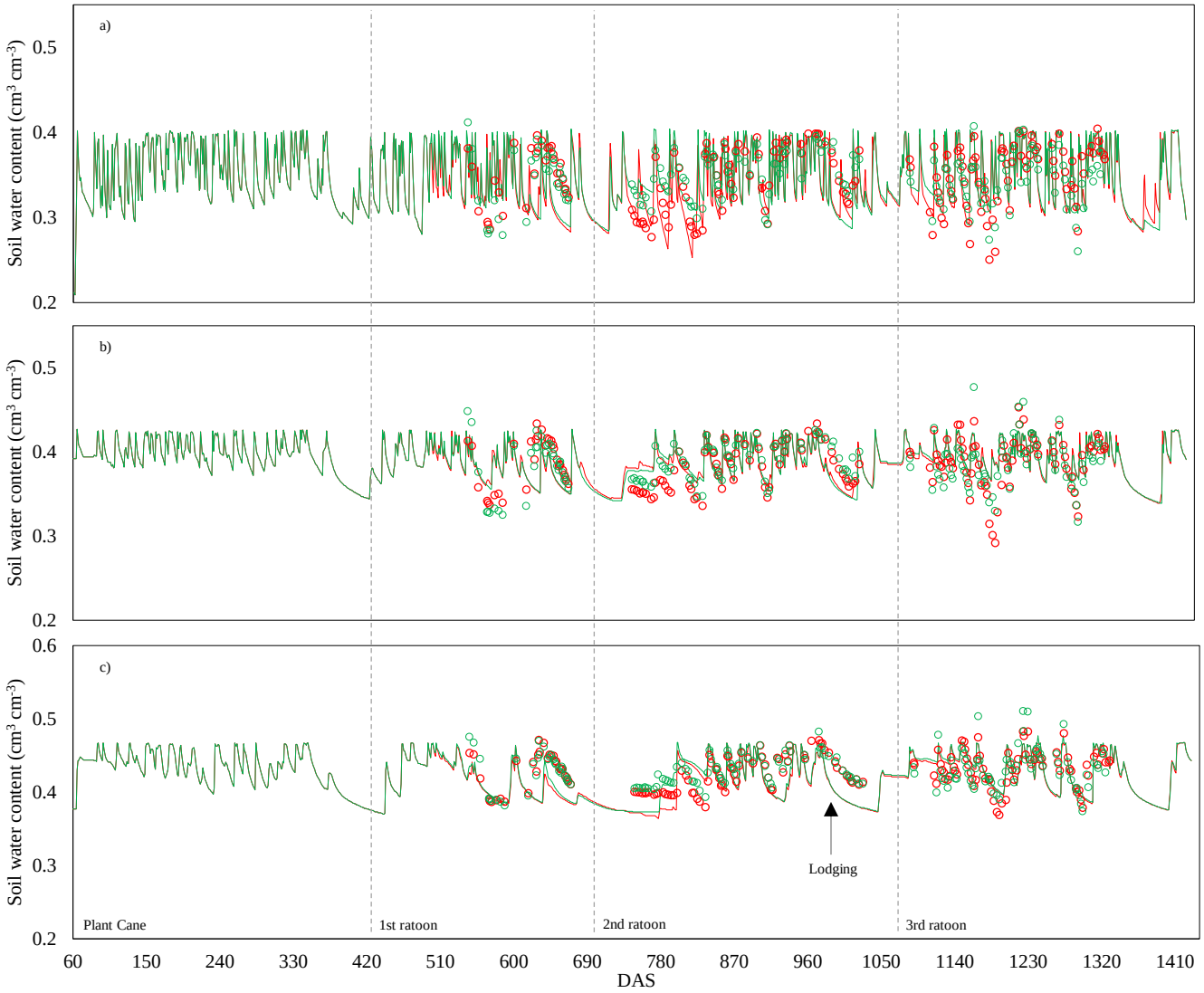

Figure 25. Soil water content simulated (lines) and measured (open circles) at 10cm (a), 30cm (b) and 60cm (c) depth for the WM (green) and NM (red) treatments during the long-term experiment (DAS= Days After Simulations Started)

The simulated evapotranspiration range for the treatment NM was within the measurement range. Although presenting poor statistical agreement, all simulations for the treatment NM at different seasons (but 1st ratoon) agreed well with the MRB measurement range (Figure 26a). In the treatment WM, evapotranspiration rates were underestimated at mid-season of 1nd and 2rd ratooning sugarcane and overestimated for the 3rd ratoon (Figure 26b). At the 3rd ratoon, measured data showed that soil water content reached critical levels, at which the model was not able to capture transpiration, and possibly, a lower reduction of potential transpiration was computed. In addition, the model could simulate the evapotranspiration fractions (evaporation and transpiration) during the seasons; soil evaporation was the major fraction at early crop development and stabilised at around 0.5 mm d^{-1} after canopy closure (Figure 26).

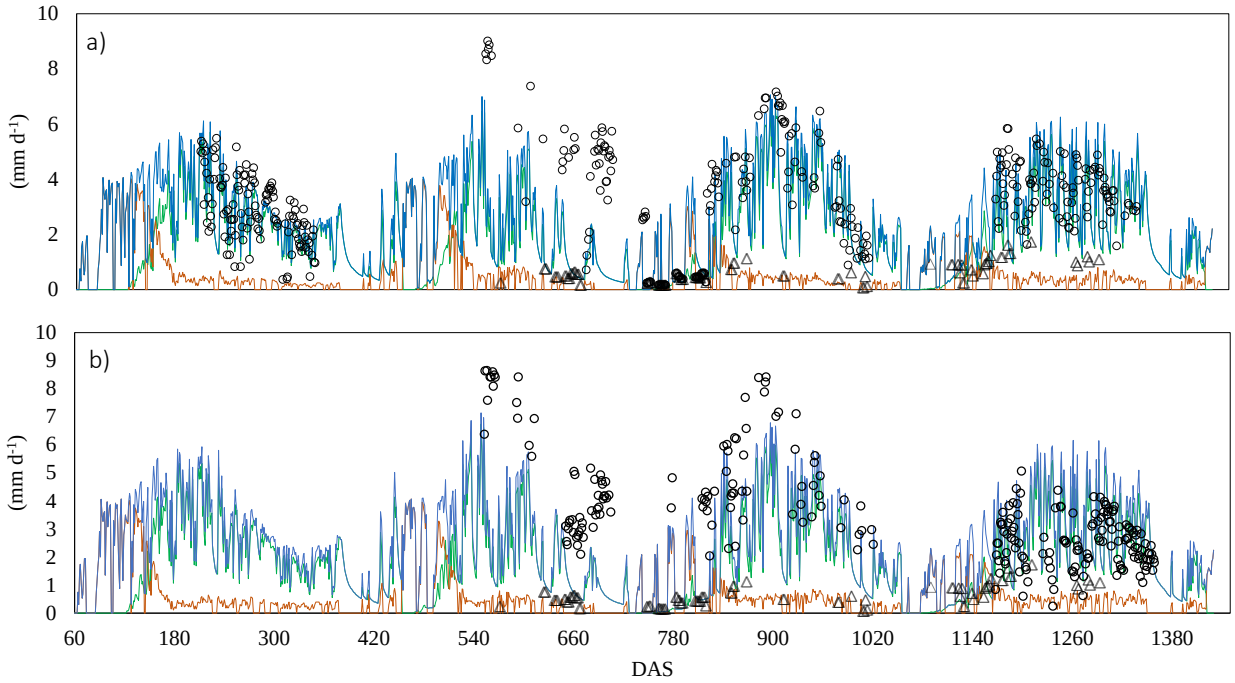

Figure 26. Simulated (lines) and measured (markers) evapotranspiration (o) and soil evaporation (Δ) for the with (b) and without(a) mulch during the long-term experiment (DAS= Days After Simulations Started)

Soil temperature was better simulated for the treatment without mulch (NM) due to the high temperature variation in bare soil. In addition, soil temperature was affected by the soil water content and the rapid canopy development. When canopy closure was anticipated, soil surface temperature in the treatment NM was underestimated due to a combination of light transmission and heat diffusivity resistance (rH). On the other hand, in the treatment WM, the root mean squared error (RMSE) was 1.2°C, agreeing with the measurements, while in the treatment without mulch, it was around 3°C. Nevertheless, in the long term, both treatments agreed well with soil temperature measurements (Figure 28), and the average values of the simulated soil temperatures were considerably similar to the observed values (Table 10). Although soil temperature data for transition periods were not available, the model was sufficiently robust to simulate the difference in soil temperature among seasons because of the mulch cover and the abrupt soil temperature transitions between seasons (DAS 726 to 735 and DAS 1064 to 1097 in Figure 28).

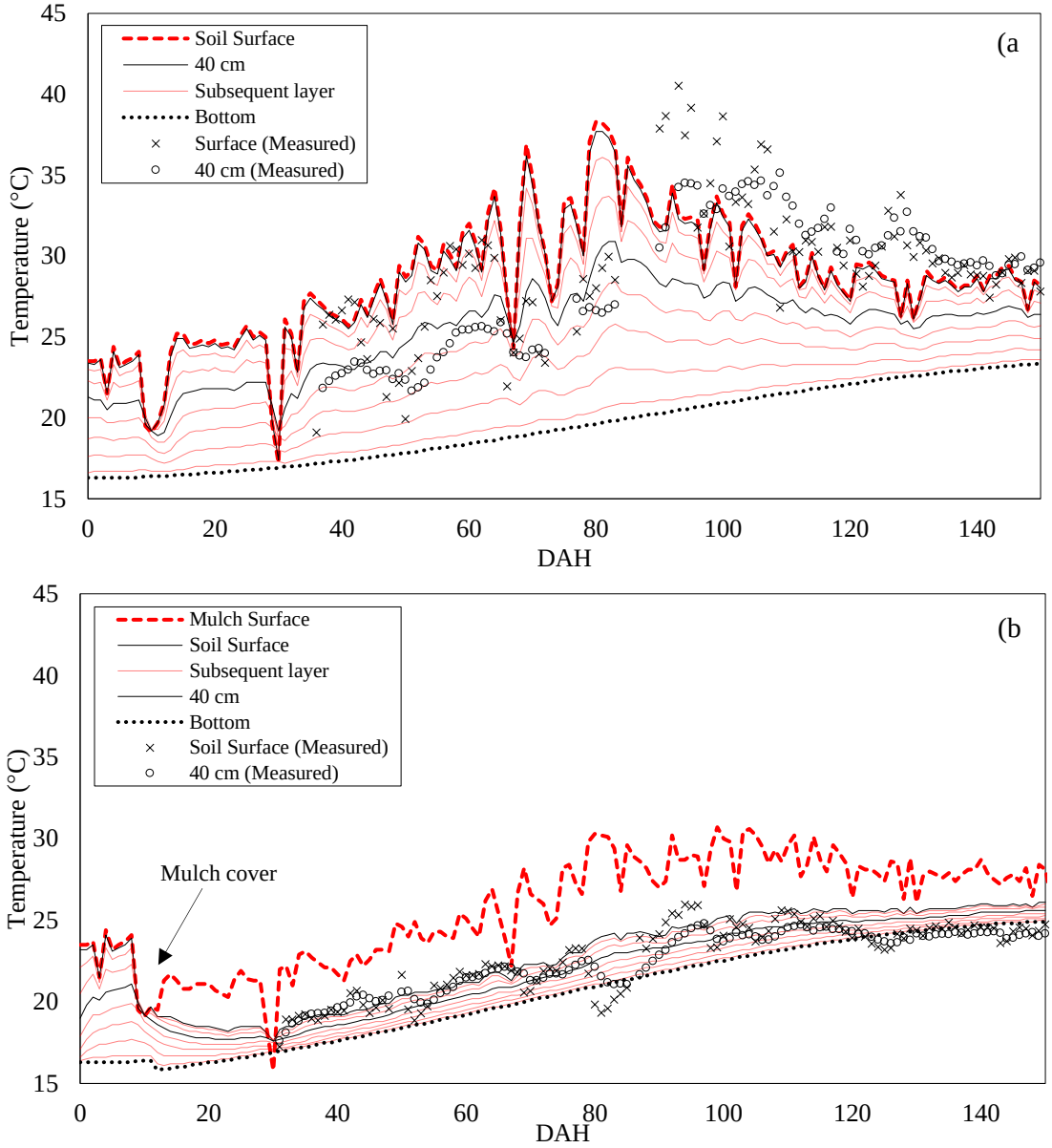

Figure 27. Simulated (lines) and measured (markers) temperature at soil surface, in subtending layers and at bottom soil profile for without mulch treatment (a); Simulated (lines) and measured (markers) temperature at mulch surface, soil surface beneath mulch, subsequent layers and at bottom soil profile for with mulch treatment (b) (DAH is Days after Harvesting)

Table 10. Statistical indexes of model performance of soil water content, soil temperature and evapotranspiration during the long-term experiment for With Mulch (WM and Without Mulch (NM) treatments. RMSE is the root mean squared error, EF is the modelling efficiency, r^2 the precision index, d is the Wilmot accuracy index. Observed and simulated averaged values are also presented as Obs and Sim respectively

Variables	Treatment	Bias	RMSE	EF	r^2	d	Obs	Sim
θ (cm^3 cm^{-3})	WM	-0.005	0.030	0.539	0.604	0.874	0.338	0.333
	NM	-0.005	0.032	0.488	0.552	0.853	0.338	0.332
Soil Temperature (°C)	WM	0.771	1.227	0.591	0.837	0.916	24.200	23.433
	NM	-0.471	3.056	-0.019	0.075	0.506	28.334	28.958
Evapotranspiration (mm d^{-1})	WM	-0.928	2.663	-1.412	0.001	0.378	3.576	2.648
	NM	-0.587	1.978	-0.252	0.179	0.668	3.292	2.705

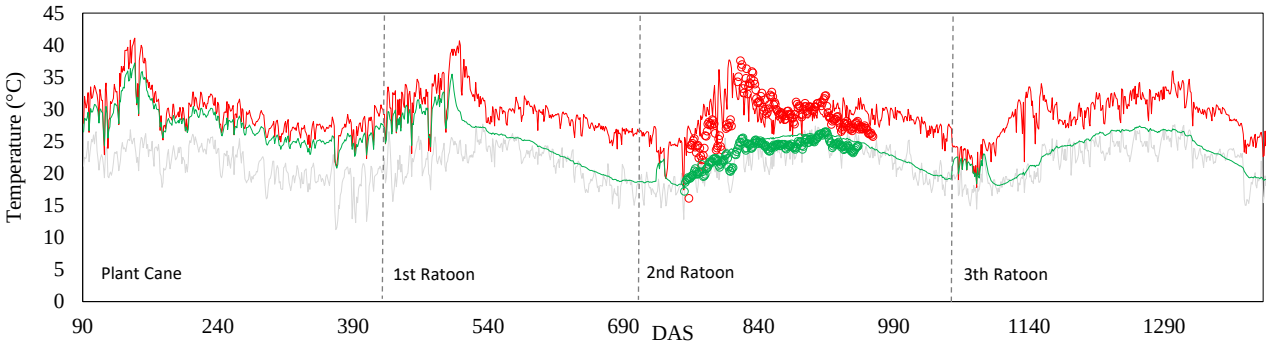

Figure 28. Simulated (lines) and measured (circles) soil temperature in the long-term experiment for the WM (green) and NM (red) treatments throughout days after simulations started (DAS). Grey line is the air temperature measured at 2m

The overall performance of SAMUCA to simulate crops components and processes in the long-term experiment was satisfactory (Figure 29 and Table 11). The average accuracy and determination indices for fresh and dry stalk biomass were 0.95 and 0.89, respectively, for both treatments. The slight systematic difference between treatments was accounted for due to different development rates, including soil temperature difference between treatments (Figure 29a and Figure 29b). Though generally reported in Brazilian sugarcane fields, yield decrease in successive seasons was not observed in this experiment, possibly because of the manual harvesting rather than harvesting with heavy machinery, which is common in commercial sugarcane crops. Simulation of leaf area index (LAI) presented an accuracy level of 0.84 and 0.68 for the treatments with and without mulching, respectively, and 0.28 and 0.58 precision (Table 11). A lower performance was obtained for the 1st ratoon, representing the driest season, and irrigation was suspended because of a water crisis in Sao Paulo (Coutinho, Kraenkel and Prado, 2015).

The tillering algorithm was able to satisfactorily simulate the differences in tillering peaks for the 2nd and the 3rd ratoon and for senescence s (Figure 29d), with an RMSE of 3 tillers m^{-2} and good levels of precision and accuracy (Table 11). Sucrose content of the fresh mass (POL, %) presented an averaged overestimation of 2% in both treatments in the early phase of the cycle (Figure 29e), with an RMSE of 2.57 and 2.42% for T1 and T2, respectively (Table 11). Results obtained by Singles et al (2008) in South Africa showed a similar trend, overestimating sucrose content primarily in the early phase of the cycle. Nonetheless, final values of POL ranged between 10 and 15%, which is a common range in commercial fields (van Heerden, Eggleston and Donaldson, 2013; Cardozo *et al.*, 2015). The number of developed green leaves (NDGL) yielded low precision ($r^2 = 0.046$), but simulated averaged values (sim_{T1} = 4.8 and sim_{T2} = 4.7 leaves $tiller^{-1}$) were close to the measured values (obs_{T1} = 4.6 and obs_{T2} = 5.0 leaves $tiller^{-1}$). In addition, the timing for the maximum number of green leaves matched with observations (Figure 29f); a further detailed database with all green leaves per shoot rather than only developed green leaves would enable a better assessment of phytomer initiation, possibly including the delayed time for leaf appearance. The transition of the apical meristem from soil temperature (hotter) to air (cooler) is used to mimic the "broken stick" phenomenon of leaf appearance, generally modelled with two phyllochron values (Singels, Jones and Berg, 2008; Bonnett, 2013). Stalks heights were simulated with 0.5 RMSE (m) for T1 and T2, respectively (Figure 29g and Table 11); no substantial difference between treatments were expected, since stalk height was simulated as a function of air temperature, considered equal for both treatments, and soil water condition, whereas the mulch effect on soil evapotranspiration is only pronounced before canopy closure.

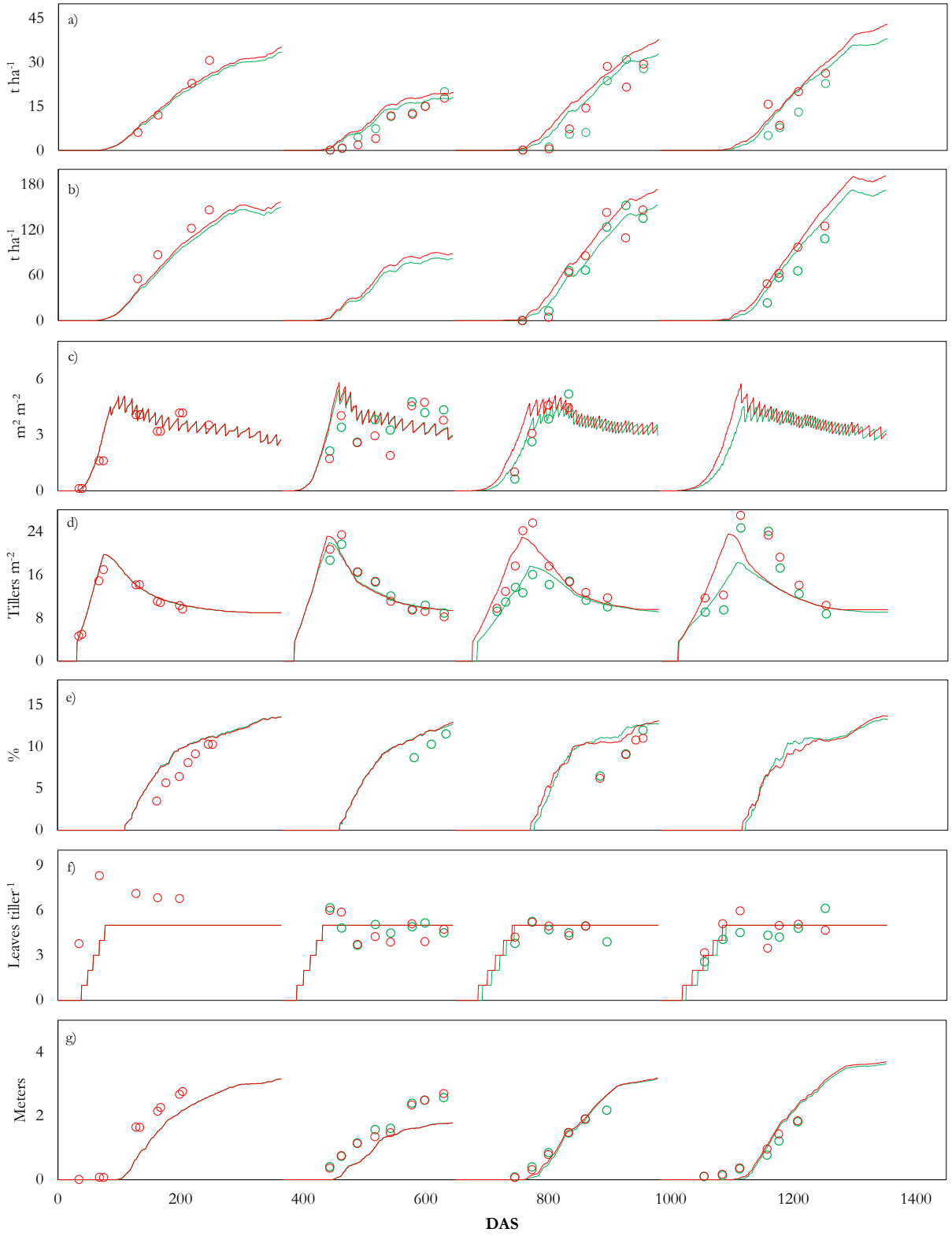

Figure 29. Simulated (lines) and measured (circles) stalk fresh mass (a), stalk dry mass (b), LAI (c), tillering (d), POL (e), developed deaf number (f) and stalks height (g) for WM (green) and NM (red) treatments throughout the days after simulation started (DAS)

Table 11. Statistical indexes of performance of SAMUCA model for the long-term experiment under WM and NM treatments, for Stalk Fresh Mass (SFM) and Stalk Dry Mass (SDM), Leaf Area Index (LAI), Tillering (TILL), Sucrose content (POL), Number of Developed Green Leaves per stalks (NDGL) and Stalk Height (HGT). RMSE is the root mean squared error, EF is the modelling efficiency, r^2 the precision index, d is the Wilmot accuracy index. Observed and simulated averaged values are also presented as Obs and Sim respectively

Variable	Treatment	Bias	RMSE	EF	r^2	d	Obs	Sim
SFM (t ha^{-1})	WM	5.824	14.442	0.911	0.926	0.976	73.686	79.510
	NM	4.193	18.979	0.828	0.848	0.956	86.225	90.418
SDM (t ha^{-1})	WM	3.324	4.539	0.768	0.893	0.942	11.286	14.610
	NM	3.080	4.927	0.747	0.847	0.934	13.316	16.396
LAI (m2 m^{-2})	WM	0.179	1.037	0.256	0.284	0.680	3.387	3.567
	NM	0.399	0.996	0.487	0.581	0.848	2.992	3.391
TILL (# m^{-2})	WM	-0.571	2.990	0.578	0.594	0.847	13.750	13.179
	NM	-0.106	3.155	0.676	0.677	0.900	14.341	14.234
POL (%)	WM	2.191	2.572	-0.927	0.738	0.570	9.703	11.893
	NM	2.174	2.420	-0.063	0.838	0.745	8.224	10.398
NDGL (# $stalk^{-1}$)	WM	0.219	0.680	0.231	0.371	0.767	4.591	4.810
	NM	-0.365	1.479	-0.449	0.046	0.439	5.045	4.680
HGT (m)	WM	-0.197	0.498	0.627	0.720	0.905	1.211	1.255
	NM	-0.314	0.502	0.724	0.835	0.920	1.014	0.942

Simulated fractions of total sugars, hexoses and sucrose content of internodes (dry weight basis) are depicted in Figure 30. Although no data was available on internode composition, the sucrose accumulation algorithm was developed to reproduce the result patterns obtained by Singels and Inman-Bamber (2011) and Lingle and Thomson (2012). The fraction of total sugars in the internodes increased with thermal age, while in early developed internodes, hexose was the major sugar fraction. As the internodes reached their full development and lignin amount, total sugar amount reached its limit, and sucrose was passively stored within internode reserves (Figure 30). At initial growth, under well-watered conditions and high temperatures, growth rates of young internodes are higher, and the hexoses fraction is proportional to the growth rate. This mechanism allowed to simulate the difference in sucrose fractions in young to mature internodes under well-watered and hot conditions. With sufficient water, the sucrose fraction of total sugars in young stalk internodes was lower than that in mature stalk internodes (Figure 30a), and at the rapid stalk expansion, temperatures were higher (DAP = 200) than at the maturation phase (DAP = 300, low hexose demand). When the crop was under severe water-stress, the difference in the sucrose fractions in stalk internodes between young and mature plants was negligible (Figure 30b).

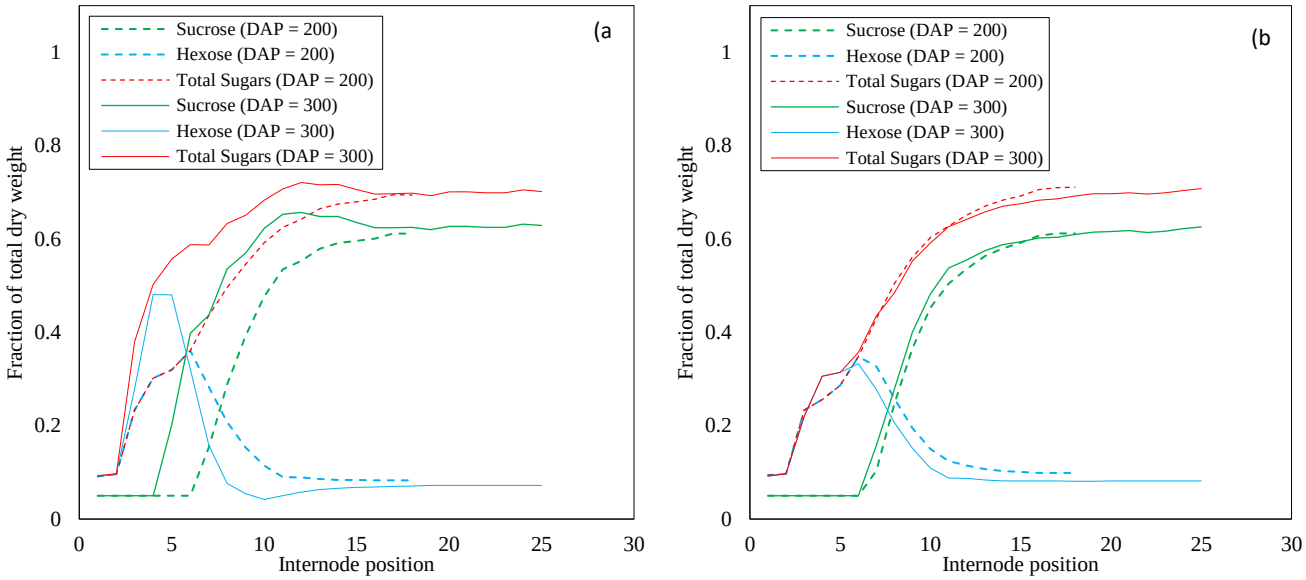

Figure 30. Simulated internode fractions of total sugars (red), hexose (blue) and sucrose (green) at grand growth (dashed lines) and maturity (solid lines) for the 1st season (plant cane) under full irrigation condition (no water stress) (a) and for the 2nd ratoon season under rainfed conditions (with water stress) (b). Internodes are counted downwards from stalks top to soil surface at corresponding Days After Planting (DAP)

The pattern of simulated root growth throughout the sugarcane season was close to geotropism, used in the last version of SAMUCA (Marin and Jones, 2014). After sprouting, roots initiated vertical expansion from the planting depth (25 cm) both up- and downwards; when the crop emerged, upward expansion ceased, and only downward roots deepened to the maximum depth parameter (MRDP = 100 cm, Table 9). At the early crop development, root length density (RLD, cm cm^{-3}) distribution was concentrated at a depth of 25 cm (Figure 31). Thereafter, RLD distribution was proportionally higher in the soil surface layers and the planting depth, with around 0.48 cm cm^{-3}, than in the deeper soil layers, with less than 0.14 cm cm^{-3} (Figure 31). The parameters for specific root length (Srl = 16 and SrlRF = 22 cm g^{-1}) were derived from Laclau and Laclau (2009), who found a mean RLD of 0.45 cm cm^{-3} at a depth of 0-20 cm and of 0.26 cm cm^{-3} at 60-100 cm at 322 days after planting under rainfed conditions.

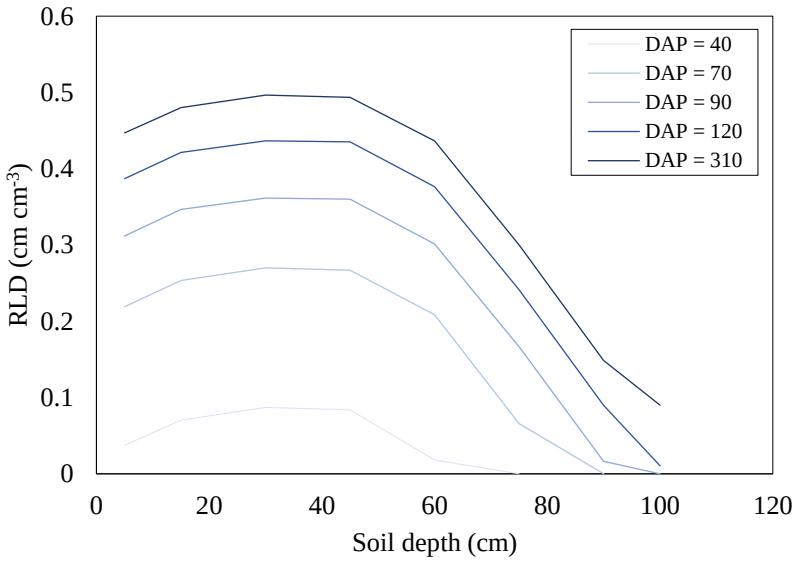

Figure 31. Simulated root length density (RLD) throughout the plant cane crop season in relation to soil depth (DAP is days after planting)

2.3.3. Model Performance for different Brazilian conditions

The model performance under different Brazilian conditions was reasonably good (Figure 32 and Table 12). Stalk dry mass was simulated with good precision and accuracy (r^2 = 0.95 and d = 0.95) and resulted in a lower RMSE of 3.3 t ha^{-1}; in the last model version, evaluation of stalk dry mass yielded an RMSE of 5.4 t ha^{-1} (Marin and Jones, 2014). Nevertheless, stalks fresh mass resulted in an RMSE of 30.3 t ha^{-1}, although with an accuracy of 0.95 and a averaged simulated value (84.5 t ha^{-1}) close to the observed value (85.5 t ha^{-1}). Marin et al (2015) found an RMSE of 20.9 and 18.7 t ha^{-1} of stalk fresh mass under different conditions in Brazil, using the APSIM-Sugar and CANEGRO model, respectively. Stalks dry and fresh mass are highly dependent on stalk population (tillering), which yielded an RMSE of 5.4 tillers m^{-2} and low values of precision (r^2 = 0.12) and accuracy (d = 0.57).

At the tillering peak, most simulations overestimated the observations and ranged between 20 and 25 tillers m^{-2}, which is in agreement with the results from the long-term experiment (Figure 29d). In all sites, observed tiller population was no higher than 20 tillers m^{-2}, where in most cases, tiller population was stable at an average value of 8.9 tillers m^{-2} (Figure 32d). For plant cane, lower tillering peaks and population variations have been observed in comparison with ratoon cane (Singels and Smit, 2009). Tiller senescence after the population peak was high, with a simulated final stalk population of around 10 tillers m^{-2} (Figure 32d). It was interesting that some unexpected patterns of tiller senescence were observed in Colina and Coruripe, where tiller population increased during tiller senescence, possibly because under severe stress, LAI is considerably reduced, and light transmitted through the canopy becomes greater than the light threshold, which in turn triggered the tillering algorithm to (erroneously) simulate new tillers (Figure 32f). Although considering senesced leaves to compute light transmission through the canopy (nsenesleaf_effect, Table 9), further parametrisation for tillering senescence under water-stress should be included to avoid this unexpected effect. The previous version yielded a considerably better performance, with an RMSE of 1.73 tillers m^{-2}, r^2 = 0.5 and d = 0.81 (Marin and Jones, 2014); however, in the previous version, the peak of the tiller population and at maturation are crop parameters (CHUPEAK and CHUMAT) and could not capture variations in tiller population due to mulch cover or competition for light (Bezuidenhout *et al.*, 2003; Singels and Smit, 2009).

Sucrose accumulation (POL) resulted in a reasonably good precision and accuracy (r^2 = 0.72 and d = 0.77), although the previous version performed slightly better, with r^2= 0.68, d = 0.87 and an RMSE of 1.2%; the RMSE values obtained with the new version were within the range of 2.46 to 6.07, as reported by O'Leary (2000) for different sugarcane crop models. The performance of the LAI algorithm was better than that in the previous version, with r^2 = 0.61 and d = 0.88, and the resulted precision, accuracy and RMSE (0.67 m^2 m^{-2}) were even superior to those simulated by CANEGRO and APSIM-Sugar for Brazilian conditions (Marin *et al.*, 2015). The best simulation performance was obtained for stalk height, with precision and accuracy values of r^2 = 0.95 and d = 0.96, an RMSE of 0.4 m and a modelling efficiency of 0.85.

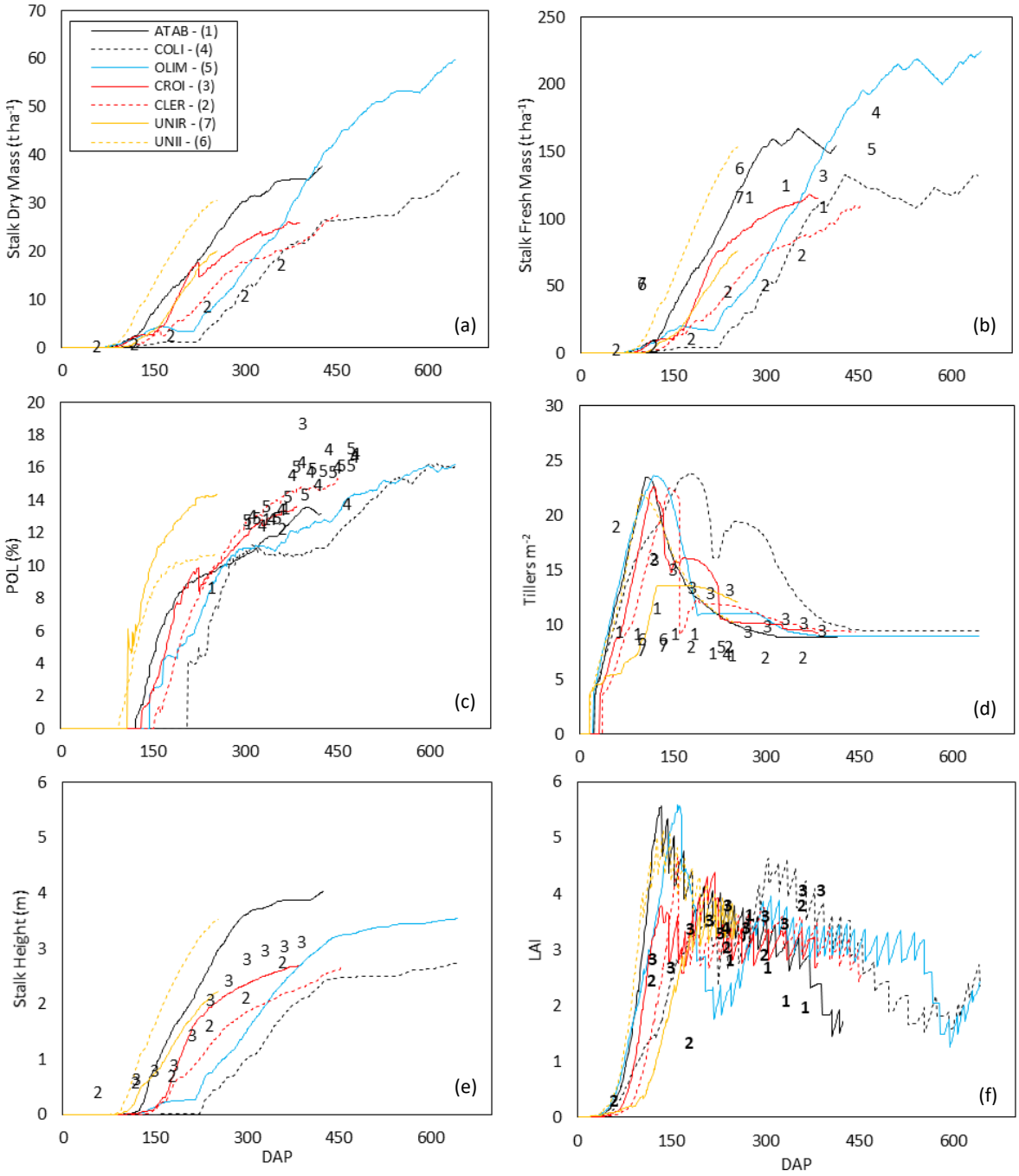

Figure 32. Simulated (lines) and measured (numbers) stalk dry mass (a), stalk fresh mass (b), POL (c), tillering (d), Stalk height (e) and LAI (f) throughout the days after planting (DAP)

Table 12. Statistical indexes of performance of SAMUCA model under different Brazilian conditions

Crop Variable	Bias	RMSE	EF	r^2	d	Obs	Sim
Stalk Fresh Mass (t ha^{-1})	-0.44	30.55	0.70	0.78	0.93	85.04	84.58
Stalk Dry Mass (t ha^{-1})	2.26	3.30	0.71	0.95	0.95	6.74	9.00
Tillering (tiller m^{-2})	2.41	5.38	-1.22	0.12	0.57	10.23	13.51
LAI	-0.01	0.67	0.59	0.61	0.88	2.98	2.97
POL (%)	-2.63	3.15	0.03	0.72	0.77	14.62	11.91
Stalk Height (m)	-0.34	0.40	0.85	0.95	0.96	1.78	1.42

2.3.4. Limitations and uncertainties

A model is a mere simplification of reality, and to quantitively represent complex systems, many assumptions need to be made to fulfil a model framework, which are mostly due to (i) simplification of a process, which does not considerably affect the system, (ii) equipment limitations in representing the system or (iii) uncertainty on how to quantify the process and all responses in the system. Although these aspects can sometimes make the model unpractical, the last one is challenging and represents one of the major advantages to use models for scientific guiding (van Ittersum K *et al.*, 2003; Vos *et al.*, 2010). By gathering all known process relations to represent the system (i.e. a cropping system), it is possible to elucidate the scientific gaps or unknowns of the system, which should then be addressed in further research. Here, the major model limitations due to computation (i.e. computer language) and process uncertainties are pointed out.

Computers were probably the most important invention of the 20th century. By enabling massive mathematical operations in fractions of time, computers supported most technological advances and affect our lives profoundly in a variety of ways, from thinking to acting. The FORTRAN language is considered the grandfather of all computer languages and was created in the mid-50ies, intended to translate scientific equations into computer codes (Chapman, 2008). Nowadays, many other computer languages are available, but FORTRAN still is the faster language and one of the most used for science and engineering due to the vast code library available (Veldhuizen and Jernigan, 1997; Levesque and Williamson, 2014; Haveraaen *et al.*, 2015). It should be clarified that a computer language is not a model, it is only the tool ("equipment") used to translate the model into computer calculations. Nevertheless, in most cases, a model needs be considerably simplified to meet the language requirements, and much of its robustness is therefore lost. For instance, photosynthesis has been widely studied and is well known at the cellular and the organ level (Farquhar, von Caemmerer and Berry, 1980; von Caemmerer and Farquhar, 1981; Ehleringer, Cerling and Helliker, 1997; Sage, 1999; Ghannoum, 2008; Sage, Peixoto and Sage, 2013); however, to simulate light interception within a canopy, considering the orientation of all plants and leaves, is unpractical and not intuitively for a computer language such as FORTRAN; thus, simplifications are needed to represent photosynthesis at the canopy level (Hikosaka, Niinemets and Anten, 2016).

In the new version of SAMUCA, the layered canopy photosynthesis method is implemented (Goudriaan, 2016) to enable a more robust photoassimilate partitioning among sinking phytomers. Nevertheless, the idealising of the model for canopy photosynthesis could be criticised because real canopies exhibit fuzzy features that are superimposed on the regular and smooth model framework. Assuming that the light extinction coefficient (k_{dif}) and optical properties (albedo) of leaves are constant are also method limitations. The extinction coefficient is dependent on leaf orientation and insertion angle, which vary within a single sugarcane stalk (Rae, Martinelli and Dornellas, 2013). In addition, in the cultivar RB867515, a considerable number of dried leaves remain attached to the stalks, and besides having different optical properties, these dry structures may significantly shade out younger tillers (Figure 11). Because the tillering process is driven by temperature and competition for light, efforts to more effectively parameterise these features may reduce simulation uncertainties (Figure 32d).

In a tillering algorithm, only light quantity is considered affecting the tillering process, while light quality (especially red: far-red ratio), an important factor for plant morphogenesis and elementary processes such as germination, stem elongation, tillering and flowering, is neglected (Evers *et al.*, 2006, 2007; Chelle *et al.*, 2007). On the other hand, to simulate light quality within a canopy with an acceptable level of accuracy and precision, it is crucial to include plant structures into simulations, which still is an extremely arduous task in the FORTRAN language rather

than in other languages developed on an object-oriented base (Chapter 4) (Vos *et al.*, 2010). The nitrogen effect on tillering and photosynthesis is also neglected, whereas the model considers adequate nutrient conditions. Sugarcane photosynthesis rate is directly related to leaf nitrogen concentrations, depicted as Photosynthesis Nitrogen Use Efficiency (PNUE), and a lack of leaf nitrogen increases the CO_2 leakiness from bundle sheath cells, leading to a decrease in sugarcane PNUE (Sage, Peixoto and Sage, 2013). Moreover, nitrogen stress affects leaf area expansion and senescence, tillering and reproductive organ growth in sugarcane plantations (Thorburn, Meier and Probert, 2005).

To date, sucrose accumulation is not fully understood (Wang *et al.*, 2013; Braun, Wang and Ruan, 2014), and modelling sucrose accumulation remains a challenge, especially in terms of scaling-up of this variable at the plant level (Inman-Bamber *et al.*, 2009). In this new SAMUCA version, it is assumed that sucrose is passively stored within internodes as the difference between total sugar and hexose demand for structural growth. This approach roughly represented the sucrose/hexose content within internodes (Figure 30); however, the detailed process still remains unknown, and efforts have been made to understand the relations of sucrose synthase enzymes to sucrose accumulation and source-sink relations (Mccormick, Cramer and Watt, 2006; Uys *et al.*, 2007; Bonnett *et al.*, 2009; Inman-Bamber *et al.*, 2009; R. V. Ribeiro *et al.*, 2017; Verma *et al.*, 2017).

Much of the model uncertainties are related to belowground processes, and sugarcane belowground internodes must be self-sufficient to survive and re-grow after successive crop harvesting in ratoon systems. By using the phytomer creation rule, it was possible to include an approximation of belowground internode number, based on planting depth and soil temperature. However, the quantitative contribution of belowground internodes to sugarcane re-growth is unknown. Furthermore, the extents of the fraction of roots senesced after harvesting and its substrate reserves used to keep ratoon sugarcane until emergence remain uncertain (Smith, Inman-Bamber and Thorburn, 2005). Apart from adequate substrate reserves, ratoon re-growth is also significantly influenced by other abiotic factors such as soil physical and chemical conditions (i.e. compaction or salinity) (Qureshi, Madramootoo and Dodds, 2002; Braunack, Arvidsson and Håkansson, 2006; Usaborisut and Sukcharoenvipharat, 2011). Also, there must be a linkage between belowground phytomer number and tiller emergence, mostly because each phytomer has its underlying axillary bud that in turn will sprout and form a new tiller. For simplicity, the model assumes tillers are individual plants, and no substrate exchange among primary to subsequent tillers is simulated (Evers *et al.*, 2005).

Maximum root length density (RLD, cm cm^{-3}) values reported for sugarcane range from 0.45 cm cm^{-3} to up to 5 cm cm^{-3} (Smith, Inman-Bamber and Thorburn, 2005; Laclau and Laclau, 2009). This considerable variation can be attributed to crop regulations of specific root length (SRL, cm g^{-1}) to improve soil root extension and soil structure and chemical properties (Laclau and Laclau, 2009; Azevedo, Chopart and Medina, 2011). This variation uncertainty is reflected in root water uptake simulations, whereas potential root water uptake is highly affected by root length density (Figure 33) (Ritchie, 1998; Singels *et al.*, 2010).

Up to now, only crop-related simulation limitations were mentioned, and soil physical and atmosphere processes were simplified. The widely tested tipping bucket approach is a parameterised method, derived from the detailed physically-based Richards model, to 'mimic' the redistribution process in the, convenient, 1-day time-step (van Ittersum K *et al.*, 2003). Only soil moisture is considered as soil-related limiting factor; nutrient uptake and dynamics in the soil still need to be further implemented to account for crop responses to limited nutrients. Moreover, the use of the Curve Number is more suitable to represent runoff rates on the watershed scale, and its use may be criticised for the small field plots, such as experimental trials. At the bottom soil boundary condition, this model only assumes that deep drainage out of the soil profile and root water uptake (when roots are present) drive soil moisture variations, neglecting the effect of the groundwater table (Kroes *et al.*, 2009). At the atmospheric compartment, although using

the standard Penman-Monteith-FAO methodology, a wide range of sugarcane potential evapotranspiration values has been reported in the last decades, calling for further parameterisation under high atmospheric demand (Grantz, 2013; Marin *et al.*, 2016).

Although many uncertainties and limitations were pointed out, most of them are still challenging to include in a crop PBM framework due to computer language limitations in representing process spatial scales and up-scaling. Advances in the crop modelling approach were achieved by including a higher robustness to canopy photosynthesis, organ level growth and development (phytomers) and carbon balance-based or source-sink relations. Tillering was also parameterised to respond to soil temperature and competition for light, which appears to be more reasonable compared to the previous version, which only relied on air temperature (Inman-Bamber, 1991; Marin and Jones, 2014). Tillering in the key process impacting final sugarcane final yields, and further research must be conducted to investigate its responses to light intensity and quality.

2.4. CONCLUSIONS

A new version of the SAMUCA model was developed, calibrated and tested for a long-term detailed field experiment and under different Brazilian regions. The model included the soil mulch cover effect on crop development and soil evaporation, including soil water stress effects on crop growth and differences regarding plant and ratoon crops. The soil-water balance routine implemented was able to simulate soil water variations throughout the crop season, with reasonably good levels of precision and accuracy, including the effect of mulch cover on the soil. Simulated sugarcane plant and ratoon mostly differ in terms of initial crop conditions (i.e. planting depth and substrate reserves available). Yield decay through successive ratooning was not observed in the long-term experiment, possibly due to manual harvesting; thus, this effect was not included and may be better assessed under effects of heavy machinery and soil managements.

The simple calibration routine implemented was useful to calibrate the model crop and soil parameters; however, translation of calibration methods to FORTRAN language could considerably increase the calibration time. The model performance in the long-term experiment and in different Brazilian conditions was satisfactory, and agreement indices were close to those of other widely used crop models for sugarcane (CANEGRO and APSIM-Sugar). In addition, by including the atmospheric CO_2 effect, the model could be incorporated into future sugarcane climate change impact studies.

REFERENCES

ALLEN, R. G.; LUIS, S. P.; RAES, D.; SMITH, M. FAO Irrigation and Drainage Paper No. 56. Crop Evapotranspiration (guidelines for computing crop water requirements). **Irrigation and Drainage**, v. 300, n. 56, p. 300, 1998.

ALLEN, R. G.; PEREIRA, L. S.; RAES, D.; SMITH, M. Crop evapotranspiration: guidelines for computing crop water requirements. **FAO (Irrigation and Drainage)**, v. 56, 1998.

AZEVEDO, M. C. B. DE; CHOPART, J. L.; MEDINA, C. D. C. Sugarcane root length density and distribution from root intersection counting on a trench-profile. **Scientia Agricola**, v. 68, n. February, p. 94–101, 2011.

BAKER, C. J.; STERLING, M.; BERRY, P. A generalised model of crop lodging. **Journal of Theoretical Biology**, v. 363, p. 1–12, 2014.

BEZUIDENHOUT, C. N.; O'LEARY, G. J.; SINGELS, A.; BAJIC, V. B. A process-based model to simulate changes in tiller density and light interception of sugarcane crops. **Agricultural Systems**, v. 76, n. 2, p. 589–599, 2003.

BONNETT, G. D. Developmental Stages (Phenology). *In*: MOORE, P. H.; BOTHA, F. C. (Eds.). . **Sugarcane. Physiology, Biochemistry and Functional Biology**. [s.l.] WILEY Blackwell, 2013. p. 35–53.

BONNETT, G. D. B.; SPILLMAN, M. F. A.; HEWITT, M. L. C.; B, J. X. Source – sink differences in genotypes and water regimes in fl uencing sucrose accumulation in sugarcane stalks. p. 316–327, 2009.

BOTTCHER, A. *et al.* Ligni fi cation in Sugarcane : Biochemical Characterization , Gene Discovery , and Expression Analysis in Two Genotypes Contrasting for Lignin Content 1 [W]. v. 163, n. December, p. 1539–1557, 2013.

BOUGHTON, W. C. A review of the USDA SCS curve number method. **Soil Research**, v. 27, n. 3, p. 511–523, 1989.

BRAUN, D. M.; WANG, L.; RUAN, Y. Understanding and manipulating sucrose phloem loading , unloading , metabolism , and signalling to enhance crop yield and food security. v. 65, n. 7, p. 1713–1735, 2014.

BRAUNACK, M. V; ARVIDSSON, J.; HÅKANSSON, I. Effect of harvest traffic position on soil conditions and sugarcane (Saccharum officinarum) response to environmental conditions in Queensland, Australia. **Soil and Tillage Research**, v. 89, n. 1, p. 103–121, 2006.

BROWN, S. E.; PREGITZER, K. S.; REED, D. D.; BURTON, A. J. Predicting Daily Mean Soil Temperature from Daily Mean Air Temperature in Four Northern Hardwood S oil temperature is a very important climatic variable. v. 46, n. 2, p. 297–301, 2000.

BYRD, R. H.; LU, P.; NOCEDAL, J.; ZHU, C. A Limited Memory Algorithm for Bound Constrained Optimization. **SIAM Journal on Scientific Computing**, v. 16, n. 5, p. 1190–1208, 1995.

CAEMMERER, S. VON; FARQUHAR, G. D. Some relationships between the biochemistry of photosynthesis and the gas exchange of leaves. **Planta**, v. 153, n. 4, p. 376–387, 1981.

CARDOZO, N. P.; SENTELHAS, P. C.; PANOSSO, A. R.; PALHARES, A. L.; IDE, B. Y. Modeling sugarcane ripening as a function of accumulated rainfall in Southern Brazil. **International Journal of Biometeorology**, v. 59, n. 12, p. 1913–1925, 2015.

CHAPMAN, S. J. **Fortran for scientist and engineers: 1995-2003**. [s.l.] McGraw-Hill, 2008.

CHELLE, M.; EVERS, J. B.; COMBES, D.; VARLET-GRANCHER, C.; VOS, J.; ANDRIEU, B. Simulation of the three-dimensional distribution of the red: far-red ratio within crop canopies. **New Phytologist**, v. 176, n. 1, p. 223–234, 2007.

COSTA, L. G.; MARIN, F. R.; NASSIF, D. S. P.; PINTO, H. M. S.; LOPES-ASSAD, M. L. R. C. Simulação do efeito do manejo da palha e do nitrogênio na produtividade da cana-de-açúcar. **Revista Brasileira de Engenharia Agrícola e Ambiental**, v. 18, n. 5, p. 469–474, 2014.

COUTINHO, R. M.; KRAENKEL, R. A.; PRADO, P. I. Catastrophic Regime Shift in Water Reservoirs and S ã o Paulo Water Supply Crisis. p. 1–14, 2015.

COWAN, I. R. The interception and absorption of radiation in plant stands. **Journal of Applied Ecology**, p. 367–379, 1968.

EBRAHIM, M. K.; ZINGSHEIM, O.; EL-SHOURBAGY, M. N.; MOORE, P. H.; KOMOR, E. Growth and Sugar Storage in Sugarcane Grown at Temperatures Below and Above Optimum. **Journal of Plant Physiology**, v. 153, n. 5–6, p. 593–602, 1998.

EHLERINGER, J. R.; CERLING, T. E.; HELLIKER, B. R. C4 photosynthesis, atmospheric CO2, and climate. **Oecologia**, v. 112, n. 3, p. 285–299, 1997.

EVERS, J. B. **Tillering in spring wheat : a 3D virtual plant modelling study**. [s.l.] Wageningen University, 2006.

EVERS, J. B.; VOS, J.; ANDRIEU, B.; STRUIK, P. C. Cessation of tillering in spring wheat in relation to light interception and red: far-red ratio. **Annals of Botany**, v. 97, n. 4, p. 649–658, 2006.

EVERS, J. B.; VOS, J.; CHELLE, M.; ANDRIEU, B.; FOURNIER, C.; STRUIK, P. C. Simulating the effects of localized red: far-red ratio on tillering in spring wheat (Triticum aestivum) using a three-dimensional virtual plant model. **New Phytologist**, v. 176, n. 2, p. 325–336, 2007.

EVERS, J. B.; VOS, J.; FOURNIER, C.; ANDRIEU, B.; CHELLE, M.; STRUIK, P. C. Towards a generic architectural model of tillering in Gramineae, as exemplified by spring wheat (Triticum aestivum). **New Phytologist**, v. 166, n. 3, p. 801–812, 2005.

FARQUHAR, G. D.; CAEMMERER, S. VON; BERRY, J. A. A biochemical model of photosynthetic CO2 assimilation in leaves of C3 species. **Planta**, v. 149, n. 1, p. 78–90, 1980.

FOURNIER, C. A functional – structural model of elongation of the grass leaf and its relationships with the

phyllochron. p. 881–894, 2001.

GARSIDE, A. L.; BELL, M. J.; BERTHELSEN, J. E.; HALPIN, N. V; OTHERS. **Effect of breaks and nitrogen fertiliser on shoot development, maintenance, and cane yield in an irrigated plant crop of Q117.**Proceedings of the 2000 Conference of the Australian Society of Sugar Cane Technologists held at Bundaberg, Queensland, Australia, 2 May to 5 May 2000. **Anais**...2000

GHANNOUM, O. C4 photosynthesis and water stress. **Annals of Botany**, v. 103, n. 4, p. 635–644, 2008.

GOUDRIAAN, J. A simple and fast numerical method for the computation of daily totals of crop photosynthesis. **Agricultural and Forest Meteorology**, v. 38, n. 1, p. 249–254, 1986.

GOUDRIAAN, J. Light distribution. *In*: **Canopy Photosynthesis: From Basics to Applications**. [s.l.] Springer, 2016. p. 3–22.

HAVERAAEN, M.; MORRIS, K.; ROUSON, D.; RADHAKRISHNAN, H.; CARSON, C. High-performance design patterns for modern Fortran. **Scientific Programming**, v. 2015, p. 3, 2015.

HEERDEN, P. D. R. VAN; EGGLESTON, G.; DONALDSON, R. A. Ripening and Postharvest Deterioration. **Sugarcane: Physiology, Biochemistry, and Functional Biology**, p. 55–84, 2013.

HEERDEN, P. D. R. VAN; SINGELS, A.; PARASKEVOPOULOS, A.; ROSSLER, R. Negative effects of lodging on irrigated sugarcane productivity—An experimental and crop modelling assessment. **Field Crops Research**, v. 180, p. 135–142, 2015.

HEUVELINK, E. Dry matter partitioning in tomato: validation of a dynamic simulation model. **Annals of botany**, v. 77, n. 1, p. 71–80, 1996.

HIKOSAKA, K.; NIINEMETS, U.; ANTEN, N. P. R. **Canopy photosynthesis: from basics to applications**. [s.l.] Springer, 2016.

INMAN-BAMBER, N. G. A growth model for sugarcane based on a simple carbon balance and the CERES-Maize water balance. **South African Journal of Plant Soil**, v. 8, p. 93–99, 1991.

INMAN-BAMBER, N. G.; BONNETT, G. D.; SPILLMAN, M. F.; HEWITT, M. L.; JACKSON, J. Increasing sucrose accumulation in sugarcane by manipulating leaf extension and photosynthesis with irrigation. p. 13–26, 2008.

INMAN-BAMBER, N. G.; BONNETT, G. D.; SPILLMAN, M. F.; HEWITT, M. L.; XU, J. Source--sink differences in genotypes and water regimes influencing sucrose accumulation in sugarcane stalks. **Crop and Pasture Science**, v. 60, n. 4, p. 316–327, 2009.

ITTERSUM K, M. VAN; LEFFELAAR, P. A.; KEULEN, H. VAN; KROPFF, M. J.; BASTIAANS, L.; GOUDRIAAN, J. On approaches and applications of the Wageningen crop models. **European Journal of Agronomy**, v. 18, p. 201–234, 2003.

JONES, J. W.; HOOGENBOOM, G.; PORTER, C. H.; BOOTE, K. J.; BATCHELOR, W. D.; HUNT, L. A.; WILKENS, P. W.; SINGH, U.; GIJSMAN, A. J.; RITCHIE, J. T. **The DSSAT cropping system model**. [s.l: s.n.]. v. 18

KEATING, B. A.; ROBERTSON, M. J.; MUCHOW, R. C.; HUTH, N. I. Modelling sugarcane production systems I. Development and performance of the sugarcane module. **Field Crops Research**, v. 61, n. 3, p. 253–271, 1999.

KROES, J. G.; DAM, J. C. VAN; GROENENDIJK, P.; HENDRIKS, R. F. A; JACOBS, C. M. J. SWAP version 3.2. Theory and user manual. **Update**, n. August, p. 284, 2009.

LACLAU, P.; LACLAU, J. P. Growth of the whole root system for a plant crop of sugarcane under rainfed and irrigated environments in Brazil. **Field Crops Research**, v. 114, n. 3, p. 351–360, 2009.

LEVESQUE, J. M.; WILLIAMSON, J. W. **A Guidebook to FORTRAN on Supercomputers**. [s.l.] Academic Press, 2014.

LINGLE, S. E.; THOMSON, J. L. Sugarcane Internode Composition During Crop Development. **Bioenergy Research**, p. 168–178, 2012.

LIU, D. L.; BULL, T. A. Simulation of biomass and sugar accumulation in sugarcane using a process-based model. v. 144, p. 181–211, 2001.

LONG, S. P.; AINSWORTH, E. A.; ROGERS, A.; ORT, D. R. Rising atmospheric carbon dioxide: plants FACE the future. **Annu. Rev. Plant Biol.**, v. 55, p. 591–628, 2004.

MARENGO, J. A.; NOBRE, C. A.; SELUCHI, M. E.; CUARTAS, A.; ALVES, L. M.; MENDIONDO, E. M.; OBREGÓN, G.; SAMPAIO, G. A seca e a crise h{'\i}drica de 2014-2015 em São Paulo. **Revista USP**, n. 106, p. 31–

44, 2015.

MARIN, F. R.; ANGELOCCI, L. R.; COELHO FILHO, M. A.; VILLA NOVA, N. A. Construção e avaliação de psicrômetro aspirado de termopar. **Scientia Agricola**, v. 58, n. 4, p. 839–844, 2001.

MARIN, F. R.; JONES, J. W. Process-based simple model for simulating sugarcane growth and production. **Scientia Agricola**, v. 71, n. 1, p. 1–16, 2014.

MARIN, F. R.; THORBURN, P. J.; NASSIF, D. S. P.; COSTA, L. G. Sugarcane model intercomparison: Structural differences and uncertainties under current and potential future climates. **Environmental Modelling & Software**, v. 72, p. 372–386, 2015.

MATSUOKA, S.; GARCIA, A. A. F. Sugarcane underground organs: going deep for sustainable production. **Tropical Plant Biology**, v. 4, n. 1, p. 22–30, 2011.

MCCORMICK, A. J.; CRAMER, M. D.; WATT, D. A. Sink strength regulates photosynthesis in sugarcane. **New Phytologist,** 2006.

MONTEITH, J. Light Interception and Radiative Exchange in Crop Stands. 1969.

MONTEITH, J. L.; UNSWORTH, M. H. **Principles of Environmental Physics: Plants , Animals , and the Atmosphere**. 4th Editio ed. Oxford: Elsevier Ltd, 2012.

MOORE, P. H.; BOTHA, F. C. **Sugarcane: physiology, biochemistry and functional biology**. [s.l.] John Wiley & Sons, 2013.

MULLER, J.; NORMALE, E.; LYON, S. DE. Arithmetic Processor for Solving Tridiagonal Systems of Linear Equations. 2006.

NASH, J. C. **Compact Methods for Computers. Linear Algebra and Function Minimisation**. [s.l: s.n.].

NASSIF, D. S. P. **Evapotranspiração, transpiração e trocas gasosas em um canavial irrigado**. [s.l.] University of Sao Paulo, 2015.

NASSIF, D. S. P.; MARIN, F. R.; COSTA, L. G. Padrões m{'\i}nimos para coleta de dados experimentais para estudos sobre crescimento e desenvolvimento da cultura da cana-de-açúcar. **Embrapa Informática Agropecuária-Documentos (INFOTECA-E)**, 2013.

NELDER, J. A.; MEAD, R. A simplex algorithm for function minimization. **Computer Journal**, v. 7, p. 308–313, 1965.

O'LEARY, G. J. A review of three sugarcane simulation models with respect to their prediction of sucrose yield. **Field Crops Research**, v. 68, n. 2, p. 97–111, 2000.

OLIVIER, F. C.; SINGELS, A. The effect of crop residue layers on evapotranspiration, growth and yield of irrigated sugarcane. **Water SA**, v. 38, n. 1, p. 77–86, 2012.

PARTON, W. J.; LOGAN, J. A. A model for diurnal variation in soil and air temperature. **Agricultural Meteorology**, v. 23, p. 205–216, 1981.

PEREZ, P. J.; CASTELLVI, F.; IBA??EZ, M.; ROSELL, J. I. Assessment of reliability of Bowen ratio method for partitioning fluxes. **Agricultural and Forest Meteorology**, v. 97, n. 3, p. 141–150, 1999.

PORTER, C. H.; JONES, J.; HOOGENBOOM, G.; WILKENS, P. W.; RITCHIE, J. T.; PICKERING, N. B.; BOOTE, K. J.; BAER, B. Soil Water Balance Module (WATBAL). *In*: JONES, J. W.; HOOGENBOOM, G.; WILKENS, P. W.; PORTER, C. H.; TSUJI, G. Y. (Eds.). . **DSSAT v4.5 Documentation**. [s.l.] University of Hawaii, 2010. p. 237–262.

PORTER, C. H.; JONES, J. W.; ADIKU, S. G. K.; GIJSMAN, A. J.; GARGIULO, O.; NAAB, J. B. Modeling organic carbon and carbon-mediated soil processes in DSSAT v4.5. **Operational Research**, 2009.

PRIESTLEY, C. H. B.; PHYSICS, R. J. T. A. On the Assessment of Surface Heat Flux and Evaporation Using Large-Scale Parameters. n. February, p. 81–92, 1972.

PROVENZANO, G.; PH, D.; RALLO, G.; PH, D.; GHAZOUANI, H. Assessing Field and Laboratory Calibration Protocols for the Diviner 2000 Probe in a Range of Soils with Different Textures. v. 142, n. 2, p. 1–12, 2016.

PRUSINKIEWICZ, P.; LINDENMAYER, A. The algorithmic beauty of plants. **Plant Science**, v. 122, n. 1, p. 109–110, 1990.

QURESHI, S. A.; MADRAMOOTOO, C. A.; DODDS, G. T. Evaluation of irrigation schemes for sugarcane in Sindh , Pakistan , using SWAP93. v. 54, p. 37–48, 2002.

R., F.; REEVES, M. Function minimization by conjugate gradients. **Computer Journal**, v. 7, p. 148–154, 1964.

RAE, A. L.; MARTINELLI, L. A.; DORNELLAS, M. C. Anatomy and Morphology. *In*: MOORE, P. H.; BOTHA, F. C. (Eds.). . **Sugarcane. Physiology, Biochemistry and Functional Biology**. [s.l.] WILEY Blackwell, 2013. p. 19–34.

RIBEIRO, R. V.; MACHADO, E. C.; MAGALH??ES FILHO, J. R.; LOBO, A. K. M.; MARTINS, M. O.; SILVEIRA, J. A. G.; YIN, X.; STRUIK, P. C. Increased sink strength offsets the inhibitory effect of sucrose on sugarcane photosynthesis. **Journal of Plant Physiology**, v. 208, p. 61–69, 2017.

RITCHIE, J. T. Soil water balance and plant water stress. *In*: TSUJI, G. Y.; HOOGENBOOM, G.; THORNTON, P. K. (Eds.). . **Understanding Options for Agricultural Production**. Dordrecht: Springer Netherlands, 1998. p. 41–54.

RITCHIE, J. T.; PORTER, C. H.; JONES, J. W.; SULEIMAN, A. A. Extension of an Existing Model for Soil Water Evaporation and Redistribution under High Water Content Conditions. v. 73, n. 3, 2009.

SAGE, R. F. Why C4 photosynthesis. **C4 plant biology**, p. 3–16, 1999.

SAGE, R. F.; PEIXOTO, M. M.; SAGE, T. L. Photosynthesis in Sugarcane. **Sugarcane: Physiology, Biochemistry, and Functional Biology**, n. DECEMBER, p. 121–154, 2013.

SENTEK. **CALIBRATION MANUAL For Sentek Soil Moisture Sensors**. v2.0 ed. [s.l.] Sentek, 2011.

SILVA, A. L. C. DE; COSTA, W. A. J. M. DE. Growth and Radiation Use Efficiency of Sugarcane Under Irrigated and Rain-fed Conditions in Sri Lanka. **Sugar Tech**, v. 14, n. 3, p. 247–254, 2012.

SILVA, C. R. Calibração de um sensor capacitivo de umidade em Latossolo Amarelo na microrregião do Litoral Piauiense Field calibration of water capacitive sensor in a Yellow Latosol of coastal region , in the of State Piaui , Brazil. p. 303–307, 2007.

SILVA DIAS, M. A. F.; DIAS, J.; CARVALHO, L. M. V; FREITAS, E. D.; SILVA DIAS, P. L. Changes in extreme daily rainfall for S{ã}o Paulo, Brazil. **Climatic Change**, v. 116, n. 3, p. 705–722, 2013.

SINGELS, A.; BERG, M. VAN DEN; SMIT, M. A.; JONES, M. R.; ANTWERPEN, R. VAN. Modelling water uptake, growth and sucrose accumulation of sugarcane subjected to water stress. **Field Crops Research**, v. 117, n. 1, p. 59–69, 2010.

SINGELS, A.; INMAN-BAMBER, N. G. Modelling genetic and environmental control of biomass partitioning at plant and phytomer level of sugarcane grown in controlled environments. **Crop and Pasture Science**, v. 62, n. 1, p. 66–81, 2011.

SINGELS, A.; JONES, M.; BERG, M. VAN DEN. DSSAT v4. 5 Canegro sugarcane plant module: scientific documentation. **South African Sugarcane Research Inst. Mount …**, p. 1–34, 2008.

SINGELS, A.; SMIT, M. A. Sugarcane response to row spacing-induced competition for light. **Field Crops Research**, v. 113, n. 2, p. 149–155, 2009.

SMITH, D. M.; INMAN-BAMBER, N. G.; THORBURN, P. J. Growth and function of the sugarcane root system. **Field Crops Research**, v. 92, n. 2–3 SPEC. ISS., p. 169–183, 2005.

SPITTERS, C. J. T.; KEULEN, H. VAN; KRAALINGEN, D. W. G. VAN. A simple and universal crop growth simulator: SUCROS87. *In*: **Simulation and systems management in crop protection**. [s.l.] Pudoc, 1989. p. 147–181.

SPITTERS, C. J. T.; TOUSSAINT, H.; GOUDRIAAN, J. Separating the diffuse and direct component of global radiation and its implications for modeling canopy photosynthesis Part I. Components of incoming radiation. **Agricultural and Forest Meteorology**, v. 38, n. 1–3, p. 217–229, 1986.

SULEIMAN, A. A.; RITCHIE, J. T. Modeling soil water redistribution during second-stage evaporation. **Soil Science Society of America Journal**, v. 67, n. 2, p. 377–386, 2003.

TEH, C. **Introduction to mathematical modeling of crop growth: How the equations are derived and assembled into a computer model**. 1st. ed. Boca Raton, Florida (USA): Brown Walker Press, 2006.

THORBURN, P. J.; MEIER, E. A.; PROBERT, M. E. Modelling nitrogen dynamics in sugarcane systems: Recent advances and applications. **Field crops research**, v. 92, n. 2, p. 337–351, 2005.

THORNLEY, J. H. M.; JOHNSON, I. R. **Plant and crop modelling: a mathematical approach to plant and crop physiologyPlant and crop modelling: a mathematical approach to plant and crop physiology.**, 1990.

USABORISUT, P.; SUKCHAROENVIPHARAT, W. Soil compaction in sugarcane fields induced by mechanization.

American Journal of Agricultural and Biological Science, v. 6, n. 3, p. 418–422, 2011.

UYS, L.; BOTHA, F. C.; HOFMEYR, J. S.; ROHWER, J. M. Kinetic model of sucrose accumulation in maturing sugarcane culm tissue. v. 68, p. 2375–2392, 2007.

VANDERPLAATS, G. N. **Numerical optimization**. [s.l: s.n.].

VELDHUIZEN, T. L.; JERNIGAN, M. E. **Will C++ be faster than Fortran?**International Conference on Computing in Object-Oriented Parallel Environments. **Anais**...1997

VERMA, I.; ROOPENDRA, K.; SHARMA, A.; JAIN, R.; SINGH, R. K.; CHANDRA, A. Expression analysis of genes associated with sucrose accumulation in sugarcane under normal and GA3-induced source--sink perturbed conditions. **Acta Physiologiae Plantarum**, v. 39, n. 6, p. 133, 2017.

VIANNA, M. S.; MARIN, F. R. **ESTIMATIVA DA TEMPERATURA DO AR HORÁRIA PARA O ESTADO DE SÃO PAULO**Congresso Brasileiro de Agrometeorologia. **Anais**...Juazeiro: 2017

VOS, J.; EVERS, J. B.; BUCK-SORLIN, G. H.; ANDRIEU, B.; CHELLE, M.; VISSER, P. H. B. DE. Functional-structural plant modelling: A new versatile tool in crop science. **Journal of Experimental Botany**, v. 61, n. 8, p. 2101–2115, 2010.

WALLACH, D.; MAKOWSKI, D.; JONES, J. W.; BRUN, F. **Working with Dynamic Crop Models**. [s.l: s.n.].

WANG, J.; NAYAK, S.; KOCH, K.; MING, R. Carbon partitioning in sugarcane (Saccharum species). **Frontiers in Plant Science**, v. 4, n. June, p. 2005–2010, 2013.

WATT, D. A.; MCCORMICK, A. J.; CRAMER, M. D. Source and Sink Physiology. **Sugarcane: Physiology, Biochemistry, and Functional Biology**, n. DECEMBER, p. 483–520, 2013.

YIN, X.; GOUDRIAAN, J. A. N.; LANTINGA, E. A.; VOS, J. A. N.; SPIERTZ, H. J. A flexible sigmoid function of determinate growth. **Annals of botany**, v. 91, n. 3, p. 361–371, 2003.

3. COMBINED AGROHYDROLOGICAL MODEL FOR SIMULATING SUGARCANE DEVELOPMENT, GROWTH AND WATER USE

ABSTRACT

Sugarcane is the second largest source of biofuel and the main source of sugar in the world. It is a crop of major social, economic and environmental importance in many tropical countries. Brazil is the largest sugarcane producing nation, accounting for half of the global production. In the current scenario, with yields reaching 80 t ha^{-1}, the crop has strongly expanded towards central-western regions, where irrigation is mandatory to offset water stress risks. The effects of crop management, land use change, climate variability and change as well as agro-economic factors on crop production and associated quantities can be assessed using process-based crop simulation models (PBM). Despite its great importance and in contrast to other major crops, only two specific sugarcane crop growth models are available for end users worldwide. A new sugarcane PBM, developed for Brazilian farming systems, showed good performance in crop component predictions; however, a simplified soil-water balance routine may be assessed to reduce uncertainties in crop water use. This study aimed to couple a newly developed process-based sugarcane model (SAMUCA) to the agrohydrological model SWAP, aiming to reduce this prediction uncertainty and to provide a better tool for crop water consumption and hydrological analysis. The SAMUCA-SWAP model performed slightly better in the prediction of stalk fresh and dry mass (3 and 7% lower RMSE values) and notably better in leaf area index prediction (reducing RMSE by 38%) than the standalone version of SAMUCA. Soil water balance simulations were improved (32% lower RMSE) compared to the standalone version (tipping bucket), enabling more robust predictions of crop water use. The extended ability to simulate solute transport and salinity stress of the SWAP-SAMUCA can be explored to support sugarcane irrigation strategies as well as fertigation with vinasse.

Keywords: Crop modelling; Agrohydrology; *Saccharum officinarum*

3.1. INTRODUCTION

Sugarcane is the main source of sugar globally and has emerged as the second largest source of biofuel (Scheiterle *et al.*, 2017; Tapia Carpio and Simone de Souza, 2017). In many tropical countries, sugarcane is of major social, economic and environmental importance; it also is the 6th most economically significant and the 2nd most important C4 species (FAO, 2016). On a global scale, more than 70% of sugarcane are produced in Brazil, India, China, Thailand and Pakistan. Brazil alone accounts for half of the global production, and besides sugar as end product, it also provides more than 15% of the country's energy source (liquid fuel and biomass), supplying ethanol and biomass energy mainly for electricity and heating (Walter *et al.*, 2014; EPE, 2015; Fortunato *et al.*, 2017).

Traditionally, sugarcane is cultivated under rainfed conditions in Brazil´s southeast and coastal northeastern regions. To address the increasing demand for sugar and energy, more recently, sugarcane areas have strongly expanded towards the central-western region, the area of the original Cerrado biome (Adami *et al.*, 2012; F. V. Scarpare *et al.*, 2016). In these newly exploited regions, sugarcane production faces difficulties because of higher water deficits and poor soil conditions, making supplementary irrigation mandatory for crop production (Vianna and Sentelhas, 2015; Fábio Vale. Scarpare *et al.*, 2016). In addition, average sugarcane yield levelled to a maximum of about 75 t ha^{-1}, and irrigation became a successful strategy to increase production in many parts of the country. Nowadays, Brazilian irrigated fields are the greatest water consumers, accounting for more than 55% of the total consumption, with

sugarcane representing 29% of irrigated fields (ANA, 2016). In this context, soil-water and hydrological studies have become increasingly useful for planners and policy makers (Fábio Vale. Scarpare *et al.*, 2016; Barbosa *et al.*, 2017).

Process-based crop models (PBM) integrate soil, plant, atmosphere and management effects on crop growth and development. Nowadays, more than five generic PBMs (J. R. Williams *et al.*, 1989; van Diepen *et al.*, 1989; Brisson *et al.*, 1998; Jones *et al.*, 2003; Keating *et al.*, 2003) and around 32 specific crop PBMs are available for end users. Besides, some crops have several specific PBMs, such as wheat with 27 available models, representing different modelling approaches or options to include crop and management specificities. Such models reduce the uncertainty of predictions for many crops (Tebaldi *et al.*, 2007; Asseng, 2013; Marin *et al.*, 2015; Martre *et al.*, 2015; Battisti, Sentelhas and Boote, 2017), although the underlying mechanism still unclear due to the specificity of each model and the complexity of simulated interactions.

Several PBMs for sugarcane have been developed and described in the literature (Keating *et al.*, 1999; Singels and Donaldson, 2000; Liu and Bull, 2001; J.F. and Todoroff, 2002; Villegas *et al.*, 2005; Singels, Jones and Berg, 2008). However, in contrast to other crops, only two of these are available for end users: the DSSAT-CANEGRO model and the APSIM/Sugar model. Both have been extensively used and tested in sugarcane studies worldwide (Inman-Bamber, Muchow and Robertson, 2002; Inman-Bamber and McGlinchey, 2003; Knox *et al.*, 2010; Singels *et al.*, 2014; Everingham *et al.*, 2015), including in Brazil (Marin *et al.*, 2011, 2013, 2015; Costa *et al.*, 2014; Vianna and Sentelhas, 2014, 2015). Because of the heuristic character of modelling and the specific features of sugarcane farming systems in Brazil, Marin & Jones (2014) presented a standalone sugarcane PBM (SAMUCA - *Agronomic Modular Simulator for Sugarcane*). Marin et al. (2017) applied SAMUCA in the stochastic simulation of sugarcane production and uncertainty analysis. In these publications, the authors verified the need to improve soil-water balance routines to better represent crop growth and water use under rainfed and irrigated conditions.

The SWAP model (Kroes *et al.*, 2009) is currently one of the most robust and widely used hydrological models available for end users (EITZINGER *et al.*, 2004; Lier *et al.*, 2008; VAZIFEDOUST *et al.*, 2008; Noory *et al.*, 2011; Kumar *et al.*, 2015). The model employs a robust implicit numerical solution scheme to solve the Richards equation and to simulate soil water movement in saturated or unsaturated soils. Soil physics modules are included to simulate solute transport, macropore flow, water repellency and soil heat flow. Three modular routines to simulate crop growth and development are included: a simple module, a detailed module for all crop types (WOFOST, WOrld FOod STudies) and a detailed module for grass (re)growth. Water interception by crops and/or forests is included, as well as the effects of soil water content, solute concentration and freezing on root water uptake and plant growth (Kroes *et al.*, 2009).

In this chapter, we describe the coupling of SAMUCA to the SWAP model and evaluate the resulting new approach for the dynamic simulation of sugarcane growth and development under Brazilian conditions, besides consistently considering soil water and irrigation. The coupled model (SWAP-SAMUCA) is expected to reduce prediction uncertainty, thereby representing a better tool for predicting crop water use and vadose zone hydrology under sugarcane.

3.2. MATERIAL E METHODS

The 1st version of sugarcane the PBM (SAMUCA - Agronomic Modular Simulator for Sugarcane) framework is described in detail by Marin and Jones (2014) and Marin et al. (2017). It simulates sugarcane growth and development based on crop phenology (thermal time), leaf growth (source to sink), biomass accumulation and

partitioning, root growth and water stress (Table 13). Daily time-step integration is performed to simulate biomass accumulation and crop development, whereas the daily amount of carbohydrates produced by the crop is allocated to roots, leaves and stalks (sucrose and fibre).

Table 13. Sugarcane model's main state variables, descriptions, units and categories

State Variables	Description	Units	Category
NSTK	Number of stalks per area unit	stalks m^{-2}	Phenology
LN	Number of green expanded leaves per stalk	leaves $stalk^{-1}$	Canopy Development
LNTOTAL	Number of green plus dead leaves per stalk	leaves $stalk^{-1}$	Canopy Development
LAI	Leaf area index	$m^2\ m^{-2}$	Canopy Development
W	Total plant dry biomass	t ha^{-1}	Biomass Accumulation
WA	Aerial dry biomass	t ha^{-1}	Biomass Accumulation
WR	Root dry biomass	t ha^{-1}	Biomass Accumulation
WL	Leaf dry biomass	t ha^{-1}	Biomass Accumulation
WSUC	Sucrose weight	t ha^{-1}	Biomass Accumulation
WSDM	Stalk dry biomass	t ha^{-1}	Biomass Accumulation
WSFM	Stalk fresh biomass	t ha^{-1}	Biomass Accumulation
SLENG	Stalk length	m	Plant extension
RLD	Root length density	cm cm^{-3}	Root and water Stress

In contrast to other sugarcane PBMs, sucrose accumulation is calculated on an internode basis (Uys *et al.*, 2007). The substrates partitioned to stalk dry mass are then partitioned between stalk structure and sucrose, based on the sink capacity, the thermal age of the internode and the characteristics of the cultivar. This approach relies on the concept that exceeding substrates are stored as sucrose within the non-structural biomass of mature internodes, which is thus considered the fourth priority after leaves, roots and stalk fibre (energy storage).

Temperature and water stress effects on sucrose accumulation are indirectly accounted for by the stalk extension rate, because plant extension sensitivity to low temperatures and water stress is considered higher than that to substrate production, mimicking sucrose accumulation under conditions of medium water deficits and lower temperatures (Inman-Bamber, 2004; Uys *et al.*, 2007; Marin and Jones, 2014).

To simulate soil-water balance, the SAMUCA standalone version employs a simple 'tipping bucket' routine, a downwards distribution of daily amount of rainfall and/or irrigation added to the soil (top layer) is performed. Water is then redistributed based on the potential gradient and the Richards equation (Richards, 1931; Knight and Raats, 2016). For simplicity, the hydraulic conductivity (K) is assumed to be exponentially related to the soil water content, enabling a straightforward analytical solution (Equation 42) of the Richards equation (Kendy *et al.*, 2003; Teh, 2006; Marin and Jones, 2014). Downward flux at the bottom layer is considered as drained water out to the soil profile, and groundwater is not considered to be part of the soil water balance:

$$\theta_{v(i,t)} = \theta_{v,sat(i)} - \frac{\theta_{v,sat(i)}}{\alpha} ln\left\{\frac{\alpha K_{sat(i)}\Delta t}{L_i \theta_{v,sat(i)}} + exp\left[\frac{\alpha}{\theta_{v,sat(i)}}\left(\theta_{v,sat(i)} - \theta_{v(i,t-\Delta t)}\right)\right]\right\} \quad (42)$$

where $\theta_{v(i,t)}$ and $\theta_{v,sat}$ are, respectively, volumetric water content and saturation point ($m^3\ m^{-3}$) for soil layer (i) and time-step (t); L_i is the thickness (m) of soil layer (i); $K_{sat(i)}$ is the saturated hydraulic conductivity in layer (i); Δt is the time-step set equal to 1 (day); α is an empirical parameter (dimensionless), supposed equal to 13 in a homogeneous soil (Kendy *et al.*, 2003).

When sugarcane starts growing, the root system is simulated by the amount of carbohydrates allocated to the roots and distributed throughout the soil profile and expressed as root length density (RLD, cm cm^{-3}) (Laclau and Laclau, 2009; Marin and Jones, 2014). Root water extraction is derived from the theory of radial flow to a single root

and assumes that the hydraulic conductivity of all soils is similar when normalised to the wilting point (Ritchie, 1998). Thus, a daily potential root water uptake (PRWU, mm d^{-1}) is integrated as a function of the underlying layer's water content (θ_v) and the RLD (Marin and Jones, 2014). Atmospheric demand for water is derived from potential evapotranspiration to potential crop transpiration (PTRANS, mm d^{-1}) as a function of leaf area index. Actual root water uptake and crop transpiration are set as the minimum value between potential supply and demand.

Similarly, water stress is computed as the ratio between water supply (PRWU) and demand (PTRANS), following the CERES-Maize model (Jones, Kiniry and Dyke, 1986). If the crop allocates carbon to roots, the PRWU capacity increases with RLD (Figure 33a). Two water stress factors are used for relative process reduction, one for photosynthesis rate (SWFACP) and the other for more sensitive physiological processes (SWFACE) such as plant expansion and tillering (Figure 33b). Any stress due to nutritional restrictions is not simulated in the standalone version.

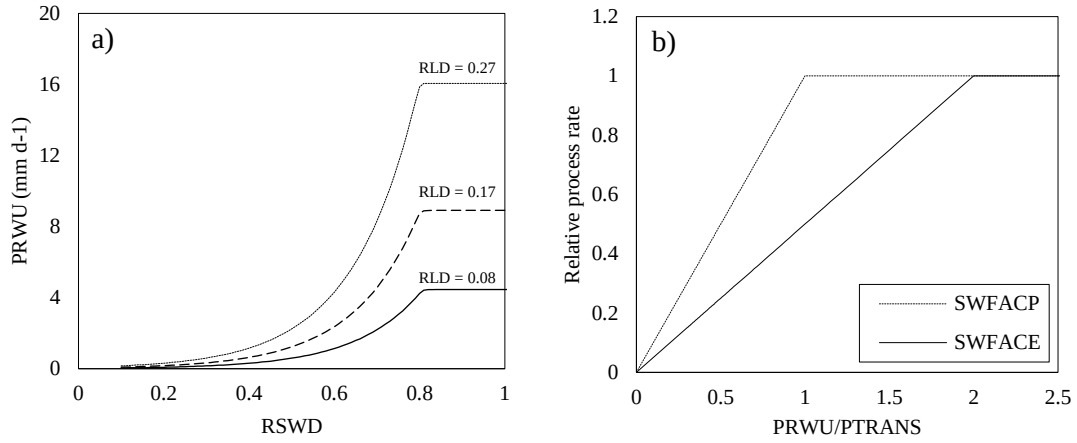

Figure 33. Potential root water uptake (PRWU) as function of relative soil water depletion (RSWD), defined as the difference between soil field capacity and wilting point, and averaged root length density (RLD) for a soil profile (a). Relative effect of water stress on photosynthesis process and plant expansion/tillering as function of potential water supply and demand ratio (b)

To compute soil water movement, the SWAP model solves the Richards equation (43) with respective sink terms. A robust numerical scheme, combined with an accurate mass balance closure and a dynamic time-step method, guarantees accurate results and rapid convergence (van Dam *et al.*, 2008; Kroes *et al.*, 2009). The Newton-Raphson iteration procedure is used to solve a set of discrete forms of the Richards equations as a function of pressure head (h), converging to mass conservation (Kroes *et al.*, 2009). In addition, a backtrack method on the Newton step is performed to ensure the convergence towards water balance closure. Various parameters can be defined to configure the numerical scheme such as a convergence criterium and maximum and minimum time-step (Kroes *et al.*, 2009):

$$\frac{\partial \theta}{\partial t} = \frac{\partial}{\partial z}\left[K(h)\left(\frac{\partial h}{\partial z} + 1\right)\right] - S_a(h) - S_d(h) - S_m(h) \qquad (43)$$

where θ is the volumetric water content ($m^3\ m^{-3}$), t is time (d), h is the soil water pressure head (cm), K(h) is hydraulic conductivity (cm d^{-1}), z is the vertical coordinate (cm), $S_a(h)$, $S_d(h)$ and $S_m(h)$ are, respectively, the sink terms for root water extraction, drain discharge in the saturated zone and exchange rate with macro pores. The hydraulic relations by Mualem–van Genuchten (1985) are used to solve Equation 43.

Maximum root water extraction (S_p), integrated over the rooting depth (D_{root}), is equal to potential transpiration (PTRANS). Root length density (RLD) distribution over soil compartments is used to compute the potential water extraction at a certain depth, $S_p(z)$ (Equation 44):

$$S_p(z) = \frac{RLD(z)}{\int_{-D_{root}}^{0} RLD(z)dz} PTRANS \quad (44)$$

Stress due to dry or wet conditions may reduce S_p by the function proposed by Feddes et al. (1978). Pressure head (h) thresholds parameters (h_1 to h_4) define five zones of potential root water extraction reduction (Figure 34). In the range of h_2 to h_3, no reduction is simulated, and root water extraction is at its potential level. When h is in the falling rate phase below h3, root water extraction is linearly reduced until zero at and below h_4. Similarly, above h_2, actual root water uptake is linearly reduced due to anoxia down to zero at and above h_1. The model allows to specify the value of h_3 for a high and low atmospheric demand (h_{3h} and h_{3l}, respectively) (Kroes *et al.*, 2009). Actual root water extraction (S_a) is then integrated over the soil compartments, and the actual transpiration rate is updated.

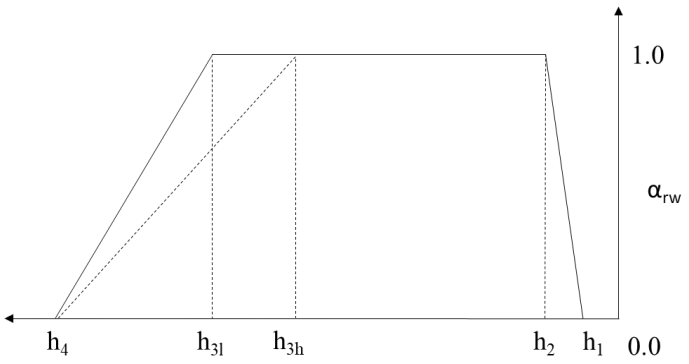

Figure 34. Reduction coefficient for root water uptake (αrw), as function of soil water pressure head (h) and potential transpiration rate (PTRANS) (after Feddes et al. 1978)

Pressure head threshold values h_1 to h_4 for sugarcane have been proposed by Qureshi (1999) and applied to simulate irrigation scheme strategies (Qureshi, Madramootoo and Dodds, 2002) and to evaluate SWAP/WOFOST model performance (Scarpare, 2011). Because potential root water uptake (PRWU) is set equal to potential transpiration (PTRANS), the plant expansion water stress factor (SWFACE) used in SAMUCA would be very restrictive (Figure 33b). Thus, PRWU based on Ritchie (1998) was re-computed only to obtain SWFACE and to avoid further calibration.

The SWAP model structure is fully described in Kroes et al. (2009), and to couple SAMUCA to the SWAP platform, the sugarcane model was re-structured into initialisation (i = 1), potential rate/state (i = 2) and actual rate/state (3) mode (Figure 35). In this way, all input and output data could be exchanged between the main structure of SWAP and sugarcane PBM during the simulations.

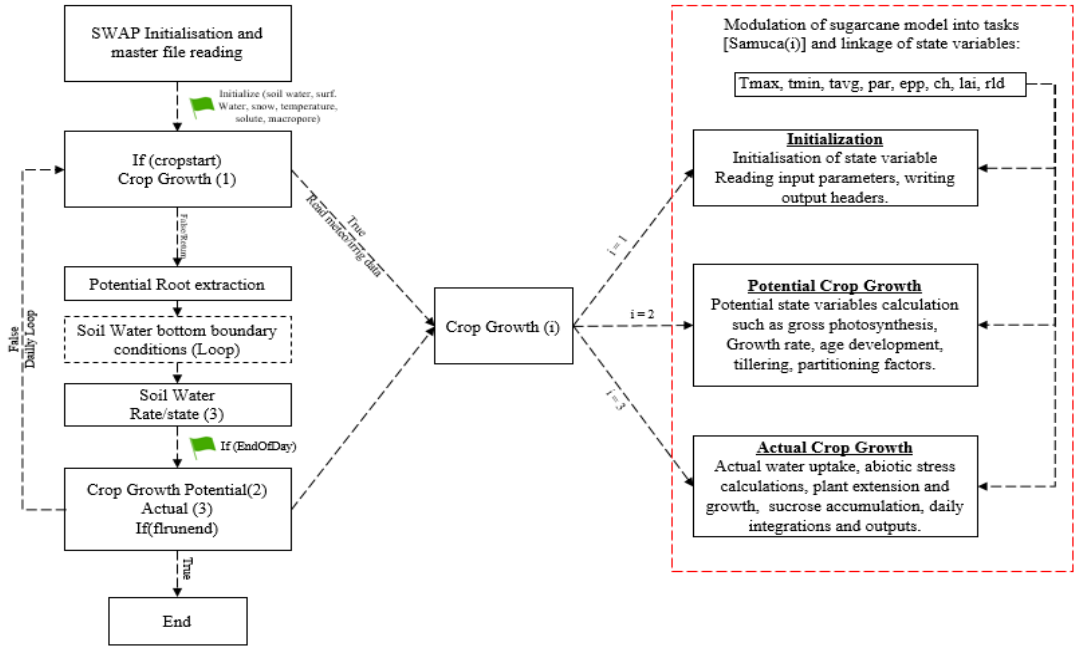

Figure 35. Simplified framework of SWAP model structure and Crop Growth module, including SAMUCA restructured subroutines (within dashed red box) and variables at initialization, potential and actual plant growth

All SWAP crop variables and process routines were compiled using the TTUTIL library (Kraalingen and Rappoldt, 2002), identified and tracked to accomplish the model coupling. The sugarcane PBM code was then included in the SWAP routine and compiled in the CropGrowth module. The SAMUCA weather, soil and control variables were identified and modified to be linked to the SWAP main structure (Figure 35). Crop parameters and controls were added to simulations in the form of an input file similar to the SWAP crop files (extension "crp").

Table 14. State variables linked, its description and modules in which it is used by SWAP main structure

Variable	Description	Module
Pleng	Plant Height	CropGrowth and ET
Llength	Leaf Length	CropGrowth and ET
Lai	Leaf Area Index	CropGrowth and ET
rld(i)	Root Length Density array(i)	CropGrowth and RootWaterUptake
Rdi	Initial Root Depth	CropGrowth and RootWaterUptake
Rdm	Maximum Root Depth	CropGrowth and RootWaterUptake
Rd	Actual Root Depth	CropGrowth and RootWaterUptake
Rdctb	Relative Root Density	CropGrowth and RootWaterUptake
Kdif	Extinction coefficient for diffuse visible light	CropGrowth
Kdir	Extinction coefficient for direct visible light	CropGrowth
Albedo	Crop reflection coefficient	CropGrowth and ET
Rsc	Minimum canopy resistance of dry crop	ET
Rsw	Canopy resistance of intercepted water	ET
Tmx	Maximum Air Temperature	CropGrowth and ET
Tmn	Minimum Air Temperature	CropGrowth and ET
Tavg	Average Air Temperature	CropGrowth and ET
Rad	Solar Radiation	CropGrowth and ET
Rh	Relative Humidity	ET
Wind	Wind Speed	ET
Etref	Reference Evapotranspiration	ET
Ptra	Potential evapotranspiration	ET and RootWaterUptake
Peva	Potential evaporation	ET and RootWaterUptake
Tra	Actual transpiration	ET and RootWaterUptake
Evap	Actual soil evaporation	ET and RootWaterUptake
h(i)	Soil water pressure head array(i)	CropGrowth and RootWaterUptake

The ability of the coupled SAMUCA-SWAP model to simulate crop yield and its components and the soil-plant atmosphere dynamics was tested and evaluated for a detailed field experiment dataset including soil water content, evapotranspiration measurements and crop growth and development (tillering, fresh and dry biomass, leaf area index, plant height and sucrose content). The experiment was conducted in Piracicaba, Brazil (Lat: 22°41'55"S Lon: 47°38'34"W Alt: 547 m), from July 2014 to May 2015 (327 days) under two treatments (with and without mulch cover) for a 2nd ratoon, cultivar RB867515 (Figure 36). The Köppen climate type is Cwa, and the soil is a Hapludox according to the USDA classification (Soil Taxonomy, 2004). Soil water content measurements were taken after every rain event and at least three times per week via a capacitance probe (FDR, "Diviner 2000®").

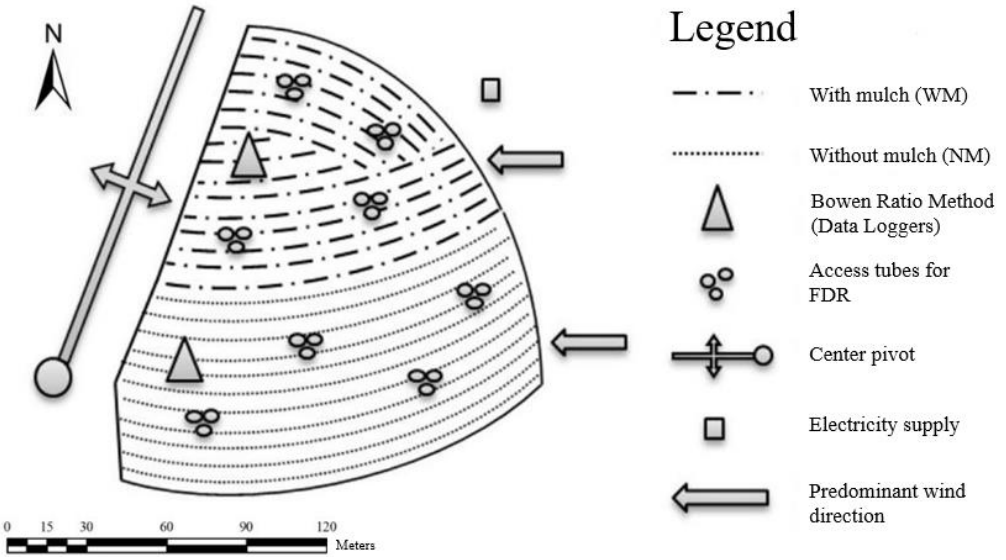

Figure 36. Experimental area sketch describing the central pivot, predominant wind direction, location of evapotranspiration measurements (Bowen Ratio Method) and access tubes for FDR soil moisture probe in treatment with mulch (WM) and without mulch (NM)

Evapotranspiration was determined via the Bowen Ratio Method (BRM), based on net radiation (Nr), soil heat flux (G), temperature and vapor pressure differences (Δt and Δe) measurements, allowing to establish the energy balance (Perez *et al.*, 1999). Two BRM equipment towers were slightly displaced to the northwest (NW) inside each treatment area, as southwest is the prevailing wind direction (Wiendll and Angelocci, 1995), to assure sufficient fetch and adequate superficial boundary layer (Heilman, Brittin and Neale, 1989). Mualem-van Genuchten soil parameters and saturated hydraulic conductivity (Ks) were determined in the laboratory, using undisturbed soil samples taken at five depths (Table 15). Further details on MRB and soil curve retention curves are depicted in section 2.2.2.1.

Table 15. Mualem-van Genuchten soil parameters and saturated hydraulic conductivity (Ks) for the Piracicaba field experiment

Parameter	depth (cm)				
	0-5	5-15	15-30	30-60	60-100
θr ($m^3\ m^{-3}$)	0.01	0.01	0.01	0.01	0.01
θs ($m^3\ m^{-3}$)	0.380	0.352	0.390	0.428	0.456
α (cm^{-1})	0.011	0.019	0.005	0.004	0.002
n (-)	1.124	1.065	1.068	1.072	1.090
Ks ($m\ d^{-1}$)	0.41	0.24	0.11	0.05	0.05

A calibration routine was implemented to optimise crop parameters by minimising the root mean squared error (RMSE) between simulated and measured data. The SWAP-SAMUCA model was embedded into an R function to compute the RMSE, based on the detailed field experiment measurements. This function was then iteratively called a "General-Purpose function" ("*optim(crop_array,fun)*"), changing the crop parameter array to converge it into the minimum RMSE for each crop component (dry biomass, tillering, LAI) (Figure 37). By default, *optim()* uses an implementation of Nelder and Mead (1965), but it is also possible to use quasi-Newton and conjugate-gradient algorithms with box-constrained optimisation (R. and Reeves, 1964; Nelder and Mead, 1965; Nash, 1990; Byrd *et al.*, 1995; Vanderplaats, 1995).

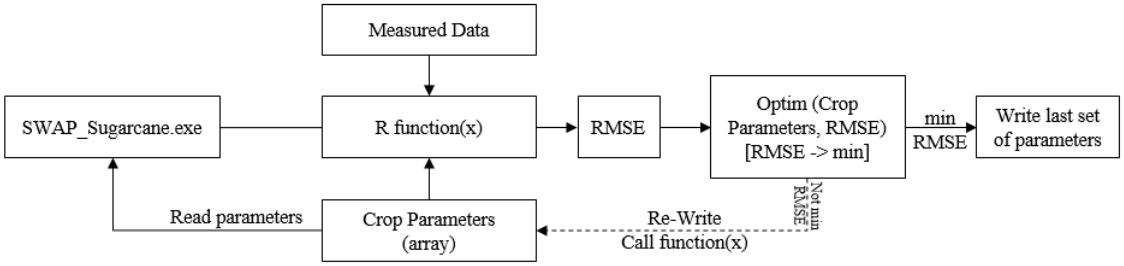

Figure 37. Schematic framework of a general-purpose calibration routine developed in R environment

The constrained BFGS (Broyden–Fletcher–Goldfarb–Shanno) optimisation method (Byrd *et al.*, 1995) was selected to calibrate the SWAP-SAMUCA model, focusing only on tillering and canopy parameters (chustk, chupeak, chudec, chumat, popmat, poppeak and maxgl), based on the detailed field experiment dataset for cultivar RB857515 described above. Initial parameter values and constrains were set according to Marin (2014) and Marin & Jones (2014), respectively.

To evaluate the SWAP-SAMUCA model performance in different weather and soil conditions, a field experiment dataset was used (Table 16). All weather input data were formatted according to the SWAP input format. As no relative humidity and wind data were available, reference evapotranspiration (ETref) was estimated according to Priestley-Taylor (1972). The soil parameters were numerically derived from soil saturation curves for each site (van Genuchten, Leij and Yates, 1991; Marin and Jones, 2014). The cultivar RB857515 was selected because at present, it is one of the most cultivated in Brazil (accounting for more than 25% of sugarcane fields) (CTC, 2012). Statistical indices such as bias, root mean squared error (RMSE), relative root mean squared error (RRMSE), determination index (r^2) and the Willmot index (d) were used to evaluate model performance in simulating plant components and soil water contents for different scenarios (Wallach *et al.*, 2014).

Table 16. Locations used in this study: data about geography, climate and sugarcane management

Site	Planting and harvesting dates	Weather	Water treatment	Soil Type	Soil depth
União/PI 4°51'S,42°52'W, 68 m	9/29/2007 and 06/16/2008	27 °C, 1500 mm, Aw	Irrigated and Rainfed	Oxisol*	125 cm
Coruripe/AL 10°07'S,36°10'W, 16 m	8/11/2007 and 11/15/2008	24.4 °C, 1400 mm, As´	2 irrigation levels	Typic Hapludox*	40 cm
Coruripe/AL 10°07'S,36°10'W, 16 m	8/16/2005 and 09/15/2006	21.6 °C 1400 mm, As´	Rainfed	Typic Hapludox*	40 cm
Aparecida do Tab./MS 20º05S,51º18'W,335 m	7/1/2006 and 09/08/2007	23.5 °C, 1560 mm, Aw	Rainfed	Typic Hapludox*	400 cm
Colina/SP 20°25'S,48°19'W, 590 m	2/10/2004 and 12/01/2005	22.8 °C, 1363 mm, Cwa	Rainfed	Typic Hapludox*	400 cm
Olímpia/SP 20°26'S,48°32'W, 500 m	2/10/2004 and 12/01/2005	23.3 °C, 1349 mm, Cwa	Rainfed	Typic Hapludox*	400 cm

3.3. RESULTS AND DISCUSSION

3.3.1. Model calibration and performance to simulate crop components and soil water content in southeast Brazil

The values obtained using the calibration routine, using a constrained range of parameters (Marin and Jones, 2014) and pre-defined parameters (Marin, 2014), are summarised in Table 17. The best RMSE values for green leaf number, LAI and tillering measurements were 1.82 green leaves tiller^{-1}, 1.36 m^2 m^{-2} and 3.64 tillers m^{-2}, respectively. The parameter values optimised for tillering on maturation and maximum green leaf number were similar to measured values in the field experiment, i.e. 10.86 tillers m^{-2} and 4.74 leaves tiller^{-1} (average values among treatments). The estimated population peak was also close to the measured data (20.77 tillers m^{-2}); however, a significant difference between the peak populations of the treatment WM and NW was observed and might be related to soil temperature and light interception (Bezuidenhout *et al.*, 2003).

Table 17. Parameter description and calibration values for the SWAP-SAMUCA model

Parameter	Description	Value	Units
maxgl	Maximum number of green leaves	5.5*	n°
tb	Base temperature	9.98	°C
rue	Radiation use efficiency	1.82	g MJ^{-1}
sla	Specific leaf area	64.0	g m^{-2}
extcoef	Light extinction coefficient	0.59	-
sgpf	Max partitioning fraction to culms	0.79	-
dpercoeff	Plant extension rate	0.352	mm °C^{-1} d^{-1}
sucmax	Max sucrose fraction of dry biomass	0.769	-
srl	Specific root length	17.38	cm g^{-1}
chustk	Heat units for start culm elongation	432.1*	°C d
chupeak	Heat units for population peak	1256.5*	°C d
chudec	Heat units for start of tiller abortion	1481.6*	°C d
chumat	Heat units for population establishment	2501.8*	°C d
popmat	Number of tillers on maturation	11.05*	tillers m^{-2}
poppeak	Maximum number of tillers	20.01*	tillers m^{-2}
phyloc	Phyllochron interval for leaf appearance	169.7	°C d
mla	Maximum leaf area	543.2	cm^2
rwep1	Soil water supply/potential threshold for expansion stress	2	-
rwep2	Soil water supply/potential threshold for photosynthesis stress	1	-

* Calibrated parameters

Crop components were well simulated by the SWAP-SAMUCA model, with focus on green leaf number, stalk dry mass and tillering. Simulated green leaf number started close to emergence observed in the field experiment (34 days after harvesting [DAH]), ranging between 4.5 and 5.5 green leaves per tiller (Figure 38a). For LAI, early season values were overestimated (Figure 38b), probably because the model neglects the effect of water stress on leaf appearance. The tillering peak occurred at 113 DAH (Figure 39a), which may have contributed to the overestimations resulting from the upscaling approach of LAI based on tillering and leaf area. The water stress effect on leaf appearance has been pointed out by Inman-Bamber (1991) and is accounted for in the DSSAT-CANEGRO model by a thermal time assumed for full crop recovery from water stress. In addition, in both APSIM-Sugar and DSSAT-CANEGRO models, leaf senescence is accelerated by water stress (Marin *et al.*, 2015).

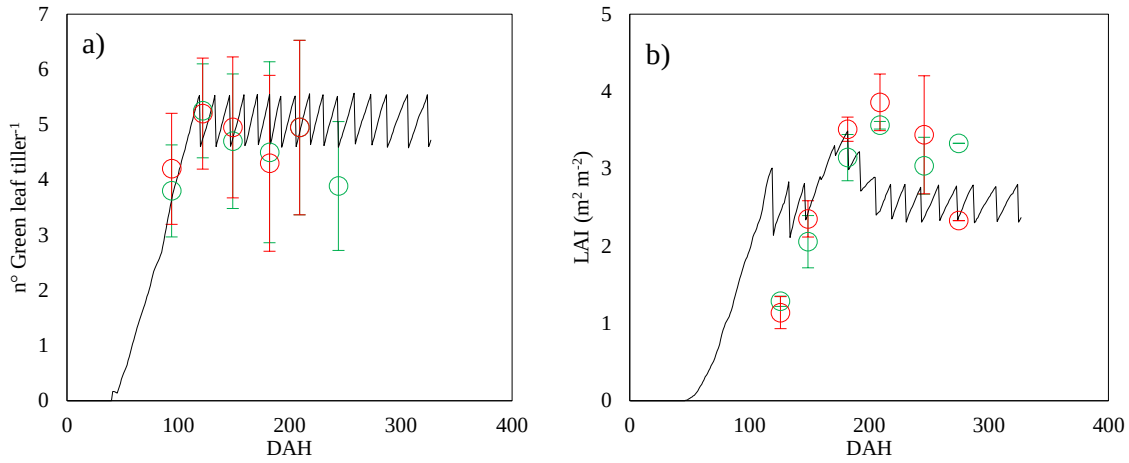

Figure 38. Number of green leaves per tiller (a) and leaf area index (b) simulated (solid lines) and measured (open circles) for With Mulch (green) and Without Mulch (red) treatments throughout days after harvesting (DAH) in the Piracicaba experiment

Tillering results were close to measured data, except at the tillering peak, when 25.5 and 16.0 tillers m^{-2} were measured in the treatment NW and WM, respectively (Figure 39a), and this version of SAMUCA does not consider the mulch effect on tillering (Marin and Jones, 2014). Tiller emergence occurs from buds at the base of the plant, and soil temperature might be a key factor driving this process (LAUDE, 1972). This was evident especially in this case, because mulch cover significantly affects soil temperature (Donk *et al.*, 2004), although the effect of soil temperature on sugarcane tillering is not included in the model (Marin and Jones, 2014). Plant height was underestimated throughout the crop season (Figure 39b), the water stress effect on plant expansion (rwep1) is considered to be higher than that on photosynthesis (rwep2) (Marin and Jones, 2014).

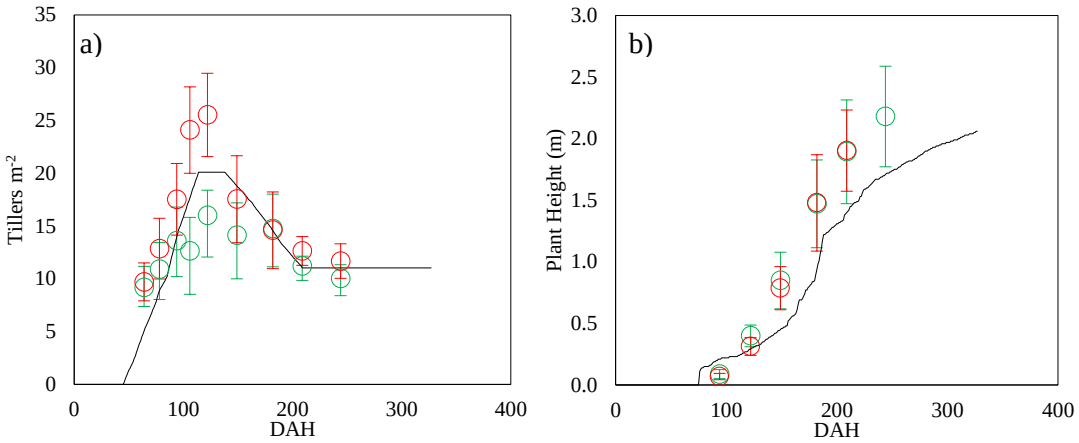

Figure 39. Tillering (a) and stalk height (b) simulated (solid lines) and measured (open circles) for With Mulch (green) and Without Mulch (red) treatments throughout days after harvesting (DAH) in the Piracicaba experiment

Stalk dry mass was simulated by the SWAP-SAMUCA, with an RMSE of 5.37 t ha^{-1} (Figure 40a), similar to previous calibration in different Brazilian regions (Marin and Jones, 2014). Despite the high variability of measured data, the simulated stalk dry mass pattern over time was close to the average field measurements. This variable is directly affected by partitioning and radiation use efficiency parameters and indirectly by almost all other parameters due to the model dynamics. Similar observations were made for stalk fresh mass, which was well simulated until the mid-season (200 DAH). Stalk fresh mass has strong relations to soil moisture and sucrose content in stalks, and the noticed underestimation of final season stalk fresh mass (Figure 40b) was possibly due to the underestimated soil water content after lodging (Figure 42) (Martine and Lebret, 2001; Marin *et al.*, 2015).

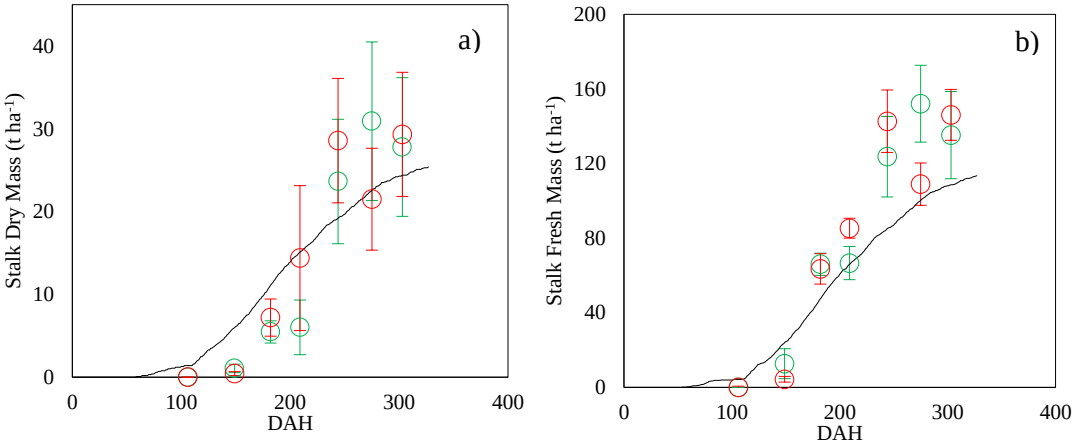

Figure 40. Stalk dry (a) and fresh (b) mass simulated (solid lines) and measured (open circles) for With Mulch (green) and Without Mulch (red) treatments throughout days after harvesting (DAH) in the Piracicaba experiment

The final sucrose content on a fresh mass basis (POL %) was simulated well, although the sucrose accumulation process was anticipated in simulations (Figure 41a). Sucrose accumulation within sugarcane stalks is accelerated by low temperatures and/or drought stress. In traditional sugarcane areas of Brazil, the humid subtropical climate (Cwa), with a dry winter from May to August, favours sucrose accumulation (Alvares *et al.*, 2013). In irrigated fields, without a dry winter, the "drying off" strategy (irrigation suppression) takes place at the final season to accelerate sucrose accumulation, in addition to saving water and energy (Inman-Bamber, 2004). The mechanism employed in the

model to simulate this effect is by using two stress parameters to regulate plant expansion and growth. The expansion parameter is more sensitive in mimicking the sucrose accumulation as a passive energy storage ("sugar leftovers").

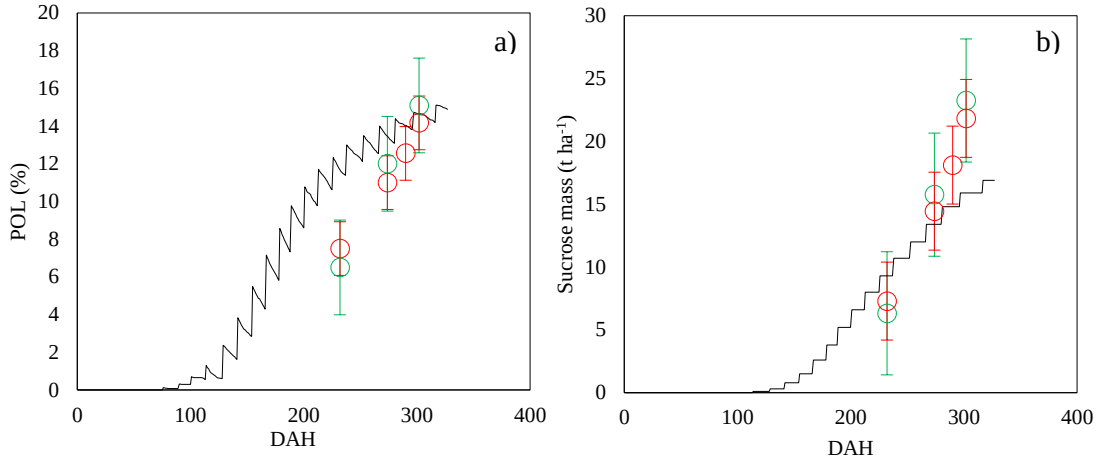

Figure 41. Sucrose content in fresh stalks (POL%) (a) and sucrose mass (b) simulated (solid lines) and measured (open circles) for With Mulch (green) and Without Mulch (red) treatments throughout days after harvesting (DAH) in the Piracicaba experiment

In general, the coupled model resulted in improved statistical indices for crop components than the standalone version of SAMUCA (Table 18). Green leaf number and stalk dry and fresh mass simulation performance were not considerably affected by the SWAP coupling. On the other hand, tillering and LAI were the most improved simulation variables, with RMSE decreases of 7 and 27%, respectively, whilst stalk height showed an increased RMSE compared to the standalone version.

Table 18. Statistical performance indexes for SWAP-SAMUCA and SAMUCA standalone versions compared computed for Piracicaba field experiment (averaging with and without mulch treatment). RMSE is the root mean squared error, EF is the modelling efficiency, r^2 the precision index, d is the Wilmot accuracy index

Variable	SWAP-SAMUCA				SAMUCA-Standalone			
	Bias	RMSE	r^2	d	Bias	RMSE	r^2	d
Green Leaf Number tiller^{-1}	0.09	0.58	0.83	0.95	0.08	0.59	0.84	0.96
Tillers m^{-2}	-0.86	3.34	0.67	0.90	-0.09	3.21	0.73	0.89
LAI (m^2 m^{-2})	-0.15	0.83	0.46	0.79	0.15	1.16	0.14	0.65
Stalk Height (m)	-0.26	0.37	0.96	0.92	-0.07	0.18	0.98	0.98
Stalk dry mass (t ha^{-1})	0.23	5.37	0.87	0.93	3.15	5.98	0.82	0.90
Stalk fresh mass (t ha^{-1})	-15.72	27.33	0.93	0.92	-5.34	28.30	0.87	0.91
POL (%)	7.87	2.81	0.97	0.67	9.33	3.05	0.95	0.69

The soil water content in layers down to 60 cm was well simulated by SWAP-SAMUCA throughout the crop season (Figure 43), except for the period after 242 DAH, when a lodging event occurred in the experimental area (Figure 42). This kind of field perturbation is not included in model predictions, leading to a prediction mismatch. Lodging is frequent in "Cwa" climates and has increased over the past years (Silva Dias *et al.*, 2013). After lodging, the soil water content was mostly underestimated by the model; this may also explain the lower predicted yields for stalk fresh mass (Figure 40b).

Figure 42. Lodging event occurred on 242 Days After Harvesting (DAH) when a storm occurred (10.2 mm in 15 minutes and over 12.6 m s^{-1} max wind speed)

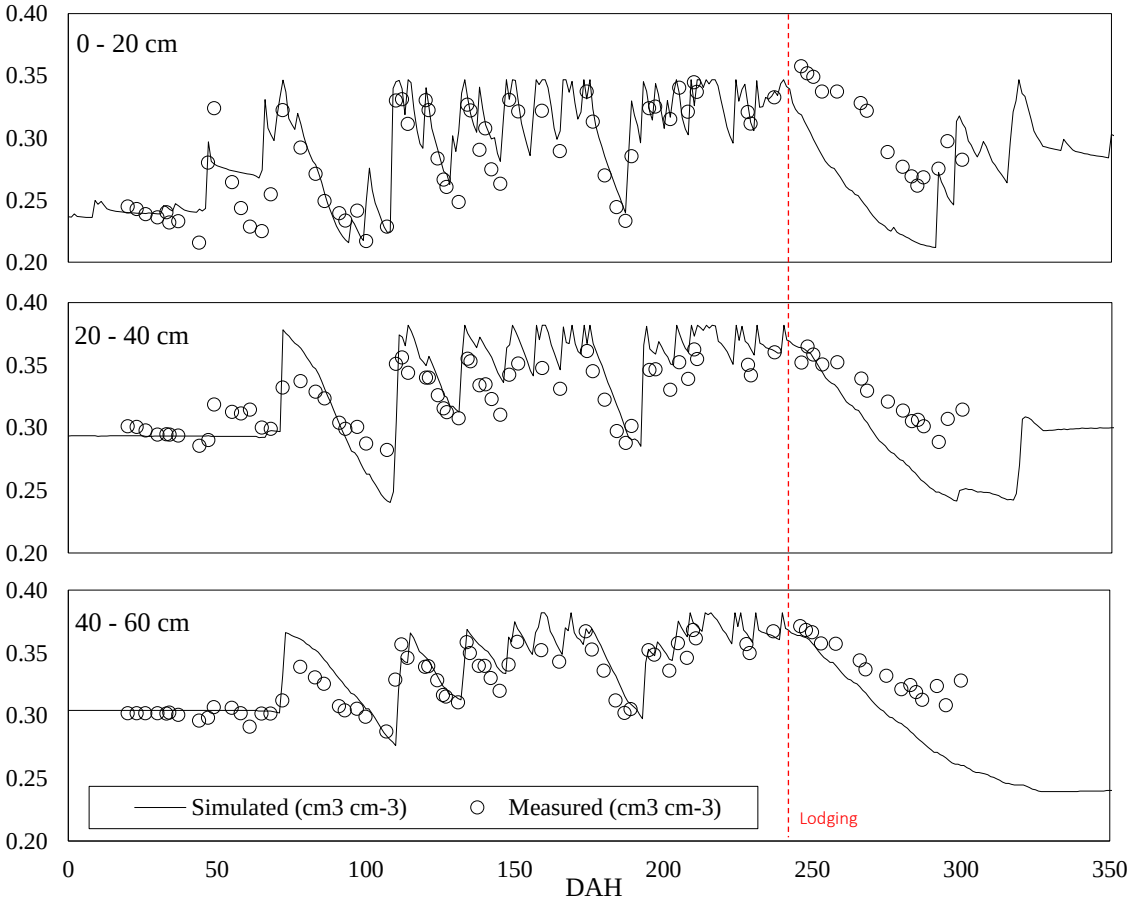

Figure 43. Soil water content (cm^3 cm^{-3}) in three soil layers simulated by SWAP-SAMUCA model (solid line) and measured (open circles) in the Piracicaba experiment (average of WM and NM treatments). Red-dotted line indicates the lodging event occurred on 242 Days after Harvesting (DAH)

The soil-water balance routine used in the standalone sugarcane model also yielded good results over the crop season (Figure 44). Although predicting a higher temporal variability of soil water content in all soil layers, the model simulated the main soil water content ranges and variation. As in the coupled version, soil water contents were underestimated after the lodging event. The CERES-based models predict a considerably more abrupt root water uptake reduction than observed, whereas simple models based on soil water content thresholds simulate a more gradual decline, which mimics observations more accurately (Singels *et al.*, 2010). Under limited water availability, this approach

may overestimate soil water stress, drastically reducing crop yield (Kendy *et al.*, 2003; López-cedrón *et al.*, 2008). Alternatively, root water uptake thresholds limit (e.g. wilting point) can be crop-specific, allowing root water extraction below or above -15MPa on the APSIM platform (Keating *et al.*, 1999). Moreover, hydrological models usually do not include compensation mechanisms allowing for reductions in the uptake from dry layers to be compensated by an increased uptake from wetter layers, as included in the SWAP platform (Jarvis, 1989; Lier *et al.*, 2008).

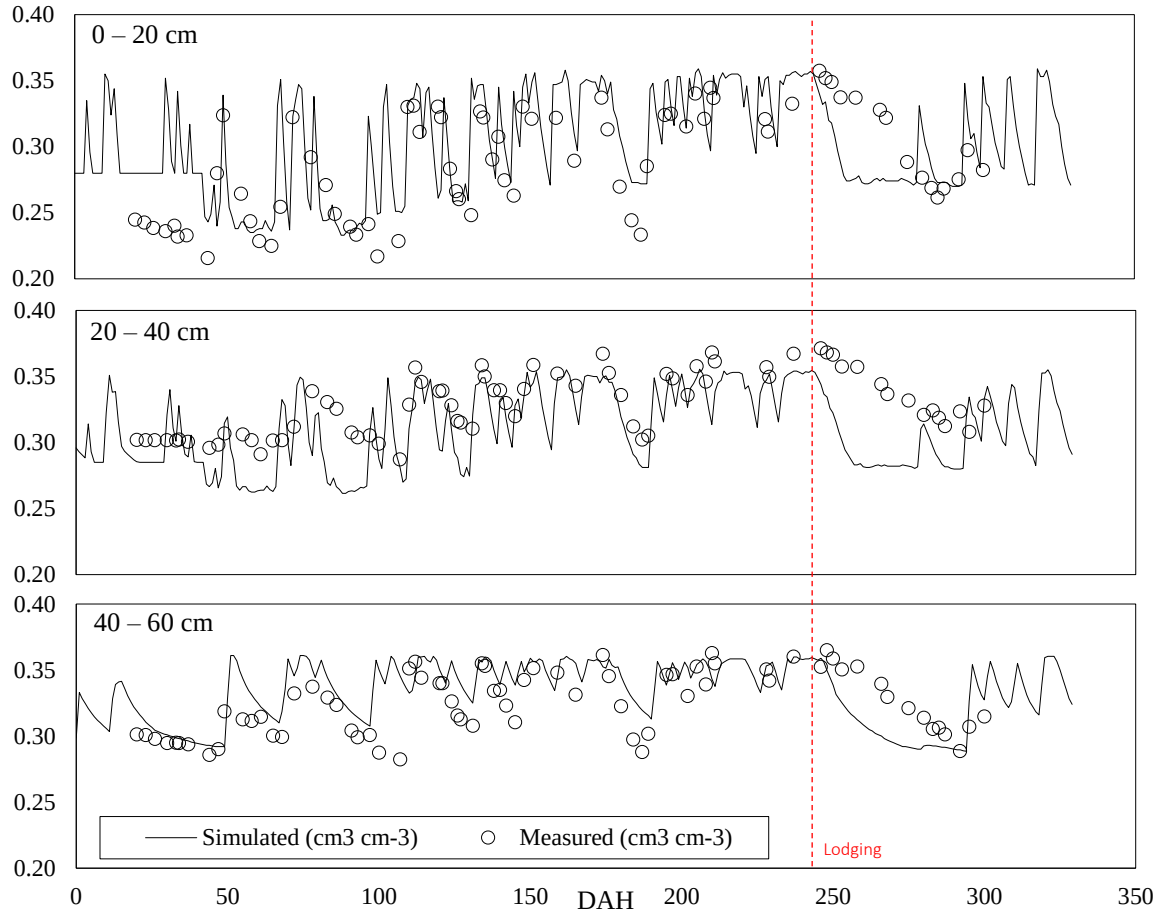

Figure 44. Soil water content ($cm^3\ cm^{-3}$) in three soil layers simulated by the SAMUCA standalone water balance routine and measured in Piracicaba experiment (average both treatments). Red-dotted line indicates the lodging event occurred on 242 Days after Harvesting (DAH)

Evapotranspiration can be expected to diminish after lodging due to damaged stems and/or root systems (affecting transpiration) and increased soil coverage by biomass (reducing evaporation). Lodging affects not only the sugarcane crop, but many crops cultivated under irrigated and windy conditions (Baker, Sterling and Berry, 2014). Physiologically, sugarcane lodging results in a reduction of radiation use efficiency and sucrose accumulation due to stalk damage and geotropic expansion. The occurrence can be simulated by empirical relations, using plant height and wind speed (van Heerden *et al.*, 2015), or physically through moment forces, soil conditions and crop canopy and root system characteristics (Baker, Sterling and Berry, 2014).

The SWAP-SAMUCA predictions for soil water content were better than the results of the SAMUCA standalone approach (Figure 45). The soil water content values simulated by SWAP-SAMUCA, applying the full Richards equation water balance module of SWAP, showed a higher precision ($r^2 = 0.82$) and accuracy ($d = 0.93$), with a 32% lower RMSE value than the original bucket-type simple water balance routine. Thus, besides the quantitative

improvement in simulation performance when using SWAP-SAMUCA, there is a qualitative advantage by enabling the inherent ability of SWAP to simulate process-based soil water dynamics.

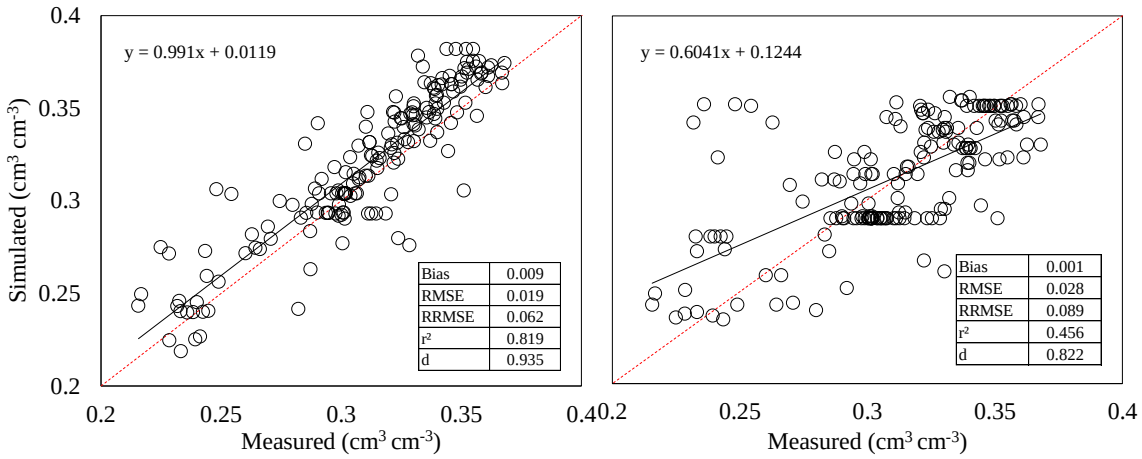

Figure 45. Measured versus simulated water contents over the cropping season and statistical indexes of performance using SWAP-SAMUCA (left) and SAMUCA standalone (right). Red dotted line is the line 1:1, RMSE is the root mean squared error, RRMSE is the relative root mean squared error, r^2 is the precision index and d is the Wilmot accuracy index

Actual evapotranspiration simulated by both models accompanied the observed values during the season (Figure 46). A small underestimation in the mid-season (around 150 DAH) occurred for the SWAP-SAMUCA model, which may be due to differences in root water uptake and/or root system growth. The effect of lodging after 242 DAH can be observed, but the used models cannot be expected to simulate this.

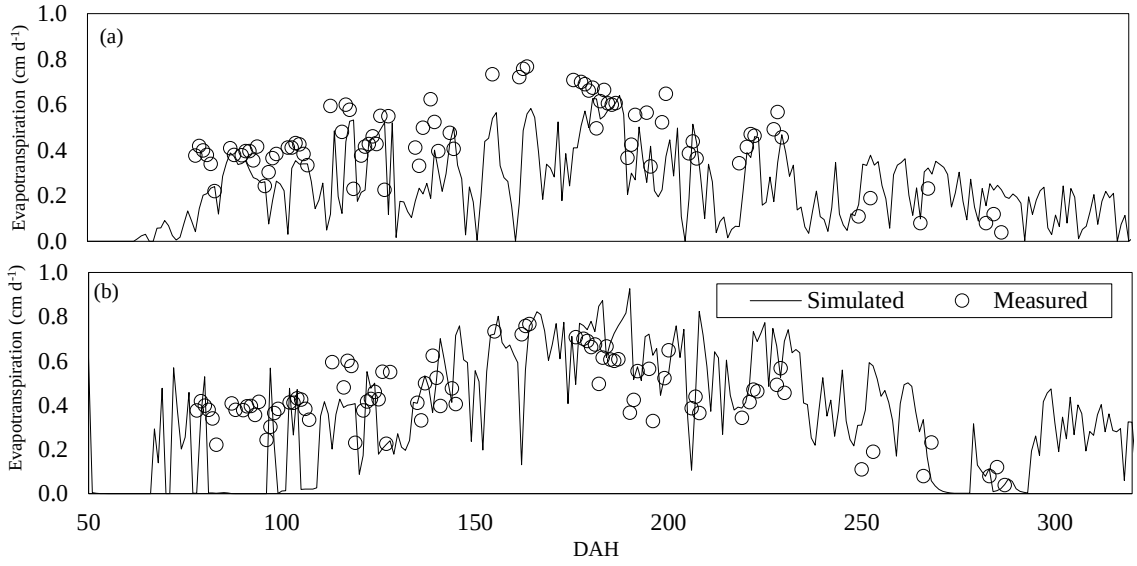

Figure 46. Crop actual evapotranspiration simulated by SWAP-SAMUCA model (a) and SAMUCA standalone version (b) in the Piracicaba experiment (average both treatments).

The PBMs for sugarcane have shown satisfactory performance to simulate crop components for Brazilian conditions (Marin *et al.*, 2015; Vianna and Sentelhas, 2015). Nevertheless, uncertainty about LAI and, especially, about the tillering process requires attention mostly because the canopy and population density are directly affecting the upscaling. In addition, mulch cover management techniques are used in many Brazilian sugarcane fields (De Souza *et*

al., 2005; Costa *et al.*, 2014; de Aquino and de Conti Medina, 2014), increasing the importance of physiologically accounting for mulch cover. Soil temperature is lower under the mulch cover, which might be a driving factor for tillering and initial crop development.

3.3.2. Model performance to simulate crop components for other regions in Brazil

For the other study sites, SWAP-SAMUCA showed good performance in stalk dry and fresh mass predictions (Figure 47), with an RMSE of 3.4 and 24.1 t ha^{-1} among the five different regions. Compared to previous studies with DSSAT-CANEGRO and APSIM-Sugar, the model presented a higher RMSE for stalk fresh and dry mass simulations, earlier reported as 18.2 and 20.9 t ha^{-1} respectively (Marin *et al.*, 2015), but improved in relation to the standalone version RMSE, reported as 5.38 t ha^{-1} (Marin and Jones, 2014). In contrast, for a longer season in Colina, São Paulo State, the model did not satisfactory simulate stalk fresh mass, whereas in Olimpia, São Paulo State, also with a longer crop cycle and similar climatic conditions, the result was good. In both sites, sugarcane was cultivated under rainfed conditions, whereas the production is dependent on soil hydraulic properties, and quick variations in fresh mass increase the uncertainty in fresh biomass simulations. No expressive improvements regarding crop components were noticed compared to the standalone version of SAMUCA, with an overall 6% lower RMSE value (Marin and Jones, 2014). Despite the low precision in LAI, the RMSE was 38% lower than in the standalone version, and the simulation pattern was reproduced during the season under different conditions.

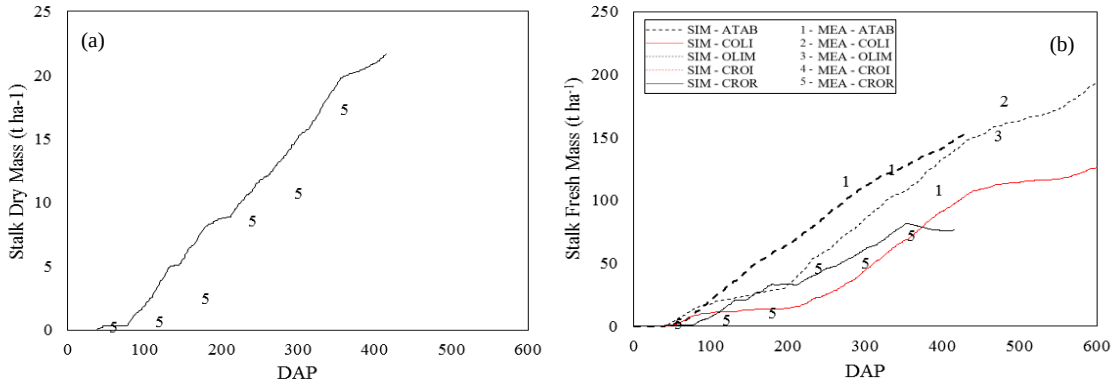

Figure 47. Stalk dry (a) and fresh biomass (b) simulated by SWAP-SAMUCA model (lines) and measured data (numbers) for several Brazilian conditions throughout Days After Planting (DAP)

The model could simulate the tillering pattern over time, such as peak population time and quantities. However, in some regions, the tillering peak did not match the simulated pattern. There is a lack of data describing the management of each site regarding soil mulch coverage (Aparecida do Taboado, MS), which may have a great effect on tillering, as discussed before (LAUDE, 1972). A similar effect was noted for LAI, and the model was able to simulate its pattern over time, although not very accurately.

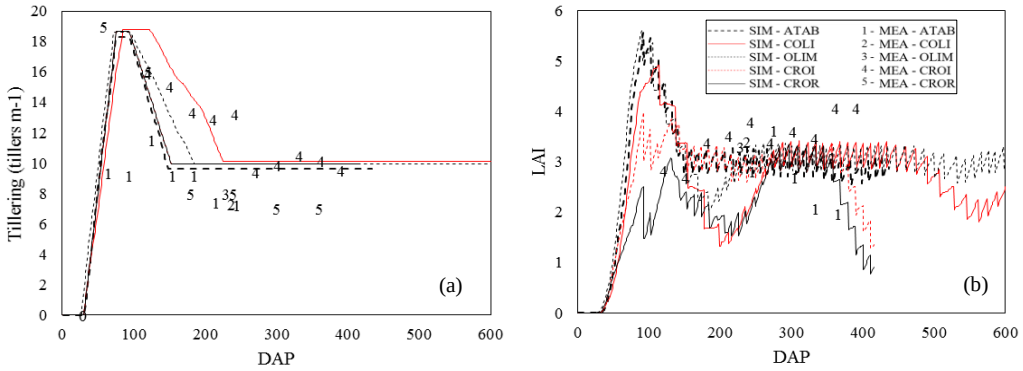

Figure 48. Tillering (a) and leaf area index (b) simulated by SWAP-SAMUCA model (lines) and measured data (numbers) for several Brazilian conditions throughout Days After Planting (DAP)

Excepting Coruripe (AL), where sucrose contents were overestimated for the whole season, resulting in an unexpected additional accumulation at the end of the season (320 DAH), sucrose accumulation on a fresh basis was well simulated, better than discussed earlier (Figure 49a). Stalk height was evaluated only at one site but under two treatments (irrigated and rainfed), and the model predictions were accurate throughout the season.

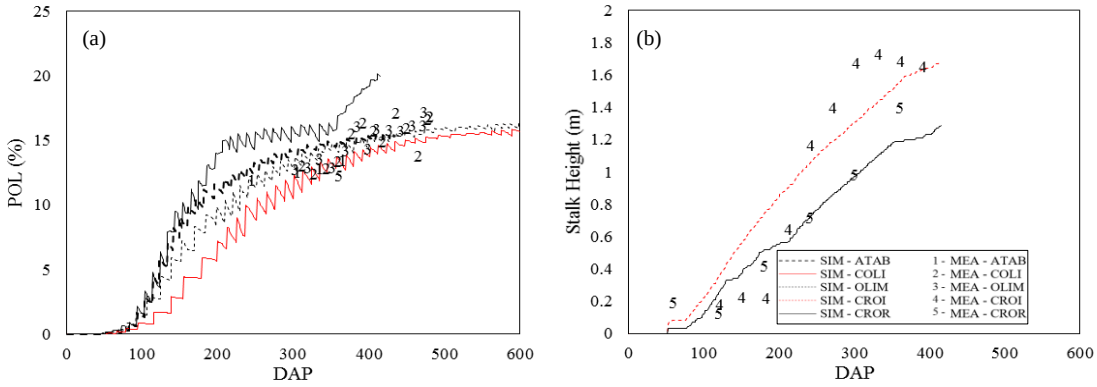

Figure 49. Sucrose content in fresh stalks (a) and stalk height (b) simulated by SWAP-SAMUCA model (lines) and measured data (numbers) for several Brazilian conditions throughout Days After Planting (DAP)

Table 19. Statistical indexes of performance of SWAP-SAMUCA computed for different Brazilian regions. RMSE is the root mean squared error, EF is the modelling efficiency, r^2 the precision index, d is the Wilmot accuracy index

Variable	Bias	RMSE	d	r^2
Stalk Dry Mass (t ha^{-1})	2.95	3.44	0.93	0.93
Stalk Fresh Mass (t ha^{-1})	-0.21	24.06	0.95	0.83
POL (%)	-0.20	1.49	0.95	0.85
LAI (m^2 m^{-2})	-0.23	0.85	0.64	0.18
Tillering (# m^{-2})	0.46	3.26	0.89	0.67
Height (m)	0.03	0.23	0.95	0.88

Besides soil water relations, SWAP has also been used in solute transport simulation and soil salinization studies (Jiang *et al.*, 2011; Noory *et al.*, 2011). Salt stress in the vadose zone can also be included in root water uptake simulations as a function of soil water electrical conductivity (Kroes *et al.*, 2009). In many Brazilian sugarcane fields in

expanding and traditional regions, emergency irrigation is required to maintain very young plants alive during the dry season. To save water and fertiliser resources, growers add vinasse (a by-product of ethanol production) to the irrigation water on sugarcane fields (Christofoletti *et al.*, 2013; dos Santos *et al.*, 2013). Moreover, vinasse application to sugarcane fields has been adopted as an alternative water and fertiliser source in water scarcity regions (Franco, Marques and de Melo, 2008; Barbosa *et al.*, 2017). These strategies are considered as good environmental practices in soil restoration; however, the inadequate and indiscriminate disposal of sugarcane vinasse in soils and water bodies has been receiving considerable attention for several decades due to the related environmental problems (Christofoletti *et al.*, 2013). The threshold of the amount of these alternative water resources and the potential salt stress and soil salinization impact on sugarcane production and groundwater contamination could be assessed by using SWAP. Further experimental data on solute transport and salinization stress could be used to evaluate the model's ability to simulate these processes to facilitate decision making in sugarcane management (Kumar *et al.*, 2015).

3.4. CONCLUSIONS

The coupling of a new sugarcane PBM (SAMUCA) to a robust agrohydrological model (SWAP) was fully accomplished, enabling more robust and less uncertain simulations of crop water consumption. Although non-expressive improvements in model performance regarding crop yield were noticed (with an overall 6% lower RMSE), the SWAP-SAMUCA ability to simulate soil water content proved to be quite superior compared to the original "tipping bucket" approach (32% lower RMSE values). Moreover, it opens new room for improvements and the testing of sugarcane groundwater consumption and the crop´s response to soil temperature, agrohydrology and salt stress on the PBM level.

Since any Brazilian sugarcane PBM is available for end users (for any crop), efforts on crop modelling may be a reasonably good strategy not only to support decisions of policy makers, farmers and investors, but also as a tool in education and scientific guiding (van Ittersum K *et al.*, 2003). Further modifications on these models, aiming to overcome limitations, and the addition of more detailed outputs on crop water consumption and key plant process (tillering, sugar accumulation, carbon partitioning) interactions between weather and management strategies are required to better assess and support sustainable sugarcane production in Brazil.

REFERENCES

ALLEN, R. G.; LUIS, S. P.; RAES, D.; SMITH, M. FAO Irrigation and Drainage Paper No. 56. Crop Evapotranspiration (guidelines for computing crop water requirements). **Irrigation and Drainage**, v. 300, n. 56, p. 300, 1998.

ALLEN, R. G.; PEREIRA, L. S.; RAES, D.; SMITH, M. Crop evapotranspiration: guidelines for computing crop water requirements. **FAO (Irrigation and Drainage)**, v. 56, 1998.

AZEVEDO, M. C. B. DE; CHOPART, J. L.; MEDINA, C. D. C. Sugarcane root length density and distribution from root intersection counting on a trench-profile. **Scientia Agricola**, v. 68, n. February, p. 94–101, 2011.

BAKER, C. J.; STERLING, M.; BERRY, P. A generalised model of crop lodging. **Journal of Theoretical Biology**, v. 363, p. 1–12, 2014.

BEZUIDENHOUT, C. N.; O'LEARY, G. J.; SINGELS, A.; BAJIC, V. B. A process-based model to simulate changes in tiller density and light interception of sugarcane crops. **Agricultural Systems**, v. 76, n. 2, p. 589–599, 2003.

BONNETT, G. D. Developmental Stages (Phenology). *In*: MOORE, P. H.; BOTHA, F. C. (Eds.). **Sugarcane. Physiology, Biochemistry and Functional Biology**. [s.l.] WILEY Blackwell, 2013. p. 35–53.

BONNETT, G. D. B.; SPILLMAN, M. F. A.; HEWITT, M. L. C.; B, J. X. Source – sink differences in genotypes and

water regimes in fl uencing sucrose accumulation in sugarcane stalks. p. 316–327, 2009.

BOTTCHER, A. *et al.* Ligni fi cation in Sugarcane : Biochemical Characterization , Gene Discovery , and Expression Analysis in Two Genotypes Contrasting for Lignin Content 1 [W]. v. 163, n. December, p. 1539–1557, 2013.

BOUGHTON, W. C. A review of the USDA SCS curve number method. **Soil Research**, v. 27, n. 3, p. 511–523, 1989.

BRAUN, D. M.; WANG, L.; RUAN, Y. Understanding and manipulating sucrose phloem loading , unloading , metabolism , and signalling to enhance crop yield and food security. v. 65, n. 7, p. 1713–1735, 2014.

BRAUNACK, M. V; ARVIDSSON, J.; HÅKANSSON, I. Effect of harvest traffic position on soil conditions and sugarcane (Saccharum officinarum) response to environmental conditions in Queensland, Australia. **Soil and Tillage Research**, v. 89, n. 1, p. 103–121, 2006.

BROWN, S. E.; PREGITZER, K. S.; REED, D. D.; BURTON, A. J. Predicting Daily Mean Soil Temperature from Daily Mean Air Temperature in Four Northern Hardwood S oil temperature is a very important climatic variable. v. 46, n. 2, p. 297–301, 2000.

BYRD, R. H.; LU, P.; NOCEDAL, J.; ZHU, C. A Limited Memory Algorithm for Bound Constrained Optimization. **SIAM Journal on Scientific Computing**, v. 16, n. 5, p. 1190–1208, 1995.

CAEMMERER, S. VON; FARQUHAR, G. D. Some relationships between the biochemistry of photosynthesis and the gas exchange of leaves. **Planta**, v. 153, n. 4, p. 376–387, 1981.

CARDOZO, N. P.; SENTELHAS, P. C.; PANOSSO, A. R.; PALHARES, A. L.; IDE, B. Y. Modeling sugarcane ripening as a function of accumulated rainfall in Southern Brazil. **International Journal of Biometeorology**, v. 59, n. 12, p. 1913–1925, 2015.

CHAPMAN, S. J. **Fortran for scientist and engineers: 1995-2003**. [s.l.] McGraw-Hill, 2008.

CHELLE, M.; EVERS, J. B.; COMBES, D.; VARLET-GRANCHER, C.; VOS, J.; ANDRIEU, B. Simulation of the three-dimensional distribution of the red: far-red ratio within crop canopies. **New Phytologist**, v. 176, n. 1, p. 223–234, 2007.

COSTA, L. G.; MARIN, F. R.; NASSIF, D. S. P.; PINTO, H. M. S.; LOPES-ASSAD, M. L. R. C. Simulação do efeito do manejo da palha e do nitrogênio na produtividade da cana-de-açúcar. **Revista Brasileira de Engenharia Agrícola e Ambiental**, v. 18, n. 5, p. 469–474, 2014.

COUTINHO, R. M.; KRAENKEL, R. A.; PRADO, P. I. Catastrophic Regime Shift in Water Reservoirs and S ã o Paulo Water Supply Crisis. p. 1–14, 2015.

COWAN, I. R. The interception and absorption of radiation in plant stands. **Journal of Applied Ecology**, p. 367–379, 1968.

EBRAHIM, M. K.; ZINGSHEIM, O.; EL-SHOURBAGY, M. N.; MOORE, P. H.; KOMOR, E. Growth and Sugar Storage in Sugarcane Grown at Temperatures Below and Above Optimum. **Journal of Plant Physiology**, v. 153, n. 5–6, p. 593–602, 1998.

EHLERINGER, J. R.; CERLING, T. E.; HELLIKER, B. R. C4 photosynthesis, atmospheric CO2, and climate. **Oecologia**, v. 112, n. 3, p. 285–299, 1997.

EVERS, J. B. **Tillering in spring wheat : a 3D virtual plant modelling study**. [s.l.] Wageningen University, 2006.

EVERS, J. B.; VOS, J.; ANDRIEU, B.; STRUIK, P. C. Cessation of tillering in spring wheat in relation to light interception and red: far-red ratio. **Annals of Botany**, v. 97, n. 4, p. 649–658, 2006.

EVERS, J. B.; VOS, J.; CHELLE, M.; ANDRIEU, B.; FOURNIER, C.; STRUIK, P. C. Simulating the effects of localized red: far-red ratio on tillering in spring wheat (Triticum aestivum) using a three-dimensional virtual plant model. **New Phytologist**, v. 176, n. 2, p. 325–336, 2007.

EVERS, J. B.; VOS, J.; FOURNIER, C.; ANDRIEU, B.; CHELLE, M.; STRUIK, P. C. Towards a generic architectural model of tillering in Gramineae, as exemplified by spring wheat (Triticum aestivum). **New Phytologist**, v. 166, n. 3, p. 801–812, 2005.

FARQUHAR, G. D.; CAEMMERER, S. VON; BERRY, J. A. A biochemical model of photosynthetic CO2 assimilation in leaves of C3 species. **Planta**, v. 149, n. 1, p. 78–90, 1980.

FOURNIER, C. A functional – structural model of elongation of the grass leaf and its relationships with the phyllochron. p. 881–894, 2001.

GARSIDE, A. L.; BELL, M. J.; BERTHELSEN, J. E.; HALPIN, N. V; OTHERS. **Effect of breaks and nitrogen fertiliser on shoot development, maintenance, and cane yield in an irrigated plant crop of Q117.**Proceedings

of the 2000 Conference of the Australian Society of Sugar Cane Technologists held at Bundaberg, Queensland, Australia, 2 May to 5 May 2000. **Anais**...2000

GHANNOUM, O. C4 photosynthesis and water stress. **Annals of Botany**, v. 103, n. 4, p. 635–644, 2008.

GOUDRIAAN, J. A simple and fast numerical method for the computation of daily totals of crop photosynthesis. **Agricultural and Forest Meteorology**, v. 38, n. 1, p. 249–254, 1986.

GOUDRIAAN, J. Light distribution. *In*: **Canopy Photosynthesis: From Basics to Applications**. [s.l.] Springer, 2016. p. 3–22.

HAVERAAEN, M.; MORRIS, K.; ROUSON, D.; RADHAKRISHNAN, H.; CARSON, C. High-performance design patterns for modern Fortran. **Scientific Programming**, v. 2015, p. 3, 2015.

HEERDEN, P. D. R. VAN; EGGLESTON, G.; DONALDSON, R. A. Ripening and Postharvest Deterioration. **Sugarcane: Physiology, Biochemistry, and Functional Biology**, p. 55–84, 2013.

HEERDEN, P. D. R. VAN; SINGELS, A.; PARASKEVOPOULOS, A.; ROSSLER, R. Negative effects of lodging on irrigated sugarcane productivity—An experimental and crop modelling assessment. **Field Crops Research**, v. 180, p. 135–142, 2015.

HEUVELINK, E. Dry matter partitioning in tomato: validation of a dynamic simulation model. **Annals of botany**, v. 77, n. 1, p. 71–80, 1996.

HIKOSAKA, K.; NIINEMETS, U.; ANTEN, N. P. R. **Canopy photosynthesis: from basics to applications**. [s.l.] Springer, 2016.

INMAN-BAMBER, N. G. A growth model for sugarcane based on a simple carbon balance and the CERES-Maize water balance. **South African Journal of Plant Soil**, v. 8, p. 93–99, 1991.

INMAN-BAMBER, N. G.; BONNETT, G. D.; SPILLMAN, M. F.; HEWITT, M. L.; JACKSON, J. Increasing sucrose accumulation in sugarcane by manipulating leaf extension and photosynthesis with irrigation. p. 13–26, 2008.

INMAN-BAMBER, N. G.; BONNETT, G. D.; SPILLMAN, M. F.; HEWITT, M. L.; XU, J. Source--sink differences in genotypes and water regimes influencing sucrose accumulation in sugarcane stalks. **Crop and Pasture Science**, v. 60, n. 4, p. 316–327, 2009.

ITTERSUM K, M. VAN; LEFFELAAR, P. A.; KEULEN, H. VAN; KROPFF, M. J.; BASTIAANS, L.; GOUDRIAAN, J. On approaches and applications of the Wageningen crop models. **European Journal of Agronomy**, v. 18, p. 201–234, 2003.

JONES, J. W.; HOOGENBOOM, G.; PORTER, C. H.; BOOTE, K. J.; BATCHELOR, W. D.; HUNT, L. A.; WILKENS, P. W.; SINGH, U.; GIJSMAN, A. J.; RITCHIE, J. T. **The DSSAT cropping system model**. [s.l: s.n.]. v. 18

KEATING, B. A.; ROBERTSON, M. J.; MUCHOW, R. C.; HUTH, N. I. Modelling sugarcane production systems I. Development and performance of the sugarcane module. **Field Crops Research**, v. 61, n. 3, p. 253–271, 1999.

KROES, J. G.; DAM, J. C. VAN; GROENENDIJK, P.; HENDRIKS, R. F. A; JACOBS, C. M. J. SWAP version 3.2. Theory and user manual. **Update**, n. August, p. 284, 2009.

LACLAU, P.; LACLAU, J. P. Growth of the whole root system for a plant crop of sugarcane under rainfed and irrigated environments in Brazil. **Field Crops Research**, v. 114, n. 3, p. 351–360, 2009.

LEVESQUE, J. M.; WILLIAMSON, J. W. **A Guidebook to FORTRAN on Supercomputers**. [s.l.] Academic Press, 2014.

LINGLE, S. E.; THOMSON, J. L. Sugarcane Internode Composition During Crop Development. **Bioenergy Research**, p. 168–178, 2012.

LIU, D. L.; BULL, T. A. Simulation of biomass and sugar accumulation in sugarcane using a process-based model. v. 144, p. 181–211, 2001.

LONG, S. P.; AINSWORTH, E. A.; ROGERS, A.; ORT, D. R. Rising atmospheric carbon dioxide: plants FACE the future. **Annu. Rev. Plant Biol.**, v. 55, p. 591–628, 2004.

MARENGO, J. A.; NOBRE, C. A.; SELUCHI, M. E.; CUARTAS, A.; ALVES, L. M.; MENDIONDO, E. M.; OBREGÓN, G.; SAMPAIO, G. A seca e a crise h{'\i}drica de 2014-2015 em São Paulo. **Revista USP**, n. 106, p. 31–44, 2015.

MARIN, F. R.; ANGELOCCI, L. R.; COELHO FILHO, M. A.; VILLA NOVA, N. A. Construção e avaliação de psicrômetro aspirado de termopar. **Scientia Agricola**, v. 58, n. 4, p. 839–844, 2001.

MARIN, F. R.; JONES, J. W. Process-based simple model for simulating sugarcane growth and production. **Scientia Agricola**, v. 71, n. 1, p. 1–16, 2014.

MARIN, F. R.; THORBURN, P. J.; NASSIF, D. S. P.; COSTA, L. G. Sugarcane model intercomparison: Structural differences and uncertainties under current and potential future climates. **Environmental Modelling & Software**, v. 72, p. 372–386, 2015.

MATSUOKA, S.; GARCIA, A. A. F. Sugarcane underground organs: going deep for sustainable production. **Tropical Plant Biology**, v. 4, n. 1, p. 22–30, 2011.

MCCORMICK, A. J.; CRAMER, M. D.; WATT, D. A. Sink strength regulates photosynthesis in sugarcane. **New Phytologist,** 2006.

MONTEITH, J. Light Interception and Radiative Exchange in Crop Stands. 1969.

MONTEITH, J. L.; UNSWORTH, M. H. **Principles of Environmental Physics: Plants , Animals , and the Atmosphere**. 4th Editio ed. Oxford: Elsevier Ltd, 2012.

MOORE, P. H.; BOTHA, F. C. **Sugarcane: physiology, biochemistry and functional biology**. [s.l.] John Wiley & Sons, 2013.

MULLER, J.; NORMALE, E.; LYON, S. DE. Arithmetic Processor for Solving Tridiagonal Systems of Linear Equations. 2006.

NASH, J. C. **Compact Methods for Computers. Linear Algebra and Function Minimisation**. [s.l: s.n.].

NASSIF, D. S. P. **Evapotranspiração, transpiração e trocas gasosas em um canavial irrigado**. [s.l.] University of Sao Paulo, 2015.

NASSIF, D. S. P.; MARIN, F. R.; COSTA, L. G. Padrões m{'\i}nimos para coleta de dados experimentais para estudos sobre crescimento e desenvolvimento da cultura da cana-de-açúcar. **Embrapa Informática Agropecuária-Documentos (INFOTECA-E)**, 2013.

NELDER, J. A.; MEAD, R. A simplex algorithm for function minimization. **Computer Journal**, v. 7, p. 308–313, 1965.

O'LEARY, G. J. A review of three sugarcane simulation models with respect to their prediction of sucrose yield. **Field Crops Research**, v. 68, n. 2, p. 97–111, 2000.

OLIVIER, F. C.; SINGELS, A. The effect of crop residue layers on evapotranspiration, growth and yield of irrigated sugarcane. **Water SA**, v. 38, n. 1, p. 77–86, 2012.

PARTON, W. J.; LOGAN, J. A. A model for diurnal variation in soil and air temperature. **Agricultural Meteorology**, v. 23, p. 205–216, 1981.

PEREZ, P. J.; CASTELLVI, F.; IBA??EZ, M.; ROSELL, J. I. Assessment of reliability of Bowen ratio method for partitioning fluxes. **Agricultural and Forest Meteorology**, v. 97, n. 3, p. 141–150, 1999.

PORTER, C. H.; JONES, J.; HOOGENBOOM, G.; WILKENS, P. W.; RITCHIE, J. T.; PICKERING, N. B.; BOOTE, K. J.; BAER, B. Soil Water Balance Module (WATBAL). *In*: JONES, J. W.; HOOGENBOOM, G.; WILKENS, P. W.; PORTER, C. H.; TSUJI, G. Y. (Eds.). . **DSSAT v4.5 Documentation**. [s.l.] University of Hawaii, 2010. p. 237–262.

PORTER, C. H.; JONES, J. W.; ADIKU, S. G. K.; GIJSMAN, A. J.; GARGIULO, O.; NAAB, J. B. Modeling organic carbon and carbon-mediated soil processes in DSSAT v4.5. **Operational Research**, 2009.

PRIESTLEY, C. H. B.; PHYSICS, R. J. T. A. On the Assessment of Surface Heat Flux and Evaporation Using Large-Scale Parameters. n. February, p. 81–92, 1972.

PROVENZANO, G.; PH, D.; RALLO, G.; PH, D.; GHAZOUANI, H. Assessing Field and Laboratory Calibration Protocols for the Diviner 2000 Probe in a Range of Soils with Different Textures. v. 142, n. 2, p. 1–12, 2016.

PRUSINKIEWICZ, P.; LINDENMAYER, A. The algorithmic beauty of plants. **Plant Science**, v. 122, n. 1, p. 109–110, 1990.

QURESHI, S. A.; MADRAMOOTOO, C. A.; DODDS, G. T. Evaluation of irrigation schemes for sugarcane in Sindh , Pakistan , using SWAP93. v. 54, p. 37–48, 2002.

R., F.; REEVES, M. Function minimization by conjugate gradients. **Computer Journal**, v. 7, p. 148–154, 1964.

RAE, A. L.; MARTINELLI, L. A.; DORNELLAS, M. C. Anatomy and Morphology. *In*: MOORE, P. H.; BOTHA, F. C. (Eds.). . **Sugarcane. Physiology, Biochemistry and Functional Biology**. [s.l.] WILEY Blackwell, 2013. p. 19–

34.

RIBEIRO, R. V.; MACHADO, E. C.; MAGALH??ES FILHO, J. R.; LOBO, A. K. M.; MARTINS, M. O.; SILVEIRA, J. A. G.; YIN, X.; STRUIK, P. C. Increased sink strength offsets the inhibitory effect of sucrose on sugarcane photosynthesis. **Journal of Plant Physiology**, v. 208, p. 61–69, 2017.

RITCHIE, J. T. Soil water balance and plant water stress. *In*: TSUJI, G. Y.; HOOGENBOOM, G.; THORNTON, P. K. (Eds.). . **Understanding Options for Agricultural Production**. Dordrecht: Springer Netherlands, 1998. p. 41–54.

RITCHIE, J. T.; PORTER, C. H.; JONES, J. W.; SULEIMAN, A. A. Extension of an Existing Model for Soil Water Evaporation and Redistribution under High Water Content Conditions. v. 73, n. 3, 2009.

SAGE, R. F. Why C4 photosynthesis. **C4 plant biology**, p. 3–16, 1999.

SAGE, R. F.; PEIXOTO, M. M.; SAGE, T. L. Photosynthesis in Sugarcane. **Sugarcane: Physiology, Biochemistry, and Functional Biology**, n. DECEMBER, p. 121–154, 2013.

SENTEK. **CALIBRATION MANUAL For Sentek Soil Moisture Sensors**. v2.0 ed. [s.l.] Sentek, 2011.

SILVA, A. L. C. DE; COSTA, W. A. J. M. DE. Growth and Radiation Use Efficiency of Sugarcane Under Irrigated and Rain-fed Conditions in Sri Lanka. **Sugar Tech**, v. 14, n. 3, p. 247–254, 2012.

SILVA, C. R. Calibração de um sensor capacitivo de umidade em Latossolo Amarelo na microrregião do Litoral Piauiense Field calibration of water capacitive sensor in a Yellow Latosol of coastal region , in the of State Piaui , Brazil. p. 303–307, 2007.

SILVA DIAS, M. A. F.; DIAS, J.; CARVALHO, L. M. V; FREITAS, E. D.; SILVA DIAS, P. L. Changes in extreme daily rainfall for S{ã}o Paulo, Brazil. **Climatic Change**, v. 116, n. 3, p. 705–722, 2013.

SINGELS, A.; BERG, M. VAN DEN; SMIT, M. A.; JONES, M. R.; ANTWERPEN, R. VAN. Modelling water uptake, growth and sucrose accumulation of sugarcane subjected to water stress. **Field Crops Research**, v. 117, n. 1, p. 59–69, 2010.

SINGELS, A.; INMAN-BAMBER, N. G. Modelling genetic and environmental control of biomass partitioning at plant and phytomer level of sugarcane grown in controlled environments. **Crop and Pasture Science**, v. 62, n. 1, p. 66–81, 2011.

SINGELS, A.; JONES, M.; BERG, M. VAN DEN. DSSAT v4. 5 Canegro sugarcane plant module: scientific documentation. **South African Sugarcane Research Inst. Mount …**, p. 1–34, 2008.

SINGELS, A.; SMIT, M. A. Sugarcane response to row spacing-induced competition for light. **Field Crops Research**, v. 113, n. 2, p. 149–155, 2009.

SMITH, D. M.; INMAN-BAMBER, N. G.; THORBURN, P. J. Growth and function of the sugarcane root system. **Field Crops Research**, v. 92, n. 2–3 SPEC. ISS., p. 169–183, 2005.

SPITTERS, C. J. T.; KEULEN, H. VAN; KRAALINGEN, D. W. G. VAN. A simple and universal crop growth simulator: SUCROS87. *In*: **Simulation and systems management in crop protection**. [s.l.] Pudoc, 1989. p. 147–181.

SPITTERS, C. J. T.; TOUSSAINT, H.; GOUDRIAAN, J. Separating the diffuse and direct component of global radiation and its implications for modeling canopy photosynthesis Part I. Components of incoming radiation. **Agricultural and Forest Meteorology**, v. 38, n. 1–3, p. 217–229, 1986.

SULEIMAN, A. A.; RITCHIE, J. T. Modeling soil water redistribution during second-stage evaporation. **Soil Science Society of America Journal**, v. 67, n. 2, p. 377–386, 2003.

TEH, C. **Introduction to mathematical modeling of crop growth: How the equations are derived and assembled into a computer model**. 1st. ed. Boca Raton, Florida (USA): Brown Walker Press, 2006.

THORBURN, P. J.; MEIER, E. A.; PROBERT, M. E. Modelling nitrogen dynamics in sugarcane systems: Recent advances and applications. **Field crops research**, v. 92, n. 2, p. 337–351, 2005.

THORNLEY, J. H. M.; JOHNSON, I. R. **Plant and crop modelling: a mathematical approach to plant and crop physiologyPlant and crop modelling: a mathematical approach to plant and crop physiology.**, 1990.

USABORISUT, P.; SUKCHAROENVIPHARAT, W. Soil compaction in sugarcane fields induced by mechanization. **American Journal of Agricultural and Biological Science**, v. 6, n. 3, p. 418–422, 2011.

UYS, L.; BOTHA, F. C.; HOFMEYR, J. S.; ROHWER, J. M. Kinetic model of sucrose accumulation in maturing sugarcane culm tissue. v. 68, p. 2375–2392, 2007.

VANDERPLAATS, G. N. **Numerical optimization**. [s.l: s.n.].

VELDHUIZEN, T. L.; JERNIGAN, M. E. **Will C++ be faster than Fortran?**International Conference on Computing in Object-Oriented Parallel Environments. **Anais**...1997

VERMA, I.; ROOPENDRA, K.; SHARMA, A.; JAIN, R.; SINGH, R. K.; CHANDRA, A. Expression analysis of genes associated with sucrose accumulation in sugarcane under normal and GA3-induced source--sink perturbed conditions. **Acta Physiologiae Plantarum**, v. 39, n. 6, p. 133, 2017.

VIANNA, M. S.; MARIN, F. R. **ESTIMATIVA DA TEMPERATURA DO AR HORÁRIA PARA O ESTADO DE SÃO PAULO**Congresso Brasileiro de Agrometeorologia. **Anais**...Juazeiro: 2017

VOS, J.; EVERS, J. B.; BUCK-SORLIN, G. H.; ANDRIEU, B.; CHELLE, M.; VISSER, P. H. B. DE. Functional-structural plant modelling: A new versatile tool in crop science. **Journal of Experimental Botany**, v. 61, n. 8, p. 2101–2115, 2010.

WALLACH, D.; MAKOWSKI, D.; JONES, J. W.; BRUN, F. **Working with Dynamic Crop Models**. [s.l: s.n.].

WANG, J.; NAYAK, S.; KOCH, K.; MING, R. Carbon partitioning in sugarcane (Saccharum species). **Frontiers in Plant Science**, v. 4, n. June, p. 2005–2010, 2013.

WATT, D. A.; MCCORMICK, A. J.; CRAMER, M. D. Source and Sink Physiology. **Sugarcane: Physiology, Biochemistry, and Functional Biology**, n. DECEMBER, p. 483–520, 2013.

YIN, X.; GOUDRIAAN, J. A. N.; LANTINGA, E. A.; VOS, J. A. N.; SPIERTZ, H. J. A flexible sigmoid function of determinate growth. **Annals of botany**, v. 91, n. 3, p. 361–371, 2003.

4. FUNCTIONAL-STRUCTURAL SUGARCANE MODEL FOR SIMULATING SUGARCANE GROWTH AND DEVELOPMENT

ABSTRACT

Sugarcane crop is the main source of sugar and the second largest source of biofuel in the world. In contrast to other crops, all aerial parts are harvested and processed, increasing the importance of its structural composition (sugars and fibre). Moreover, different row spacings have been adopted on sugarcane fields to decrease damage to plants and soil structure from harvest equipment, although potentially affecting the tillering process and productivity due to increased shading. Functional-structural plant (FSP) models are capable to simulate plant growth under competition for light at the organ level and have been used to assess and optimise crop arrangements and intercropping for other cultures. The aim of this paper was to develop and test a simple FSP model to simulate sugarcane growth and development, notably the tillering process and sucrose build-up. The FSP model was developed by integrating the main crop components from the organ level (phytomer), based on a relative source-sink approach, and a robust light model embedded into a three-dimensional modelling platform (GroIMP). The effect of soil water content on plant extension was added with a soil-plant-atmosphere with a tipping bucket water balance routine implemented in the model. A sugarcane field experiment dataset, with standard row spacing (1.40 m), was used for parameter deriving and model evaluating and testing. The FSP model was able to satisfactorily simulate sugarcane aboveground dry biomass ($r^2 = 0.87$, d = 0.91), stalk dry mass ($r^2 = 0.87$, d = 0.84), sucrose content ($r^2 = 0.57$, d = 0.49) and tillering ($r^2 = 0.76$, d = 0.85). Further model testing against experimental data may be performed to better assess the model applicability for different spacing row arrangements.

Keywords: Functional-structural plant model; Sugarcane; Agricultural system

4.1. INTRODUCTION

Sugarcane is the main source of sugar in the world and a major crop of social, economic and environmental importance in many tropical countries (Scheiterle *et al.*, 2017; Tapia Carpio and Simone de Souza, 2017). Globally, more than 70% of sugarcane are produced in Brazil, India, China, Thailand and Pakistan, with Brazil being the largest producer (50% global production); the crop is not only responsible for sugar production, but also accounts for 15% of the country's energy source, providing ethanol ["*flexfuel*" vehicles and gasoline mixture (27%)] and biomass energy mainly for electricity and heating (Walter *et al.*, 2014; EPE, 2015; Marin, 2016; Fortunato *et al.*, 2017). Despite of an increasing Brazilian production (7 mi tons $year^{-1}$), sugarcane yield has plateaued (around 80 t_{stalks} ha^{-1}) in the last years (FAO, 2016), which a strong expansion of crop areas towards the central-western region, the area of the original Cerrado biome (Adami *et al.*, 2012; F. V. Scarpare *et al.*, 2016).

In contrast to other crops, all parts of sugarcane plants are harvested (aerial parts), processed to extract sucrose or burnt for heating and electricity. Thus, differences in sucrose and fibre content between upper internodes of the stalks have attracted attention from molecular biologists attempting to identify enzymes and genes involved in rapid sucrose accumulation in parenchyma tissue (Whittaker and Botha 1997). Sucrose accumulation has also been studied extensively at cell and molecular levels, producing a wealth of information about processes at these levels (Moore, 2005). Nevertheless, the reductionist approach has reached its limits for altering sucrose accumulation at the crop level due to complex interactions among simultaneous processes (Singels and Inman-Bamber, 2011).

Numerous crossing and selection programs have aimed to improve the sucrose content trait to offset the low yield level, and much of the research effort has been directed towards molecular means for improving sucrose content. While some breakthroughs have been made in the laboratory , no plants modified for this purpose have been grown successfully in the field (Wu and Birch, 2007; Singels and Inman-Bamber, 2011; Braun, Wang and Ruan, 2014). Moreover, the increasing use of stalk biomass for renewable energy in the form of electricity from fibre and bio-ethanol from fermentable sugars has increased the importance of the identification of enzymes and genes involved in sucrose accumulation in parenchyma tissues (Moore, 2005).

Tillering is a key process for final yield in sugarcane, with competition for light and temperature being the most important driving factors (Bezuidenhout *et al.*, 2003). Several studies have been dedicated to the understanding of crop responses to row spacing (RS) to maximise final tiller population, and generally, their findings indicate that yield responses to row spacing are reduced with crop age and lower for ratoon crops than for plant crops (Singels and Smit, 2002; Garside *et al.*, 2005; Berthelsen *et al.*, 2006). Singels & Smit (2009) have investigated the underlying mechanisms of the impact of competition for light on leaf and tiller development, radiation capture and conversion to biomass as well as partitioning of biomass between leaves and stalks at the crop level in a wide range of row spacings (0.36 to 2.66 m).

The progression of intercepted radiation at the inter-row level differed substantially between the different row-spacings, while no influence of intra-row competition was observed among row-spacing arrangements. No inter-row competition for light was observed for a row spacing of 2.15 m. As soon as inter-row intercepted radiation exceeded a value of 90%, a drastic reduction in green leaf number due to a sharp acceleration in leaf senescence rate was reported (Singels and Smit, 2009). Inter-row competition had an effect on aboveground biomass accumulation at an RS of less than 1.37 m from before the first sampling at 730 8Cd (base temperature of 16 8C). For an RS of 1.73 m, the competition effect commenced sometime between the first and second sampling (at 948 8Cd) while there appeared to be no inter-row competition effect for an RS of 2.15 m.

Generally, these findings indicate that yield responses to row spacing diminish with crop age and are lower for ratoon crops than for plant crops. However, the apparent discrepancies between these studies demonstrate the need for a better understanding of the underlying processes of crop responses to row spacing, such as tiller and leaf development, radiation capture and biomass partitioning. Final and peak tiller densities are generally strongly dependent on row spacing, as shown in a review by Singels and Smit (2002), but the responses are not always consistent. The authors also demonstrated that the rate of tiller senescence due to shading is higher for narrower RS. Not much is known regarding the impact of row spacing on leaf appearance rate and leaf size or on the partitioning of biomass between the different plant components. This lack of knowledge extends to crop models, which causes uncertainty when these are used in RS-sensitive applications. In the Canesim model (Singels and Donaldson, 2000), canopy development (and interception of photosynthetically active radiation, PAR) is driven by thermal time.

The RS effect is simulated by adjusting the thermal time requirement to reach 50% canopy by 125 8Cd (base of 10 8C) per meter change in RS. In the Canegro model (Inman-Bamber, 1991), a more complex approach is followed by simulating the development of individual leaves and tiller cohorts, both driven by thermal time. The leaf area index (LAI) is calculated by multiplying leaf area per tiller by tiller density; the fractional interception of PAR across cane rows (FIINTER)is then calculated according to Beer's law. The RS effect is accounted for by simulating an increase in tiller appearance rate, inversely proportional to RS; tiller density is capped at 30 m^2. Simulated yield responses for the two models are then indirectly determined by the changed interception of radiation through the

impacts on the rates of biomass accumulation and water consumption. The APSIM (Keating et al., 1999) and Qcane (Liu and Bull, 2001) sugarcane models do not account for differences in row spacing, as far as we could establish.

Despite of the great contribution to understanding and predictions of sugarcane growth and development (Keating *et al.*, 1999; Singels, Jones and Berg, 2008), the sugarcane process-based model (PBM) reductionist approach has reached its limits for altering sucrose accumulation at crop level due to complex interactions among simultaneous processes (Singels and Inman-Bamber, 2011), limiting its use to support plant breeding towards sucrose maximisation, as reported previously by O'Leary (2000). In this sense, studies have been conducted on phytomer level to understand and integrate whole-plant carbon partitioning and sucrose accumulation (Singels and Inman-Bamber, 2011; Lingle and Thomson, 2012).

Functional-Structural Plant (FSP) studies have evolved in the last decades with the aid of computing processing techniques (Vos, Marcelis and Evers, 2007), such as ray-tracking algorithms and extensible languages. The Functional-Structural Plant Models (FSPM) explicitly describe the growth and development over time of the three dimensional (3D) architecture or structure of plants as governed by physiological processes, which, in turn, depend on environmental factors (Vos *et al.*, 2010). Those models have been used for intercropping and planting row arrangements due their ability to simulate competition for light among different plant structures (Mao *et al.*, 2016).

The sugarcane crop displays a high competition for light among tillers, which determines the final crop population and thus yield. Moreover, attempts to better understand sucrose accumulation and feedback responses of sucrose in plant tissues to whole-plant net photosynthesis rates on phytomer level have been made, and the scaling-up of these processes to the whole-plant level could be enabled by using FSP models (McCormick, Cramer and Watt, 2008). Therefore, the aim of this paper was to develop and test a simple functional-structural plant model (FSPM) to simulate sugarcane growth and development, integrating it from plant organs and competition for light.

4.2. MATERIAL E METHODS

To simulate light competition among tillers, sucrose accumulation and carbon partitioning on organ level, a simple FSPM for sugarcane was developed. The framework was based on a prior model for maize, developed in the Centre for Crop Systems Analysis (CSA), Wageningen University (WUR), The Netherlands. As other models, it was included in a main structure designed to link weather and soil data for plant growth and development simulations.

The FSPM is driven by rule-creation, which is, in turn, governed by environmental conditions (solar radiation, temperature and soil moisture). A sugarcane phytomer (re-writing) rule was created to reproduce a node, an axillary bud, a leaf sheath, a leaf blade, an internode and the apex (Vos *et al.*, 2010; Singels and Inman-Bamber, 2011; Moore and Botha, 2013a). The growth grammar was set to replicate (develop) and modify (growth) this phytomer pattern over time, based on crop responses to the environment (light, temperature and water stress). Each plant's state variables, such as leaf area, photosynthesis rate, height, stem weight and sucrose content, were integrated based on topology (Figure 50). Plant topology simulation is an important feature of FSPM, enabling feedback responses of specific organs to plant processes or structures (Vos *et al.*, 2010; Xu *et al.*, 2011).

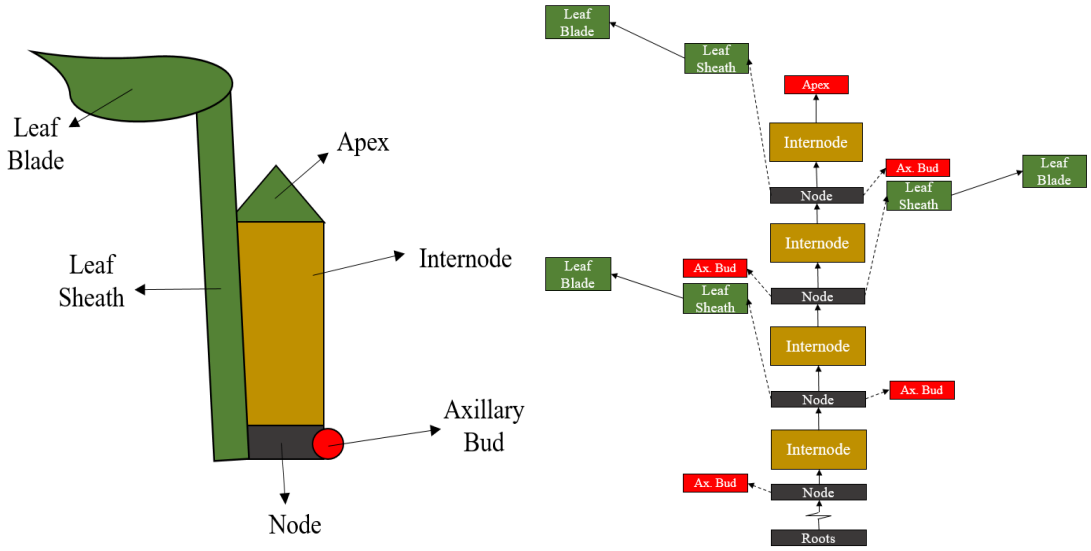

Figure 50. Sugarcane's phytomer (left) and topology (right) schematic details considered on the functional-structural model

For simplicity, a root growth rate (mm degree day^{-1}) was adopted to calculate the emergence time from planting depth and temperature (Marin and Jones, 2014). To simulate ratooning conditions, random positions for buds were set within 20 cm of the row to avoid self-shedding and overlapping. In this way, each tiller was considered as a single plant due its difficulty to differentiate among tillers of 1st and 2nd order and so on. Thus, tillers were set to emerge from the soil base (ratoon stool) based on a plastochron interval, and the abortion starts based on a light interception threshold, according to Bezuidenhout et al. (2003).

Leaves were initiated and appeared considering two phyllochron intervals to account for the "broken stick" phenomena of leaf creation (Inman-Bamber, 1994; Singels, Jones and Berg, 2008). A maximum number of green leaves was set for each tiller and considered as crop parameter threshold for leaf senescence. Therefore, the oldest leaf will shed when the corresponding tiller produces a number of leaves greater than the MaxGreenLeafNumber parameter (Keating *et al.*, 1999; Singels, Jones and Berg, 2008; Marin and Jones, 2014).

A relative sink strength approach is used to simulate carbohydrate demand at the organ scale (Heuvelink, 1996), which dictates that substrates are allocated to growing organs according to their relative sink strength. A derivative sigmoidal curve as a function of organ age was used to simulate the sink strength of each organ over time (Figure 51). Sink strength across all organs is summarised, and the relative sink strength is recalculated; the daily amount of plant substrates (previously calculated and integrated for all photosynthesising organs and reserve pools) is allocated for all organs, based on its relative sink strength. The substrates not used in organ allocation are then stored in a reserve pool for substrates.

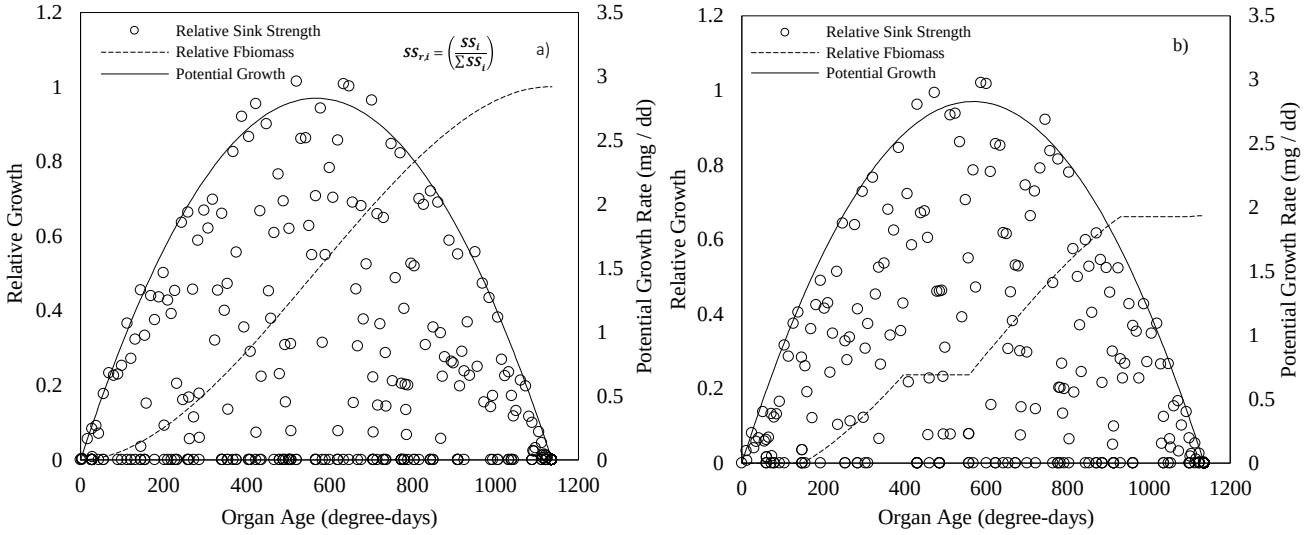

Figure 51. Potential growth, relative sink strength and fraction of potential biomass allocated to an organ under potential substrates supply (a) and intense substrates competition among organs (b)

As sugarcane is a C4 plant with highly efficient sucrose accumulation, it seems reasonable to consider the substrates pool as a total sugar pool, which can be partitioned into hexose and sucrose. Thus, to simulate sucrose accumulation in each culm's internode, the plant substrate pool is partitioned among internodes according to its structural biomass and age, following the Singels & Inman-Bamber (2011) approach and data derived from Lingle & Thomson (2012). The amount of hexose required by each internode for growth and maintenance respiration is calculated based on the classical method, and the sucrose amount for each internode is then considered the difference of total sugars and hexoses (Singels and Inman-Bamber, 2011; Lingle and Thomson, 2012).

More than 40 specific parameters for sugarcane can be modified to run the FSPM (Table 20). Most of them were derived from the literature and from experimental data, such as leaf insertion angle and curvature, phyllotaxis, shape coefficient and canopy development. Although a calibration routine was not implemented, due to its stochastic functions (light direction, plant orientations and position), many parameters are easily measured in field experiments (sizes, weights, angles) or derived from PBMs.

Table 20. Plant parameters and description for the sugarcane FSPM. Reference values are given at the bottom of table

Parameter	Value	Description
plastochron	72	Time between creation of two phytomers (dd) [2]
phyllochron	72	Time between appearance of two leaves (dd) [2]
plastochron2	172	Time between creation of two phytomers (dd) [3]
phyllochron2	172	Time between appearance of two leaves (dd) [3]
tillochron	120	Time between appearance of two tillers (dd) [4, 8]
MaxGreenLeafNumber	10	Max green leaf number per tiller [8]
MaxDewlapNumber	5	Max developed number of leaves per tiller [8]
MaxPop	26	Max population (tillers m^{-2}) [2, 8]
Tiller_light	0.3	Light interception threshold for tiller aborting [4]
nrShortInternodes	5	Number of short internodes that should not elongate [8]
TillerbelowG	0.08	Below ground growth rate for tiller (cm dd^{-1}) [5]
plas_change	10	Number of created plastochron for plastochron change [3, 8]
phyl_change	10	Number of created phyllochron for phyllochron change [3, 8]
wmaxRoot	20000	Maximum root system biomass [6]
wmaxInt	20000	Maximum internode dry biomass [1]
wmaxSucrose	8700	Maximum sucrose mass within an internode [1]
wmaxLeaf	3000	Maximum leaf biomass [8]
teRoot	4000	Root growth duration [3]
teInt	688	Internode growth duration [1]
teLeaf	1008	Leaf growth duration [2,8]
maxWidthInt	0.03	Maximum internode width [8]
PerCoeff	0.16	Fraction of plant elongation attributable to stalk elongation [3]
StrucBiom	0.06	Specific structural volume change (mg cm-3 dd^{-1}) [1]
MaxStrucBiom	0.12	Maximum specific structural volume (mg cm^{-3}) [1]
amax	44	Max photosynthesis rate (mmol m^{-2} s^{-1}) [7]
eff	0.05	Initial light use efficiency (initial slope of light response curve) [7]
LMA	4	Leaf mass per unit area (mg cm-) [2, 8]
lwRatio	30	Ratio between leaf blade length and width [8]
maxWidth	0.65	Location on the leaf where width is maximal (fraction of length) [8]
shapeCoeff	0.4	Leaf shape coefficient [8]
fPet	0.15	Petiole length (expressed as fraction of leaf blade length) [8]
leafAngle	35	Insertion angle of all leaves [8]
leafCurve	60	Leaf curvature - angle between bottom and top of leaf blade [8]
phyllotaxis	180	Angle between consecutive leaves along a stem [8]
varDelay	10	Max variation in germination delay [8]
seedMass	1000	Seed endosperm mass (mg)
PlantingDepth	0.25	Planting Depth [8]
tb	10	Base temperature for thermal time calculation [2,3]
eoratio	1.15	Ratio ETp from fully developed canopy to grass ETo (Kc from FAO-56) [3]

[1]Lingle & Thomson (2012); [2]Marin & Jones (2014); [3]Singels et al (2008); [4]Bezuidenhout et al (2003); [5]Keating et al (1999); [6]Laclau & Laclau (2009); [7]Sage et al (2014); [8]Experimental Data.

In contrast to crop PBM, all organs are simulated individually, interacting (or not) with the simulated environment and with other plants. A re-writing rule determines each organ´s creation and abortion, whilst an updating rule is also used to update all organ state variables such as age, sink strength, amount of light intercepted and dimensions. Therefore, all organs have a form and function inherent to each process, which, in turn, can be modified by the environment and at the same time affects the environment (FSPM paradigm) (Vos *et al.*, 2010; Godin, Dejong and Nikinmaa, 2014).

Due to its nature, the model is modulated in hierarchical levels of objects, classes and methods. For instance, to calculate leaf area index (LAI), it is required to add to the scene (simulate) a field base, in which several plants will stand and each plant will have a number of leaves (created systematically by the L-system), which, in turn, has its own dimension information to be integrated over that field base. In this way, all organs and objects (light sources, soil surface, glasshouse structure, etc.) are indexed to a corresponding class based on plant topology and structure. At the

same way, methods are operated to compute rate/state variables of all organs or objects inherent to its class at the same time, considering topology and structure hierarchy.

Based on this system, the FSPM main structure is operated by 12 modules (Table 21). The sugarcane module was implemented within organ and base modules, and the parameters can be set in the "parameters11" module. Re-writing rules for sugarcane phytomere creation were also included in the re-write module routines as well as update rules in update modules.

Table 21. Sugarcane FSPM main modules and description

Module	Description
main	• Initiation and run control (init(), run(), steps()) • Read/Reset parameters • Write outputs
parameters	• Parameters declaration and definitions for simulation control • Datasets declarations and shaders
rewrite	• Re-writing rules for plant development
updates	• Updating rules for rate/state variables calculations • Field and plant level integrations
initiation	• Axiom declarations • Dataset and charts reset
modules_base	• Field base classes and methods: Field, plant and branch bases
modules_organs	• Organ level class and methods: Growing organ, Visible organs, Seed, RootSystem, Flower, Apex, StemNode, Internode and leaf.
modules_light	• "Light dome" setup and partitioning into direct and diffuse radiation • Tile sensor and independent sensors creation
environment	• Meteorological data reading and calculation (solar radiation, tmax tmin, rain, rh, wind, et0) • Evapotranspiration routines: PM-method, priestley-Taylor or Etref input (crop factor)
parameters0 to 11	• Specific crop parameters of 12 plants (including sugarcane): • Dicots1 and 2, *Chenopodium*, *Arabidopsis thaliana*, cereal, wild, progenitor, weed, sunflower, maize, quinoa, sugarcane. • Parameters related to: plastochron, phyllochron, phyllotaxis and structure, sink strengths, specific organ's area and volume, photosynthesis.
modules_soil	• Soil layer and profile declarations • Simple tipping bucket water balance routines • Soil-Plant-Atmosphere routines • Soil temperature method
read_file	• Reading CSV file routines (input daily weather data)

The FSPM framework and main processes are summarised in Figure 52. To account for plant water use, the FAO-56 Penman-Monteith method (Allen, Pereira, Raes and M. Smith, 1998), Priestley-Taylor (Ritchie, 1998) and crop coefficient (Allen, Luis, *et al.*, 1998) were included into environment routines. Moreover, a "tipping bucket" soil-water balance method (Ritchie, 1998; Jones *et al.*, 2003; Suleiman and Ritchie, 2003a) was implemented to simulate belowground water movement, water uptake by roots (Ritchie, 1998), root development (Marin and Jones, 2014) and soil temperature (Sharpley and Williams, 1990). All these routines follow the PBMs concepts and were developed for entire canopies or large areas, thereby roughly simulating the soil-plant-atmosphere conditions, and further modifications to account for organ level may be required.

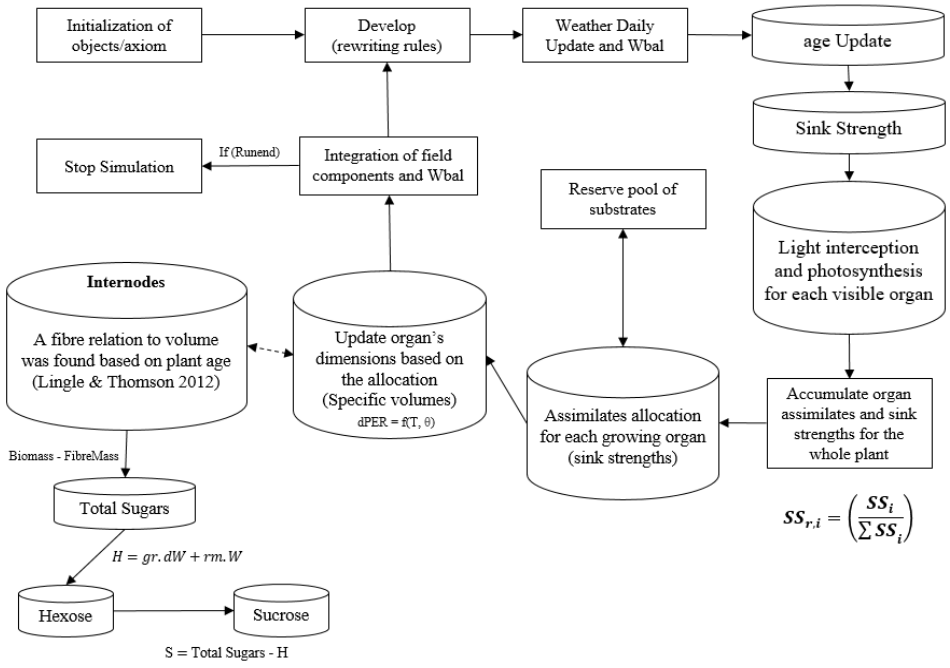

Figure 52. Schematic framework of the sugar FSPM main processes and modules since simulation's axiom to integrations

All routines were implemented in GroIMP v1.2 (Growth Grammar-related Interactive Modelling Platform), which is a 3D modelling platform that includes growth grammars by the XL language (ruled-based). It also includes a robust light model that simulates the amounts of light absorbed, reflected and transmitted for each object in a scene via Monte-Carlo stochastic sampling (Hemmerling *et al.*, 2008).

One experiment was carried out in an irrigated sugarcane field cropped with the second ratoon cultivar RB867515, which is planted on 27% of the Brazilian sugarcane fields. The planting date was on October 16, 2012, using a single line spacing of 1.4 m between rows and distributing 13-15 shoots per linear meter to a depth of 0.25 m. Thus, the current experiment was carried out during the second ratoon, starting on July 17, 2014, until June 8, 2015. The experiment was performed in the Department of Biosystems Engineering of the College of Agriculture "Luiz de Queiroz", Piracicaba, São Paulo (Lat: 22°41'55"S Lon: 47°38'34"W Alt: 540m). The climate is Cwa based on the Köppen classification, and the soil is a Hapludox (Soil Taxonomy, 2004). Fertilisation and agricultural pesticides were applied at the beginning of the second crop cycle, according to conventional practices of São Paulo State. Although an irrigation system was present, only two irrigations were performed in January due to droughts; the treatments were therefore mainly conducted under rainfed conditions. Plant growth and development biometric data were collected, including tillering, stalk diameter and stalk height, number of green and dead leaves, leaf area index (LAI), leaf insertion angle, length and width, stalk weight and leaf dry and fresh mass.

Field data was used to derive plant functional-structural parameters. When scaling up from organ level to field level, it is possible to evaluate the FSPM simulations with the same level of the PBM. In this, case, as only one detailed dataset (Piracicaba) was available and due to the difficulty in implementing a straightforward calibration routine, the sugarcane FSPM was only tested and evaluated based on the Piracicaba experiment. A set of 15 runs was performed due to the stochastic nature of the plant positions on scene. Statistical indices such as bias, root mean squared error (RMSE), relative root mean squared error (RRMSE), determination index (r^2) and the Willmot index (d)

were calculated for an average of 15 simulations and, therefore, used to evaluate the model performance in simulating each plant component (Wallach, Makowski and Jones, 2006).

4.3. RESULTS AND DISCUSSION

Similarity of simulated plant structures, based on phytomers and rules-based, and sugarcane morphology was achieved with the FSPM (Figure 53). The model could graphically represent individual sugarcane organs, such as seeds (buds), internodes, leaf sheath and blade, required for simulations. The structural differentiation between planted and ratooned sugarcane is shown in Figure 53, whereas planted cane tillers emerge from a single point in contrast to ratoon tillers, which emerge from a random position of buds within plant rows.

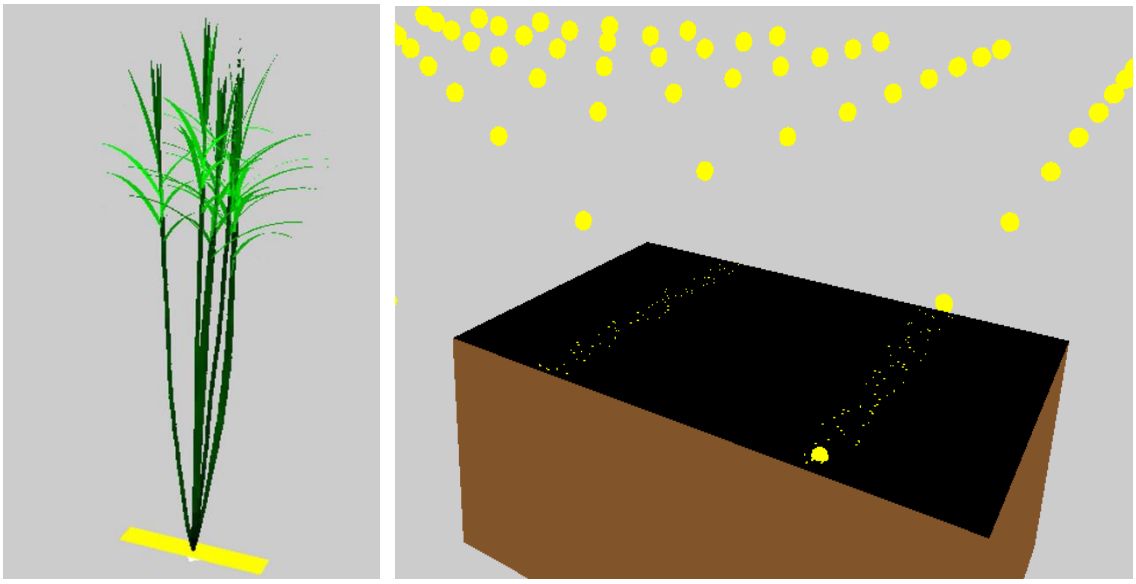

Figure 53. Structural representation of a planted sugarcane clump (left) and buds (small yellow dots) randomly positioned within planting row in ratooned sugarcane (right). The bigger yellow balls on right snapshot is a cloning feature of GroIMP to simulate extensive canopies efficiently avoiding border effects on results

Phenological development, growth and function of simulated sugarcane are shown in Figure 54. In this simulation for Piracicaba conditions, it is possible to identify crop emergence (50 DAH), tillering (between 50 to 170 DAH), stalk elongation and population establishment (from 170 DAH). Each organ in the scene has it owns structural and physiological role for crop development, such as absorbing light for photosynthesis or "sensing" the environment for plant signalling. Thus, the FSPM explicitly allows feedbacks between structure and function to be captured. Furthermore, feedbacks can be addressed between processes at the level of an individual organ (the 'local level') and the functioning of the plant or plant stand as a whole (the 'global level') (Vos *et al.*, 2010).

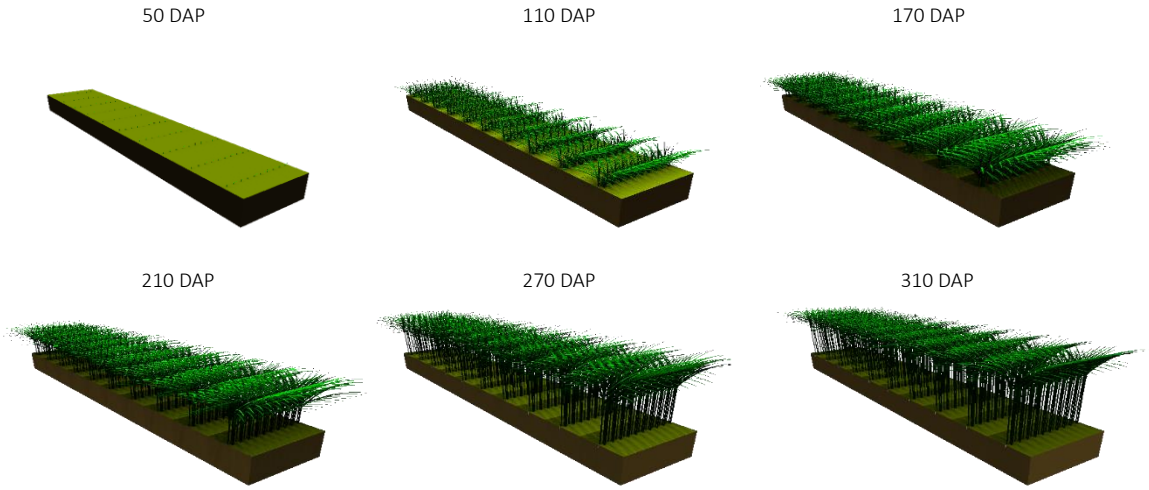

Figure 54. Rendered snapshots of a sugarcane FSPM simulation on different Days After Planting (DAP)

The fraction of intercepted fPAR (photosynthetically Active Radiation) measured over time in the Piracicaba experiment (Figure 55a) follows the same pattern as that of several sugarcane rainfed conditions evaluated by Silva & Costa (2012). The same authors also evaluated the fPAR for several sugarcane cultivars in fully-irrigated fields, which resulted in similar pattern of simulated fPAR by the sugarcane FSPM in Piracicaba (Figure 55b) (De Silva and De Costa, 2012). Water stress was not fully included in the model to account for all plant structural adaptations (e.g. leaf senescence or tiller abortion for water stress); thus, most of the simulated canopy and plant structure is still without water stress effect, explaining the "fully-irrigated" (or potential) pattern in light interception. This, in part, confirms the ability of the GROIMP's light model to precisely simulate light sources and their interception as well as the "light dome" methodology used here (Evers *et al.*, 2010).

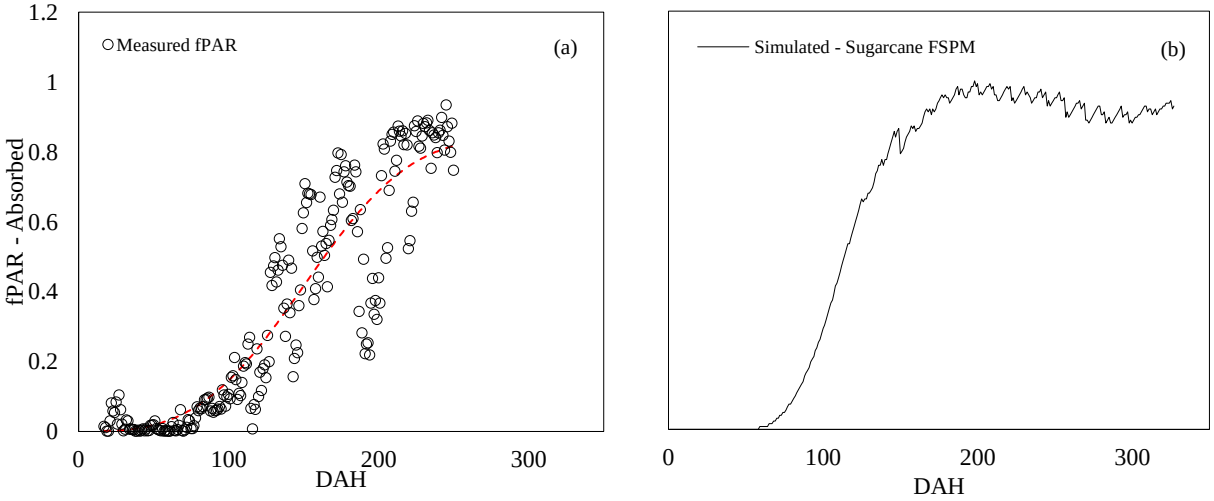

Figure 55. Fraction of photosynthetically active radiation (PAR) absorbed by the sugarcane canopy measured (open circles) over time in the Piracicaba experiment (a) and simulated fPAR by sugarcane FSPM (solid line) (b). Red dashed line is the best fit of a function of absorbed PAR and Days After Harvesting (DAH)

Many plant parameters were derived from field experiment measurements (Table 20); therefore, final leaf blade lengths ranged from 1.3 to 1.73 m, while width was approximately 6 cm. Internode expansion mainly occurs among top internodes, and the model uses an expansion parameter to regulate stalk expansion based on air temperature and water stress (Keating *et al.*, 1999; Singels, Jones and Berg, 2008; Marin and Jones, 2014). A green leaf organ dimension profile was also calculated by the model to follow up the canopy development during the crop season. The model computed continuous leaf growth from its appearance on tiller tops up to its senescence, based on maximum green leaf parameters.

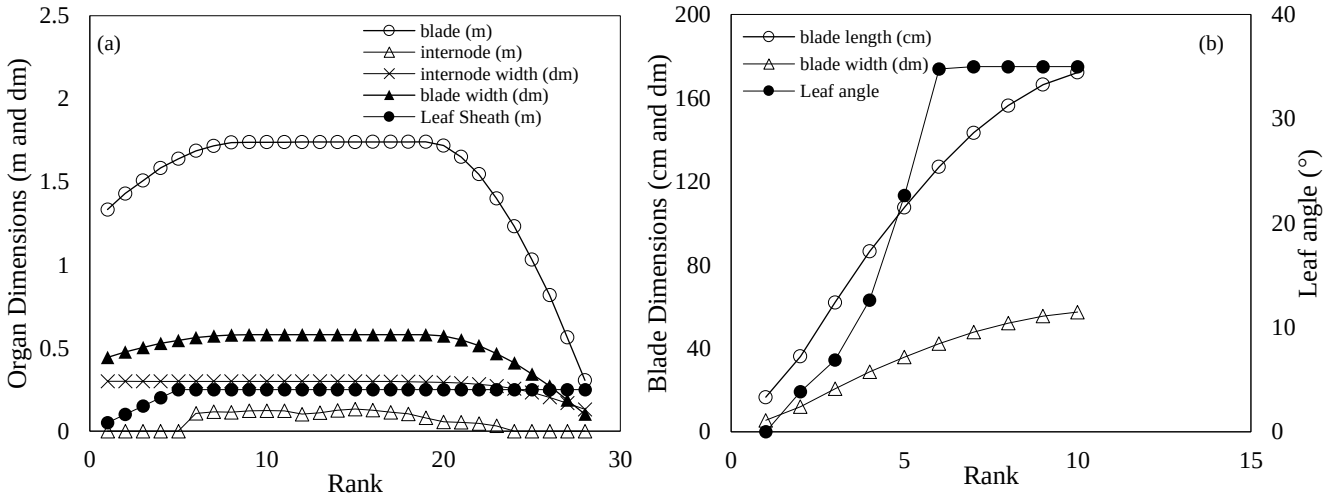

Figure 56. Organs dimension profile (a) and detailed leaf profile (b) over organs rank (phytomer creation) simulated by sugarcane FSPM in Piracicaba conditions

The internode composition profile was also determined based on data derived from Lingle & Thomson (2012). Internode specific volume (structural) was calculated based on a relation with organ age to calculate the structural allocated biomass and hexose demand; the substrate reserves were then stored in internodes as total sugar pools. Sugarcane FSPM was able to simulate this process (Figure 57a), where the hexose fraction of expanding internodes is higher due to their high growth rates, shifting to sucrose after the intense growth stage (Singels and Inman-Bamber, 2011; Lingle and Thomson, 2012). Sucrose accumulation starts after the internode expansion phase (5th top internode), as observed in Lingle & Thomson (2012) and simulated by Singels & Inman-Bamber (2011) (Figure 57b).

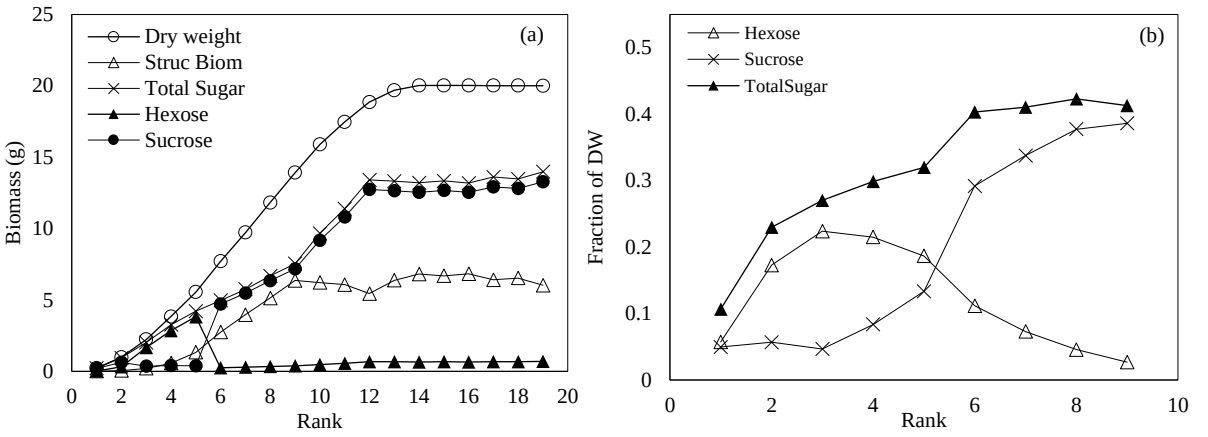

Figure 57. Composition profile of internodes over rank simulated by sugarcane FSPM in Piracicaba conditions (left), and fractions of sucrose, hexose and total sugars measured on field experiment by Lingle & Thomson (2012) (right)

The water balance routine implemented in the FSPM model simulated soil water content variations throughout the season (Figure 58). The simulated soil water content obtained was satisfactory, with an average RMSE value of 0.03 cm^3 cm^{-3}, a precision (r^2) of 0.36 and an accuracy (d) of 0.85. Although the root system was simplified and run without three-dimensional structures, further developments on the 3D root system also can be implemented in FSPMs (Leitner, Klepsch, Bodner, *et al.*, 2010; Leitner, Klepsch, Knieß, *et al.*, 2010; Or *et al.*, 2016).

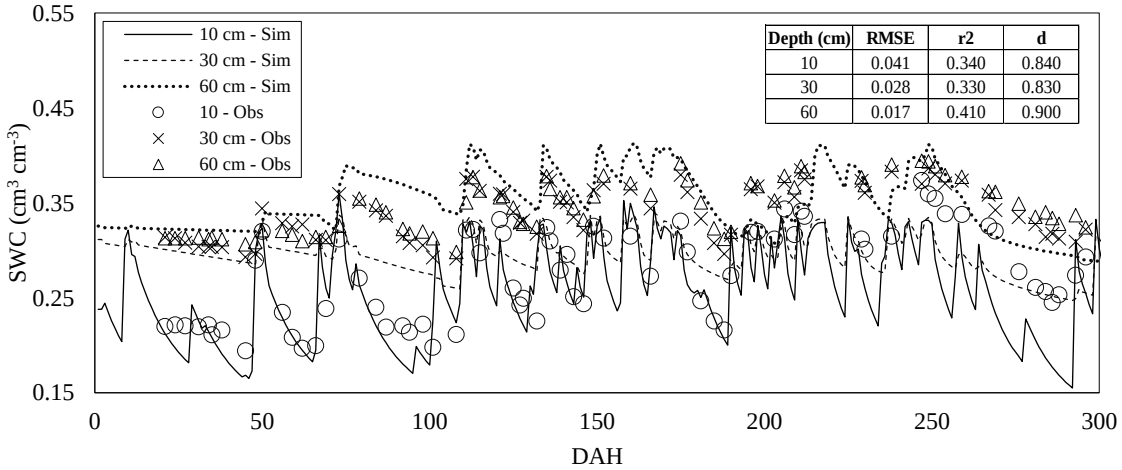

Depth (cm)	RMSE	r2	d
10	0.041	0.340	0.840
30	0.028	0.330	0.830
60	0.017	0.410	0.900

Figure 58. Soil water content (cm^3 cm^{-3}) in three soil layers simulated by the sugarcane FSPM water balance routine and measured in Piracicaba experiment throughout Days After Harvesting (DAH) and the statistical agreement indexes of simulation: Root means squared error (RMSE), precision (r2) and accuracy (d) for soil depth of 10, 30 and 60cm

Stalk height was well simulated by the sugarcane FSPM (Figure 59a), presenting high precision and accuracy (r^2 = 0.98 and d = 0.99) and an RMSE of 10 cm. Simulated tillering also presented good agreement, with 2.12 tillers m^{-2} of RMSE and elevated values of precision and accuracy (r^2 = 0.76, d = 0.85). Initial tillering until population peak was well simulated by employing the "tillocrhon" (Evers, 2006) to interval the light threshold for senescence. However, the simulated senescence rate was higher than observed data, possibly because when light was below the light threshold, younger tillers were instantly removed from crop field, while senesced tillers stands in the field for longer periods. Moreover, simulated senesced tillers and sheath leaf structures do not remain on the field, while they might still affect light distribution until the end of the crop season. Further implementation of soil temperature may improve simulations for mulch cover, since these results were only satisfactory for bare soil conditions.

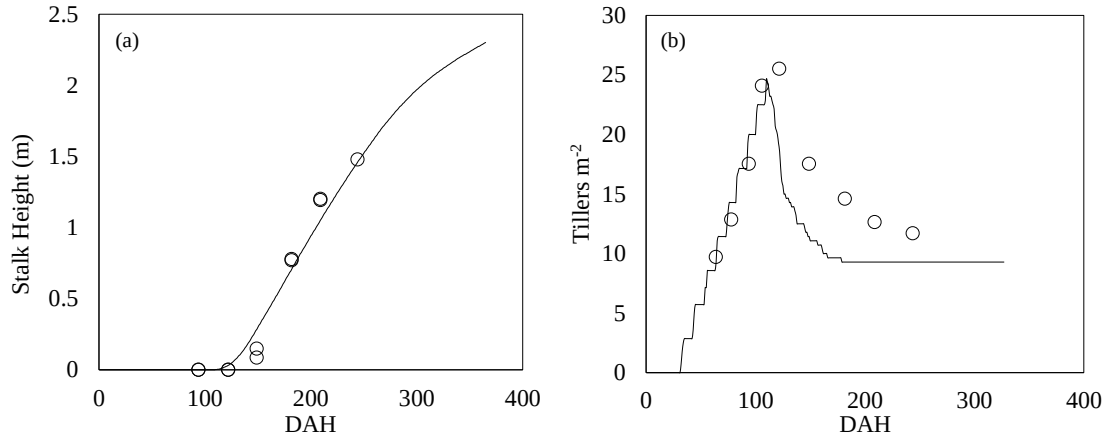

Figure 59. Stalk height (a) and tillering (b) simulated by the sugarcane FSPM (lines) and measured (open circle) in the Piracicaba conditions throughout Days After Harvesting (DAH)

The above simulated dry mass and LAI RMSE were 7.9 t ha^{-1} and 0.73, respectively, and despite of the good agreement indices (Table 22), a systemically overestimation was noticed for early crop development (Figure 60). Still, canopy integration by leaves and tillers of different ages proved to be better than the rough scaling-up methodology used in sugarcane PBMs (Marin *et al.*, 2015). The simulated decay observed for both LAI and dry biomass at 130 DAH was due to the steeper senescence rate, which may be better parameterised in further studies.

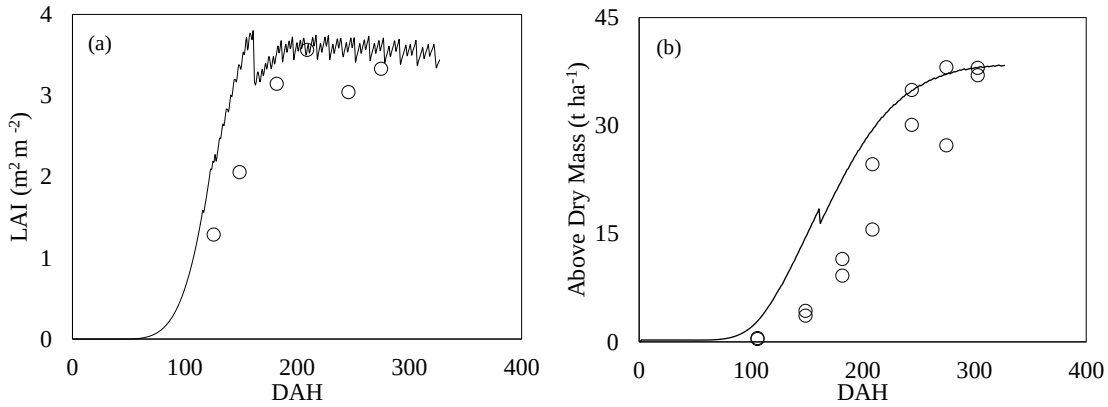

Figure 60. Leaf area index (a) and above ground dry mass (b) simulated by the sugarcane FSPM (lines) and measured (open circle) in the Piracicaba conditions throughout Days After Harvesting (DAH)

A delay time in the stalk dry weight simulation was also verified (Figure 61). The parameter related to short internodes is high and could be decreased to account for this delay in biomass accumulation. Simulated sucrose accumulation rate was high at 160 DAH; in addition, sucrose content was overestimated throughout the entire season apart from the end of the cycle. However, sucrose accumulation measured in different sites exhibited the same pattern (Marin and Jones, 2014).

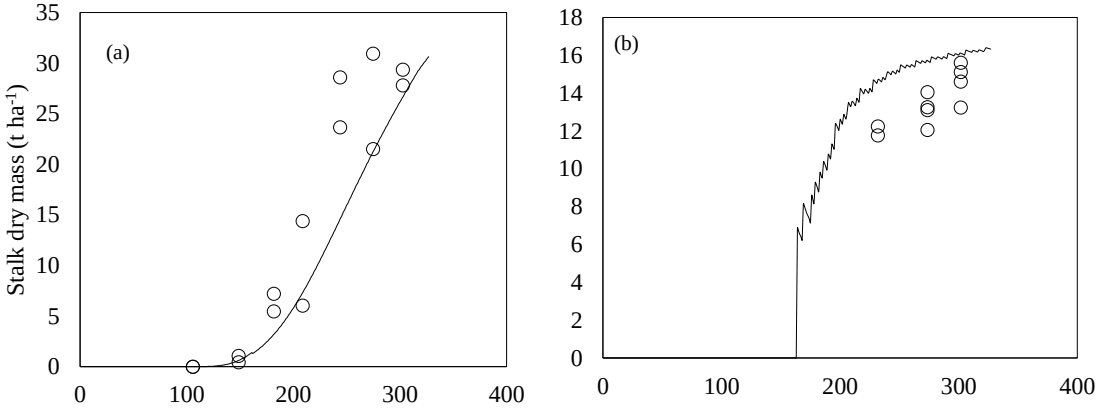

Figure 61. Stalk dry mass (a) and sucrose content on stalks (b) simulated by the sugarcane FSPM (lines) and measured (open circle) in the Piracicaba conditions throughout Days After Harvesting (DAH)

Table 22. Statistical indexes of performance of the sugarcane FSPM for the Piracicaba experiment. RMSE is the root mean squared error, EF is the modelling efficiency, r^2 the precision index, d is the Wilmot accuracy index

Crop Component	Bias	RMSE	r^2	d
Leaf area index (m^2 m^{-2})	0.516	0.73	0.78	0.89
Above Dry Mass (t ha^{-1})	6.055	7.96	0.87	0.91
Stalk Dry Mass (t ha^{-1})	-5.922	8.15	0.87	0.84
POL (%)	2.180	2.37	0.57	0.50
Stalk Height (m)	0.001	0.10	0.98	0.99
Tillering (# m^{-2})	-1.013	2.12	0.76	0.85

4.4. CONCLUSIONS

A Functional-Structural Plant Model capable to simulate sugarcane growth and development was developed. In particular, tillering and sucrose build-up were addressed by considering the intra-specific competition for light and internode composition. Satisfactory results for organ level integration to whole crop population, biomass and sucrose were obtained [aerial biomass (r^2 = 0.87, d = 0.91), stalk dry mass (r^2 = 0.87, d = 0.84), sucrose content (r^2 = 0.57, d = 0.49) and tillering (r^2 = 0.87, d = 0.95)]. The L-System was a promising approach to represent the sugarcane canopy, especially because of the non-complexity of the sugarcane plant structure. Nevertheless, some structural parts still need to be further understood, such a belowground internode and leaf sheath dimensions as well as the functional role for tillering and photosynthesis. Besides its ability to simulate competition for light, helping to understand intra-specific competition among tillers, the FSPM for sugarcane is a valuable tool for hypothesis testing, although sucrose accumulation and translocation mechanisms are still not fully understood (Wang *et al.*, 2013). Furthermore, intercropping studies for sugarcane could be supported by this FSPM framework, similar to other crops.

REFERENCES

ALLEN, R. G.; LUIS, S. P.; RAES, D.; SMITH, M. FAO Irrigation and Drainage Paper No. 56. Crop Evapotranspiration (guidelines for computing crop water requirements). **Irrigation and Drainage**, v. 300, n. 56, p. 300, 1998.

ALLEN, R. G.; PEREIRA, L. S.; RAES, D.; SMITH, M. Crop evapotranspiration: guidelines for computing crop water requirements. **FAO (Irrigation and Drainage)**, v. 56, 1998.

AZEVEDO, M. C. B. DE; CHOPART, J. L.; MEDINA, C. D. C. Sugarcane root length density and distribution from root intersection counting on a trench-profile. **Scientia Agricola**, v. 68, n. February, p. 94–101, 2011.

BAKER, C. J.; STERLING, M.; BERRY, P. A generalised model of crop lodging. **Journal of Theoretical Biology**, v. 363, p. 1–12, 2014.

BEZUIDENHOUT, C. N.; O'LEARY, G. J.; SINGELS, A.; BAJIC, V. B. A process-based model to simulate changes in tiller density and light interception of sugarcane crops. **Agricultural Systems**, v. 76, n. 2, p. 589–599, 2003.

BONNETT, G. D. Developmental Stages (Phenology). *In*: MOORE, P. H.; BOTHA, F. C. (Eds.). . **Sugarcane. Physiology, Biochemistry and Functional Biology**. [s.l.] WILEY Blackwell, 2013. p. 35–53.

BONNETT, G. D. B.; SPILLMAN, M. F. A.; HEWITT, M. L. C.; B, J. X. Source – sink differences in genotypes and water regimes in fl uencing sucrose accumulation in sugarcane stalks. p. 316–327, 2009.

BOTTCHER, A. *et al.* Ligni fi cation in Sugarcane : Biochemical Characterization , Gene Discovery , and Expression Analysis in Two Genotypes Contrasting for Lignin Content 1 [W]. v. 163, n. December, p. 1539–1557, 2013.

BOUGHTON, W. C. A review of the USDA SCS curve number method. **Soil Research**, v. 27, n. 3, p. 511–523, 1989.

BRAUN, D. M.; WANG, L.; RUAN, Y. Understanding and manipulating sucrose phloem loading , unloading , metabolism , and signalling to enhance crop yield and food security. v. 65, n. 7, p. 1713–1735, 2014.

BRAUNACK, M. V; ARVIDSSON, J.; HÅKANSSON, I. Effect of harvest traffic position on soil conditions and sugarcane (Saccharum officinarum) response to environmental conditions in Queensland, Australia. **Soil and Tillage Research**, v. 89, n. 1, p. 103–121, 2006.

BROWN, S. E.; PREGITZER, K. S.; REED, D. D.; BURTON, A. J. Predicting Daily Mean Soil Temperature from Daily Mean Air Temperature in Four Northern Hardwood S oil temperature is a very important climatic variable. v. 46, n. 2, p. 297–301, 2000.

BYRD, R. H.; LU, P.; NOCEDAL, J.; ZHU, C. A Limited Memory Algorithm for Bound Constrained Optimization. **SIAM Journal on Scientific Computing**, v. 16, n. 5, p. 1190–1208, 1995.

CAEMMERER, S. VON; FARQUHAR, G. D. Some relationships between the biochemistry of photosynthesis and the gas exchange of leaves. **Planta**, v. 153, n. 4, p. 376–387, 1981.

CARDOZO, N. P.; SENTELHAS, P. C.; PANOSSO, A. R.; PALHARES, A. L.; IDE, B. Y. Modeling sugarcane ripening as a function of accumulated rainfall in Southern Brazil. **International Journal of Biometeorology**, v. 59, n. 12, p. 1913–1925, 2015.

CHAPMAN, S. J. **Fortran for scientist and engineers: 1995-2003**. [s.l.] McGraw-Hill, 2008.

CHELLE, M.; EVERS, J. B.; COMBES, D.; VARLET-GRANCHER, C.; VOS, J.; ANDRIEU, B. Simulation of the three-dimensional distribution of the red: far-red ratio within crop canopies. **New Phytologist**, v. 176, n. 1, p. 223–234, 2007.

COSTA, L. G.; MARIN, F. R.; NASSIF, D. S. P.; PINTO, H. M. S.; LOPES-ASSAD, M. L. R. C. Simulação do efeito do manejo da palha e do nitrogênio na produtividade da cana-de-açúcar. **Revista Brasileira de Engenharia Agrícola e Ambiental**, v. 18, n. 5, p. 469–474, 2014.

COUTINHO, R. M.; KRAENKEL, R. A.; PRADO, P. I. Catastrophic Regime Shift in Water Reservoirs and S ã o Paulo Water Supply Crisis. p. 1–14, 2015.

COWAN, I. R. The interception and absorption of radiation in plant stands. **Journal of Applied Ecology**, p. 367–379, 1968.

EBRAHIM, M. K.; ZINGSHEIM, O.; EL-SHOURBAGY, M. N.; MOORE, P. H.; KOMOR, E. Growth and Sugar Storage in Sugarcane Grown at Temperatures Below and Above Optimum. **Journal of Plant Physiology**, v. 153, n. 5–6, p. 593–602, 1998.

EHLERINGER, J. R.; CERLING, T. E.; HELLIKER, B. R. C4 photosynthesis, atmospheric CO2, and climate. **Oecologia**, v. 112, n. 3, p. 285–299, 1997.

EVERS, J. B. **Tillering in spring wheat : a 3D virtual plant modelling study**. [s.l.] Wageningen University, 2006.

EVERS, J. B.; VOS, J.; ANDRIEU, B.; STRUIK, P. C. Cessation of tillering in spring wheat in relation to light interception and red: far-red ratio. **Annals of Botany**, v. 97, n. 4, p. 649–658, 2006.

EVERS, J. B.; VOS, J.; CHELLE, M.; ANDRIEU, B.; FOURNIER, C.; STRUIK, P. C. Simulating the effects of localized red: far-red ratio on tillering in spring wheat (Triticum aestivum) using a three-dimensional virtual plant model. **New Phytologist**, v. 176, n. 2, p. 325–336, 2007.

EVERS, J. B.; VOS, J.; FOURNIER, C.; ANDRIEU, B.; CHELLE, M.; STRUIK, P. C. Towards a generic architectural model of tillering in Gramineae, as exemplified by spring wheat (Triticum aestivum). **New Phytologist**, v. 166, n. 3,

p. 801–812, 2005.

FARQUHAR, G. D.; CAEMMERER, S. VON; BERRY, J. A. A biochemical model of photosynthetic CO2 assimilation in leaves of C3 species. **Planta**, v. 149, n. 1, p. 78–90, 1980.

FOURNIER, C. A functional – structural model of elongation of the grass leaf and its relationships with the phyllochron. p. 881–894, 2001.

GARSIDE, A. L.; BELL, M. J.; BERTHELSEN, J. E.; HALPIN, N. V; OTHERS. **Effect of breaks and nitrogen fertiliser on shoot development, maintenance, and cane yield in an irrigated plant crop of Q117.**Proceedings of the 2000 Conference of the Australian Society of Sugar Cane Technologists held at Bundaberg, Queensland, Australia, 2 May to 5 May 2000. **Anais**...2000

GHANNOUM, O. C4 photosynthesis and water stress. **Annals of Botany**, v. 103, n. 4, p. 635–644, 2008.

GOUDRIAAN, J. A simple and fast numerical method for the computation of daily totals of crop photosynthesis. **Agricultural and Forest Meteorology**, v. 38, n. 1, p. 249–254, 1986.

GOUDRIAAN, J. Light distribution. *In*: **Canopy Photosynthesis: From Basics to Applications**. [s.l.] Springer, 2016. p. 3–22.

HAVERAAEN, M.; MORRIS, K.; ROUSON, D.; RADHAKRISHNAN, H.; CARSON, C. High-performance design patterns for modern Fortran. **Scientific Programming**, v. 2015, p. 3, 2015.

HEERDEN, P. D. R. VAN; EGGLESTON, G.; DONALDSON, R. A. Ripening and Postharvest Deterioration. **Sugarcane: Physiology, Biochemistry, and Functional Biology**, p. 55–84, 2013.

HEERDEN, P. D. R. VAN; SINGELS, A.; PARASKEVOPOULOS, A.; ROSSLER, R. Negative effects of lodging on irrigated sugarcane productivity—An experimental and crop modelling assessment. **Field Crops Research**, v. 180, p. 135–142, 2015.

HEUVELINK, E. Dry matter partitioning in tomato: validation of a dynamic simulation model. **Annals of botany**, v. 77, n. 1, p. 71–80, 1996.

HIKOSAKA, K.; NIINEMETS, U.; ANTEN, N. P. R. **Canopy photosynthesis: from basics to applications**. [s.l.] Springer, 2016.

INMAN-BAMBER, N. G. A growth model for sugarcane based on a simple carbon balance and the CERES-Maize water balance. **South African Journal of Plant Soil**, v. 8, p. 93–99, 1991.

INMAN-BAMBER, N. G.; BONNETT, G. D.; SPILLMAN, M. F.; HEWITT, M. L.; JACKSON, J. Increasing sucrose accumulation in sugarcane by manipulating leaf extension and photosynthesis with irrigation. p. 13–26, 2008.

INMAN-BAMBER, N. G.; BONNETT, G. D.; SPILLMAN, M. F.; HEWITT, M. L.; XU, J. Source--sink differences in genotypes and water regimes influencing sucrose accumulation in sugarcane stalks. **Crop and Pasture Science**, v. 60, n. 4, p. 316–327, 2009.

ITTERSUM K, M. VAN; LEFFELAAR, P. A.; KEULEN, H. VAN; KROPFF, M. J.; BASTIAANS, L.; GOUDRIAAN, J. On approaches and applications of the Wageningen crop models. **European Journal of Agronomy**, v. 18, p. 201–234, 2003.

JONES, J. W.; HOOGENBOOM, G.; PORTER, C. H.; BOOTE, K. J.; BATCHELOR, W. D.; HUNT, L. A.; WILKENS, P. W.; SINGH, U.; GIJSMAN, A. J.; RITCHIE, J. T. **The DSSAT cropping system model**. [s.l: s.n.]. v. 18

KEATING, B. A.; ROBERTSON, M. J.; MUCHOW, R. C.; HUTH, N. I. Modelling sugarcane production systems I. Development and performance of the sugarcane module. **Field Crops Research**, v. 61, n. 3, p. 253–271, 1999.

KROES, J. G.; DAM, J. C. VAN; GROENENDIJK, P.; HENDRIKS, R. F. A; JACOBS, C. M. J. SWAP version 3.2. Theory and user manual. **Update**, n. August, p. 284, 2009.

LACLAU, P.; LACLAU, J. P. Growth of the whole root system for a plant crop of sugarcane under rainfed and irrigated environments in Brazil. **Field Crops Research**, v. 114, n. 3, p. 351–360, 2009.

LEVESQUE, J. M.; WILLIAMSON, J. W. **A Guidebook to FORTRAN on Supercomputers**. [s.l.] Academic Press, 2014.

LINGLE, S. E.; THOMSON, J. L. Sugarcane Internode Composition During Crop Development. **Bioenergy Research**, p. 168–178, 2012.

LIU, D. L.; BULL, T. A. Simulation of biomass and sugar accumulation in sugarcane using a process-based model. v. 144, p. 181–211, 2001.

LONG, S. P.; AINSWORTH, E. A.; ROGERS, A.; ORT, D. R. Rising atmospheric carbon dioxide: plants FACE the future. **Annu. Rev. Plant Biol.**, v. 55, p. 591–628, 2004.

MARENGO, J. A.; NOBRE, C. A.; SELUCHI, M. E.; CUARTAS, A.; ALVES, L. M.; MENDIONDO, E. M.; OBREGÓN, G.; SAMPAIO, G. A seca e a crise h{'\i}drica de 2014-2015 em São Paulo. **Revista USP**, n. 106, p. 31–44, 2015.

MARIN, F. R.; ANGELOCCI, L. R.; COELHO FILHO, M. A.; VILLA NOVA, N. A. Construção e avaliação de psicrômetro aspirado de termopar. **Scientia Agricola**, v. 58, n. 4, p. 839–844, 2001.

MARIN, F. R.; JONES, J. W. Process-based simple model for simulating sugarcane growth and production. **Scientia Agricola**, v. 71, n. 1, p. 1–16, 2014.

MARIN, F. R.; THORBURN, P. J.; NASSIF, D. S. P.; COSTA, L. G. Sugarcane model intercomparison: Structural differences and uncertainties under current and potential future climates. **Environmental Modelling & Software**, v. 72, p. 372–386, 2015.

MATSUOKA, S.; GARCIA, A. A. F. Sugarcane underground organs: going deep for sustainable production. **Tropical Plant Biology**, v. 4, n. 1, p. 22–30, 2011.

MCCORMICK, A. J.; CRAMER, M. D.; WATT, D. A. Sink strength regulates photosynthesis in sugarcane. **New Phytologist,** 2006.

MONTEITH, J. Light Interception and Radiative Exchange in Crop Stands. 1969.

MONTEITH, J. L.; UNSWORTH, M. H. **Principles of Environmental Physics: Plants , Animals , and the Atmosphere**. 4th Editio ed. Oxford: Elsevier Ltd, 2012.

MOORE, P. H.; BOTHA, F. C. **Sugarcane: physiology, biochemistry and functional biology**. [s.l.] John Wiley & Sons, 2013.

MULLER, J.; NORMALE, E.; LYON, S. DE. Arithmetic Processor for Solving Tridiagonal Systems of Linear Equations. 2006.

NASH, J. C. **Compact Methods for Computers. Linear Algebra and Function Minimisation**. [s.l: s.n.].

NASSIF, D. S. P. **Evapotranspiração, transpiração e trocas gasosas em um canavial irrigado**. [s.l.] University of Sao Paulo, 2015.

NASSIF, D. S. P.; MARIN, F. R.; COSTA, L. G. Padrões m{'\i}nimos para coleta de dados experimentais para estudos sobre crescimento e desenvolvimento da cultura da cana-de-açúcar. **Embrapa Informática Agropecuária-Documentos (INFOTECA-E)**, 2013.

NELDER, J. A.; MEAD, R. A simplex algorithm for function minimization. **Computer Journal**, v. 7, p. 308–313, 1965.

O'LEARY, G. J. A review of three sugarcane simulation models with respect to their prediction of sucrose yield. **Field Crops Research**, v. 68, n. 2, p. 97–111, 2000.

OLIVIER, F. C.; SINGELS, A. The effect of crop residue layers on evapotranspiration, growth and yield of irrigated sugarcane. **Water SA**, v. 38, n. 1, p. 77–86, 2012.

PARTON, W. J.; LOGAN, J. A. A model for diurnal variation in soil and air temperature. **Agricultural Meteorology**, v. 23, p. 205–216, 1981.

PEREZ, P. J.; CASTELLVI, F.; IBA??EZ, M.; ROSELL, J. I. Assessment of reliability of Bowen ratio method for partitioning fluxes. **Agricultural and Forest Meteorology**, v. 97, n. 3, p. 141–150, 1999.

PORTER, C. H.; JONES, J.; HOOGENBOOM, G.; WILKENS, P. W.; RITCHIE, J. T.; PICKERING, N. B.; BOOTE, K. J.; BAER, B. Soil Water Balance Module (WATBAL). *In*: JONES, J. W.; HOOGENBOOM, G.; WILKENS, P. W.; PORTER, C. H.; TSUJI, G. Y. (Eds.). . **DSSAT v4.5 Documentation**. [s.l.] University of Hawaii, 2010. p. 237–262.

PORTER, C. H.; JONES, J. W.; ADIKU, S. G. K.; GIJSMAN, A. J.; GARGIULO, O.; NAAB, J. B. Modeling organic carbon and carbon-mediated soil processes in DSSAT v4.5. **Operational Research**, 2009.

PRIESTLEY, C. H. B.; PHYSICS, R. J. T. A. On the Assessment of Surface Heat Flux and Evaporation Using Large-Scale Parameters. n. February, p. 81–92, 1972.

PROVENZANO, G.; PH, D.; RALLO, G.; PH, D.; GHAZOUANI, H. Assessing Field and Laboratory Calibration Protocols for the Diviner 2000 Probe in a Range of Soils with Different Textures. v. 142, n. 2, p. 1–12, 2016.

PRUSINKIEWICZ, P.; LINDENMAYER, A. The algorithmic beauty of plants. **Plant Science**, v. 122, n. 1, p. 109–110, 1990.

QURESHI, S. A.; MADRAMOOTOO, C. A.; DODDS, G. T. Evaluation of irrigation schemes for sugarcane in Sindh , Pakistan , using SWAP93. v. 54, p. 37–48, 2002.

R., F.; REEVES, M. Function minimization by conjugate gradients. **Computer Journal**, v. 7, p. 148–154, 1964.

RAE, A. L.; MARTINELLI, L. A.; DORNELLAS, M. C. Anatomy and Morphology. *In*: MOORE, P. H.; BOTHA, F. C. (Eds.). . **Sugarcane. Physiology, Biochemistry and Functional Biology**. [s.l.] WILEY Blackwell, 2013. p. 19–34.

RIBEIRO, R. V.; MACHADO, E. C.; MAGALH??ES FILHO, J. R.; LOBO, A. K. M.; MARTINS, M. O.; SILVEIRA, J. A. G.; YIN, X.; STRUIK, P. C. Increased sink strength offsets the inhibitory effect of sucrose on sugarcane photosynthesis. **Journal of Plant Physiology**, v. 208, p. 61–69, 2017.

RITCHIE, J. T. Soil water balance and plant water stress. *In*: TSUJI, G. Y.; HOOGENBOOM, G.; THORNTON, P. K. (Eds.). . **Understanding Options for Agricultural Production**. Dordrecht: Springer Netherlands, 1998. p. 41–54.

RITCHIE, J. T.; PORTER, C. H.; JONES, J. W.; SULEIMAN, A. A. Extension of an Existing Model for Soil Water Evaporation and Redistribution under High Water Content Conditions. v. 73, n. 3, 2009.

SAGE, R. F. Why C4 photosynthesis. **C4 plant biology**, p. 3–16, 1999.

SAGE, R. F.; PEIXOTO, M. M.; SAGE, T. L. Photosynthesis in Sugarcane. **Sugarcane: Physiology, Biochemistry, and Functional Biology**, n. DECEMBER, p. 121–154, 2013.

SENTEK. **CALIBRATION MANUAL For Sentek Soil Moisture Sensors**. v2.0 ed. [s.l.] Sentek, 2011.

SILVA, A. L. C. DE; COSTA, W. A. J. M. DE. Growth and Radiation Use Efficiency of Sugarcane Under Irrigated and Rain-fed Conditions in Sri Lanka. **Sugar Tech**, v. 14, n. 3, p. 247–254, 2012.

SILVA, C. R. Calibração de um sensor capacitivo de umidade em Latossolo Amarelo na microrregião do Litoral Piauiense Field calibration of water capacitive sensor in a Yellow Latosol of coastal region , in the of State Piaui , Brazil. p. 303–307, 2007.

SILVA DIAS, M. A. F.; DIAS, J.; CARVALHO, L. M. V; FREITAS, E. D.; SILVA DIAS, P. L. Changes in extreme daily rainfall for S{ã}o Paulo, Brazil. **Climatic Change**, v. 116, n. 3, p. 705–722, 2013.

SINGELS, A.; BERG, M. VAN DEN; SMIT, M. A.; JONES, M. R.; ANTWERPEN, R. VAN. Modelling water uptake, growth and sucrose accumulation of sugarcane subjected to water stress. **Field Crops Research**, v. 117, n. 1, p. 59–69, 2010.

SINGELS, A.; INMAN-BAMBER, N. G. Modelling genetic and environmental control of biomass partitioning at plant and phytomer level of sugarcane grown in controlled environments. **Crop and Pasture Science**, v. 62, n. 1, p. 66–81, 2011.

SINGELS, A.; JONES, M.; BERG, M. VAN DEN. DSSAT v4. 5 Canegro sugarcane plant module: scientific documentation. **South African Sugarcane Research Inst. Mount …**, p. 1–34, 2008.

SINGELS, A.; SMIT, M. A. Sugarcane response to row spacing-induced competition for light. **Field Crops Research**, v. 113, n. 2, p. 149–155, 2009.

SMITH, D. M.; INMAN-BAMBER, N. G.; THORBURN, P. J. Growth and function of the sugarcane root system. **Field Crops Research**, v. 92, n. 2–3 SPEC. ISS., p. 169–183, 2005.

SPITTERS, C. J. T.; KEULEN, H. VAN; KRAALINGEN, D. W. G. VAN. A simple and universal crop growth simulator: SUCROS87. *In*: **Simulation and systems management in crop protection**. [s.l.] Pudoc, 1989. p. 147–181.

SPITTERS, C. J. T.; TOUSSAINT, H.; GOUDRIAAN, J. Separating the diffuse and direct component of global radiation and its implications for modeling canopy photosynthesis Part I. Components of incoming radiation. **Agricultural and Forest Meteorology**, v. 38, n. 1–3, p. 217–229, 1986.

SULEIMAN, A. A.; RITCHIE, J. T. Modeling soil water redistribution during second-stage evaporation. **Soil Science Society of America Journal**, v. 67, n. 2, p. 377–386, 2003.

TEH, C. **Introduction to mathematical modeling of crop growth: How the equations are derived and assembled into a computer model**. 1st. ed. Boca Raton, Florida (USA): Brown Walker Press, 2006.

THORBURN, P. J.; MEIER, E. A.; PROBERT, M. E. Modelling nitrogen dynamics in sugarcane systems: Recent

advances and applications. **Field crops research**, v. 92, n. 2, p. 337–351, 2005.

THORNLEY, J. H. M.; JOHNSON, I. R. **Plant and crop modelling: a mathematical approach to plant and crop physiologyPlant and crop modelling: a mathematical approach to plant and crop physiology.**, 1990.

USABORISUT, P.; SUKCHAROENVIPHARAT, W. Soil compaction in sugarcane fields induced by mechanization. **American Journal of Agricultural and Biological Science**, v. 6, n. 3, p. 418–422, 2011.

UYS, L.; BOTHA, F. C.; HOFMEYR, J. S.; ROHWER, J. M. Kinetic model of sucrose accumulation in maturing sugarcane culm tissue. v. 68, p. 2375–2392, 2007.

VANDERPLAATS, G. N. **Numerical optimization**. [s.l: s.n.].

VELDHUIZEN, T. L.; JERNIGAN, M. E. **Will C++ be faster than Fortran?**International Conference on Computing in Object-Oriented Parallel Environments. **Anais**...1997

VERMA, I.; ROOPENDRA, K.; SHARMA, A.; JAIN, R.; SINGH, R. K.; CHANDRA, A. Expression analysis of genes associated with sucrose accumulation in sugarcane under normal and GA3-induced source--sink perturbed conditions. **Acta Physiologiae Plantarum**, v. 39, n. 6, p. 133, 2017.

VIANNA, M. S.; MARIN, F. R. **ESTIMATIVA DA TEMPERATURA DO AR HORÁRIA PARA O ESTADO DE SÃO PAULO**Congresso Brasileiro de Agrometeorologia. **Anais**...Juazeiro: 2017

VOS, J.; EVERS, J. B.; BUCK-SORLIN, G. H.; ANDRIEU, B.; CHELLE, M.; VISSER, P. H. B. DE. Functional-structural plant modelling: A new versatile tool in crop science. **Journal of Experimental Botany**, v. 61, n. 8, p. 2101–2115, 2010.

WALLACH, D.; MAKOWSKI, D.; JONES, J. W.; BRUN, F. **Working with Dynamic Crop Models**. [s.l: s.n.].

WANG, J.; NAYAK, S.; KOCH, K.; MING, R. Carbon partitioning in sugarcane (Saccharum species). **Frontiers in Plant Science**, v. 4, n. June, p. 2005–2010, 2013.

WATT, D. A.; MCCORMICK, A. J.; CRAMER, M. D. Source and Sink Physiology. **Sugarcane: Physiology, Biochemistry, and Functional Biology**, n. DECEMBER, p. 483–520, 2013.

YIN, X.; GOUDRIAAN, J. A. N.; LANTINGA, E. A.; VOS, J. A. N.; SPIERTZ, H. J. A flexible sigmoid function of determinate growth. **Annals of botany**, v. 91, n. 3, p. 361–371, 2003.

5. GENERAL CONCLUSIONS

Based on the results obtained in this study, three different sugarcane modelling approaches were developed, tested and calibrated for Brazilian conditions:

(i) The development and improvement of an existing PBM framework was achieved. A new version of the SAMUCA model was developed and embedded into a modulated crop simulation platform, which can be used to host future crop models and includes Brazilian farming system features. The model was able to simulate the soil mulch cover effect on crop development and soil evaporation, including soil water stress effects on crop growth and development, considering differences regarding plant and ratoon crops. The soil-water balance routine implemented captured soil water variations throughout the crop season, with reasonably good levels of precision and accuracy, also including the effect of mulch cover on the soil. Simulated sugarcane plants and ratoons mainly differ in terms of initial crop conditions (i.e. planting depth and substrate reserves available). The model performance in a long-term experiment and under different Brazilian conditions was satisfactory, and the agreement indices were close to those of other widely used sugarcane crop models (CANEGRO and APSIM-Sugar). In addition, by including the atmospheric CO2 effect, the model could be included in future sugarcane climate change impact studies.

(ii) The coupling of the SAMUCA model to a robust agrohydrological model (SWAP) was accomplished, and although non-expressive improvements in model performance regarding crop yield were noticed (with an overall 6% lower RMSE), the ability of SWAP-SAMUCA to simulate soil water content was superior compared to that of the original "tipping bucket" approach (32% lower RMSE). This opens new room for improvements and testing sugarcane groundwater consumption as well as its response to soil temperature, agrohydrology and salt stress at the PBM level. The coupled model (SWAP-SAMUCA) is expected to reduce prediction uncertainty and therefore represents a better tool for predicting crop water use and vadose zone hydrology under sugarcane.

(iii) A Functional-Structural Plant Model capable to simulate sugarcane growth and development was established; in particular, tillering and sucrose build-up were addressed by considering the intra-specific competition for light and internode composition. Satisfactory results of organ level integration to the whole crop population, biomass and sucrose were obtained. The L-System is a promising approach to represent the sugarcane canopy, especially because of the non-complexity of the sugarcane plant structure. Nevertheless, some structural parts still need to be further understood, such as belowground internode and leaf sheath dimensions and their functional role in tillering and photosynthesis. Besides its ability to simulate competition for light, helping to understand intra-specific competition among tillers, the FSPM for sugarcane is a valuable tool for hypothesis testing, as sucrose accumulation and translocation mechanisms are still not fully understood (Wang *et al.*, 2013). Furthermore, intercropping studies for sugarcane could be supported by the FSPM framework, which has already successfully been done for other crops.